Impact of the Removal of the Storm Surge Barrier on the Morphological Development in the Eastern Scheldt

Master thesis report

Hannah Bervoets

Impact of the Removal of the Storm Surge Barrier on the Morphological Development in the Eastern Scheldt

Master thesis report

by

Hannah Bervoets

to obtain the degree of Master of Science
at the Delft University of Technology,
to be defended publicly on Monday 31th of March, 2025 at 14:00

Faculty of Civil Engineering and Geosciences
student number: 4837746

Supervisors:

Dr. ir. Bregje van Wesenbeeck
Dr. ir. Robert Jan Labeur
Ir. Bob Smits
Dr. Ir. Lodewijk de Vet

Deltares

TU Delft Delft University of Technology

Frontpage photo: Aerial View of the Galgeplaat, Oosterschelde. Photo by Sky Pictures, 2022. Source: Natuurmonumenten.

Preface

After 6.5 years of study at the Civil Engineering Faculty at TU Delft, this master's thesis represents my final effort to fulfill the requirements for my master's degree in Civil Engineering.

First, I want to thank my supervisors for helping and advising me throughout my master's thesis. Without their guidance, this document would not be in front of you today. Thank you, Bob, for being my daily supervisor, for thinking along with me about which results I should investigate, and for advising me on how to best present them. I also appreciate you for making me feel really welcome in the ESD department of Deltares. Thank you, Bregje, for being my Chair, for asking critical questions, and for introducing me to the topic and involving me in project meetings. Thank you, Lodewijk, for always being available to answer specific questions about the Oosterschelde and for all your valuable feedback. Robert-Jan, thank you for all your help with writing and structuring my report; this undoubtedly improved the final document. Finally, thank you, Wout, for assisting me with my ASMITA-related questions and for clarifying how each parameter is defined.

Lastly, I would like to thank all my friends who made these 6.5 years of studying an incredible time, during which I not only learned a great deal but also made wonderful memories. Thank you for all the fun during rowing, coaching, committee work, cooking dinners, coffee breaks, exam weeks, lectures, online friend meetings during corona time and so much more. Without you, I would not look back on this time as fondly as I do. I also want to thank my family for being my foundation and for always being there for me. Finally, to my boyfriend, Thom, thank you for always being there for me and supporting me, even when you were over 10,000 kilometers away.

Hannah Bervoets
Delft, March '25

Abstract

The Eastern Scheldt region in the southwestern Netherlands depends on various dams and dikes for coastal protection, including the storm surge barrier (OSK) at the seaside. The OSK was built for both coastal protection and ecological preservation. Initially constructed as a compromise to avoid completely closing off the Eastern Scheldt, the OSK allows tidal exchange flows in normal conditions while it closes during storms. However, the barrier has disrupted the natural dynamics that normally govern a tidal basin, causing erosion of tidal flats as the channels 'demand' sediment from the flats. These flats are critical for the ecosystem, supporting migratory birds that forage there and playing a crucial role in wave attenuation, which reduces the wave load on dikes. Preserving these tidal flats is therefore beneficial for both flood risk reduction and ecology. Currently, this is achieved by carrying out sediment nourishments on the flats of the Eastern Scheldt to maintain them.

With rising sea levels, the OSK will need to close more frequently, potentially up to 66% of the time with a 2-meter sea level rise. This would disrupt water exchange, threatening food availability for ecosystems and mussel farming while increasing the demand for sediment nourishments on the flats. Frequent closures and ecological pressures raise concerns about the long-term viability of the OSK. Exploring alternatives, such as removing the OSK, could restore sediment exchange, reduce channel sediment demand, and promote tidal flat recovery. However, uncertainties about the long-term morphological effects of OSK removal persist, making further research essential to evaluate its potential as a sustainable solution for both ecological preservation and coastal protection. This study aims to investigate the long-term morphological development of the Eastern Scheldt following the potential removal of the OSK. To achieve this objective, the following research question will be addressed: *What is the long-term morphological development of the Eastern Scheldt, focusing on the tidal flats, when removing the storm surge barrier and under the influence of sea level rise?*

To investigate the long-term morphological development of the Eastern Scheldt without the OSK, this study adopts the equilibrium concept for tidal basins. This approach was chosen because it avoids the complexities of process-based models, in which it remains challenging to balance wave erosion and tidal sedimentation over the long term in the Eastern Scheldt. The equilibrium approach predicts aggregated volumes of the flats, channels, and ebb-tidal delta without providing spatial or depth-specific details. The methodology consists of two parts:

1. Data Analysis: Measured volumes of flats, channels, and the ebb-tidal delta are compared with equilibrium volumes derived from empirical equations to assess their alignment. Equilibrium volumes for the scenario without the OSK are then calculated to predict the likely morphological state of these elements.
2. ASMITA Model: To predict dynamic changes influenced by factors such as sea-level rise, the ASMITA numerical model is used. ASMITA simulates sediment exchange among flats, channels, and the ebb-tidal delta by also using the equilibrium concept and estimates morphological trends over time.

The results from the data analysis show that the channels will be closer to their theoretical equilibrium if the OSK is removed, which will reduce the sand demand of the channels and is expected to result in less sediment being drawn from the flats. It is also expected that, due to the removal of the OSK, sediment blockage will disappear between the channels and ebb-tidal delta. Furthermore, from the large deviations between equilibrium volumes and measured volumes of the flats and ebb-tidal delta suggest that the relations used in this research to calculate the equilibrium volumes should be refined. A good comparison should first be made between the basin on which the empirical equilibrium volumes are based and the Eastern Scheldt. Identifying these differences could lead to more specific equilibrium relations for the Eastern Scheldt.

Results modeled with ASMITA indicate that the flats will import sediment in all scenarios. Sensitivity analysis on these results show that the rate and magnitude of this sediment import largely depend on the sediment concentration entering the basin without the OSK. A reliable estimation of this sediment concentration requires further research (see Recommendations). The ASMITA results also show that the increase in flat volume depends on the balance between sediment import and sea-level rise. Most scenarios indicate an increase in total flat volume. However, for scenarios with extreme SLR rates, the flats in the Eastern Scheldt may eventually drown, even with the OSK removed.

The expected long-term morphological response of the Eastern Scheldt to removing the OSK is sediment importation to the flats. This can explained by the disappearance of the sediment blockage and the current volume of the channels matching the new equilibrium volume, therefore demanding significantly less sediment of the flats. The total increase in the volume of the flats depends on the balance between sediment import and sea-level rise. Further research is required to provide an absolute estimate of the total increase in the volume of the flats.

Contents

List of Figures

List of Tables

List of Abbreviations

ASMITA	Aggregated Scale Morphological Interaction between Tidal inlets and the Adjacent coast
MHW	Mean High Water
MLW	Mean Low Water
MSL	Mean Sea Level
OSK	Oosterscheldekering (Storm Surge Barrier)
SLR	Sea Level Rise

1 Introduction

1.1 Context

Sea level rise, a consequence of climate change, significantly impacts coastal protection worldwide. In the Netherlands, projections for sea level rise by 2100 range from 25 to 124 cm (Overbeek & van Dorland, 2023). Therefore coastal protection—both globally and in the Netherlands—must be improved, reinforced, or adapted to meet these new conditions (Haasnoot et al., 2018).

Coastal protection strategies can generally be divided into two categories: hard and soft coastal protection. Hard coastal protection refers to static structures such as dams or breakwaters. These structures occupy relatively little space, have predictable behavior, and are governed by standardized design rules, such as those for overtopping discharges and risks. On the other hand, soft coastal protection involves natural features like dunes, such as those along the northwest coast of the Netherlands. Soft protection offers additional ecological value, enhancing recreation opportunities and possibility of adapting to rising sea levels through sediment accumulation (Bosboom & Stive, 2021).

Focusing on the southwestern delta of the Netherlands, this region, prone to flooding, is predominantly protected by hard coastal defenses. The Eastern Scheldt, for instance, is surrounded by dams, dikes, and, at the sea boundary, the Oosterscheldekering (Storm Surge Barrier) (OSK). The OSK is a storm surge barrier that protects the inner Eastern Scheldt. It remains open for tidal exchange flows and closes during storms to reduce peak loads on the dikes and dams within the Eastern Scheldt. Initially, the plan was to completely close off the Eastern Scheldt with a dam, but due to protests from fishermen and other residents of Zeeland, the OSK, a storm surge barrier, was built instead (Rijkswaterstaat, 2024a). Since its construction, the tidal prism is reduced and almost no new sediment has entered the Eastern Scheldt, disrupting the equilibrium between tidal forces and tidal channels and flats. This imbalance has resulted in ongoing erosion of the tidal flats as the channels 'demand sediment,' which they source from the flats (see Figure 1.1) (van Zanten & Adriaanse, 2008). These tidal flats are critical for the ecosystem, supporting migratory birds that forage there, and play a crucial role in wave attenuation, reducing the wave load on dikes (de Ronde et al., 2013). Preserving these tidal flats is therefore beneficial for both flood risk reduction and ecological reasons. Currently, this is achieved by carrying out sediment nourishments on the flats of the Eastern Scheldt to maintain them (van der Werf et al., 2015).

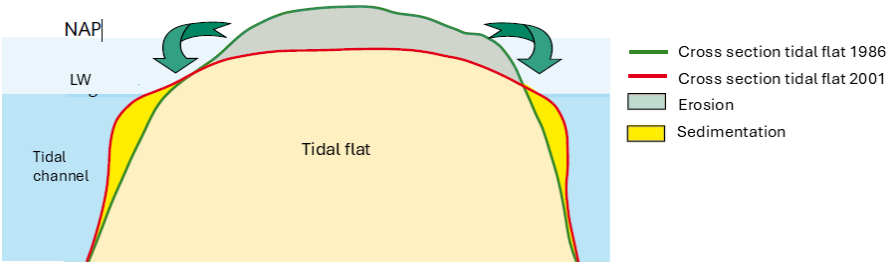

Figure 1.1: Sand demand process illustrated in the Eastern Scheldt (van Zanten & Adriaanse, 2008)

However, with rising sea levels, the barrier will need to close more frequently and for longer durations, potentially threatening its functionality. For example, with a sea level rise of 2 meters, it is estimated that the barrier would be closed for 66% of the time, assuming that the current closure protocol remains unchanged (Zandvoort et al., 2019). With such frequent closures it is expected that the food availability for the ecosystem and mussel farming sector will reduced, due to less water in and outflow in the Eastern Scheldt. Furthermore, due to higher SLR more sediment nourishment on the flats need to be carried out to maintain them. But their increased frequency harms benthic organisms, which reduces suitable forage areas for birds, and thus diminishes the nourishments' effectiveness (Zandvoort et al., 2019).

1.2 Problem statement

The Eastern Scheldt storm surge barrier was designed to as coastal protection measure and also preserve the natural environment and maintain shellfish farming in the Eastern Scheldt. However, with rising sea levels, the barrier will need to close more frequently and for longer durations, potentially threatening its functionality (Haasnoot et al., 2018). If the Eastern Scheldt storm surge barrier can no longer maintain its functionality, this raises the question whether the barrier is still the optimal solution. It may become necessary to consider alternative coastal protection strategies that allow the Eastern Scheldt to maintain its ecological values. One of these strategies could be protecting the Eastern Scheldt without the OSK. This removal could reduce channels sediment demand, restore sediment exchange, and promote tidal flat recovery, supporting soft coastal protection (De Pater, 2012). However, the effect of this removal on the morphological development in the Eastern Scheldt are not yet clear, making it difficult to determine whether this would be a beneficial and viable solution.

De Pater (2012) found that removing the OSK increases the tidal prism, tidal range, and flow velocities, promoting shoal buildup. Wisse (2022) used Delft3D to model the morphodynamics with and without the OSK but faced uncertainties regarding the balance of wave- and tide-driven transport, leaving uncertainties regarding the long-term morphological impacts of OSK removal. The study from De Pater (2012) concludes that removing the OSK could help maintain the flats, however it remains unclear how much of the flats would be preserved and what equilibrium state they might ultimately reach.

1.3 Research objective

This study aims to investigate the long-term morphological development of the Eastern Scheldt following the potential removal of the Eastern Scheldt storm surge barrier (OSK). To achieve this objective, the following research question will be addressed:

What is the long term morphological development of the Eastern Scheldt, focusing on the tidal flats, when removing the storm surge barrier and under the influence of sea level rise?

This research question will be answered using the following sub-questions.

1. How can insights gained from the historical development of the Eastern Scheldt help predict its future evolution?
2. What will be the equilibrium state of Eastern Scheldt in terms of volumes of the channels, tidal flats, and the ebb tidal delta, with and without the OSK?
3. Which factors most significantly influence the development of tidal flats in the Eastern Scheldt in terms of volume?
4. What will be the volume trends of the flats, channels, and ebb-tidal delta in the Eastern Scheldt without the OSK, and how will they evolve under sea level rise?

1.4 Method

This thesis starts by investigating existing literature and provides an overview of past, current, and expected morphological developments in the Eastern Scheldt, addressing sub-research question 1. Additionally, equilibrium equations applicable to the Eastern Scheldt are described. Using these relations, the equilibrium volumes of the flats, channels, and ebb-tidal delta are calculated and compared with the measured volumes. This comparison determines whether the Eastern Scheldt has been, is currently, or will be developing toward its equilibrium state, addressing sub-research question 2.

To investigate the rate of development toward equilibrium and the influence of factors such as Sea Level Rise (SLR), the numerical model Aggregated Scale Morphological Interaction between Tidal inlets and the Adjacent coast (ASMITA) is utilized. This model is chosen for its ability to simulate long-term morphological changes in tidal systems using equilibrium-based principles. However, accurately predicting trends using ASMITA requires well-defined model parameters, which poses a challenge due to the lack of calibration data in the version of the model used in this study. A sensitivity analysis is conducted to refine the parameter selection process, after which scenarios are simulated to provide insights therefore contribute to answering sub-research questions 3 and 4.

1.5 Scope

This research uses a method that describes and estimates the general morphological development in the Eastern Scheldt, both with and without the OSK. The prediction of the development of the tidal elements—the flats, channels, and ebb-tidal delta—is done at an aggregated volume level. This means that predictions about spatial characteristics, such as locations and depths, will not be made. The reason for this is that the equilibrium concept is used, in which these spatial characteristics are not included.

If the OSK were to be removed in the future, a new coastal protection strategy would need to be developed. This would involve, among other things, assessment of flood risks and the design of suitable coastal protection measures. However, this thesis does not address these aspects; it focuses solely on investigating the morphological development in the Eastern Scheldt with and without the OSK and whether this removal would be beneficial for the flats on the long term.

1.6 Outline

This thesis is structured into six chapters:

- **Chapter 1: Introduction**
  Introduces the research context, objectives, and the research questions guiding this study.
- **Chapter 2: Literature Review**
  Provides a review of research up till now on the Eastern Scheldt, gives an overview of how the Eastern Scheldt has developed, and describes equilibrium relations for the Eastern Scheldt.
- **Chapter 3: Methodology**
  Outlines the methodology, describing the definitions for the volumes, the implementation of the ASMITA model, parameter selection, and the scenarios considered in this study.
- **Chapter 4: Results**
  Presents the results of the comparison between the measured volumes and the equilibrium volumes, the simulations run with ASMITA, including the sensitivity analysis and the impact of sea level rise on tidal flats.
- **Chapter 5: Discussion**
  Discusses the findings in the context of the research questions, highlighting key implications, limitations, and potential uncertainties. Also a synthesis of the discussion is included in this chapter.
- **Chapter 6: Conclusions**
  Summarizes the main findings and provides recommendations for future research.

2 Literature review

This chapter reviews existing literature on the Eastern Scheldt, focusing on its historical, current, and future development. Subsequently, current and future strategies for the Eastern Scheldt are examined. Existing empirical equilibrium relationships for the Eastern Scheldt are then described. The chapter concludes with a summary of the literature findings.

2.1 Introduction Eastern Scheldt

To give an overview of the research area an introduction is given of the Eastern Scheldt. The Eastern Scheldt is located in the South-West Delta of the Netherlands and is a delta-estuarine system consisting of salt marshes, flats, channels, and human interventions. This dynamic environment has experienced a significant history of human modification, including land reclamation and flood defense systems. All these interventions have had an impact on hydrodynamics, morphodynamics, and ecology. After the devastating North Sea Flood of 1953, the Delta Works were designed and implemented. These interventions, shown in Figure 2.1, were constructed for coastal protection purposes. Initially, the plan was to completely close off the Eastern Scheldt with a dam, but due to protests from fishermen and other residents of Zeeland, the OSK, a storm surge barrier, was built instead. It is closed only during storm surge. Under normal conditions, water can still flow into the Eastern Scheldt. This allows the system to retain its tidal character and preserve more of its original ecological values on which people depend (Rijkswaterstaat, 2024a).

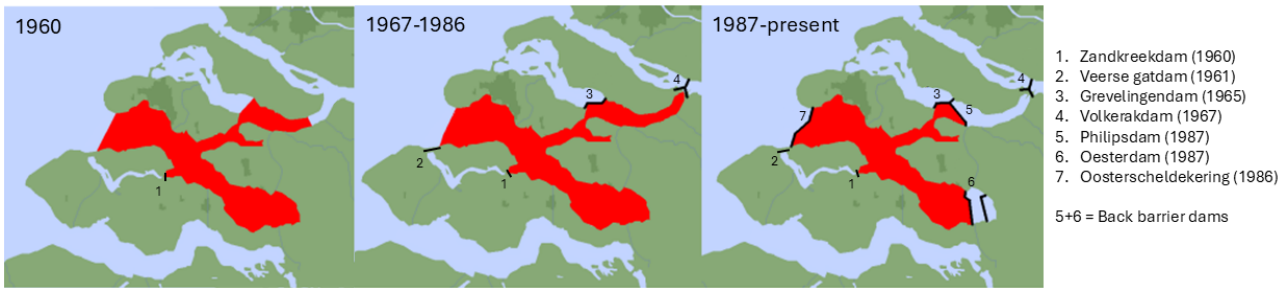

Figure 2.1: Eastern Scheldt from 1960 till now with indicated Delta works and the year in which they are completed. Per time period the estimated basin area is in red indicated (de Bok, 2001).

2.1.1 Ecological value

The Eastern Scheldt is a Natura 2000 protected site under EU law, specifically the Habitats and Birds Directives, which aim to conserve Europe's biodiversity. One of the primary reasons that the Eastern Scheldt is a Natura 2000 area is its importance as a habitat for migrating birds (Brand et al., 2016). The flats in the region are globally important, serving as resting and foraging grounds for these birds. The flats are rich in benthic organisms (benthos), which thrive in the abiotic conditions of flats. The dynamic tidal conditions create a landscape of flats and salt marshes, see Figure 2.2, which contribute to the area's unique ecological value. When flats erode they lose varied elevations, which poses a threat to the birds and other habitats that depend on them (Fitzgerald & Hughes, 2019) (De Vet, 2020). In addition to birds, the Eastern Scheldt is home to other species, including various fish, seals, pioneering plant species and mussels. These mussels are vital for the local fishing industry. Interestingly, the OSK appears to have had no significant impact on the mussel populations (Zandvoort et al., 2019).

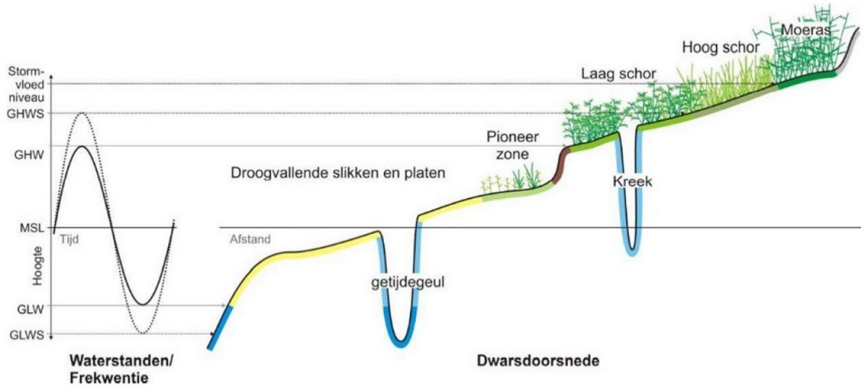

Figure 2.2: Cross-section flats and saltmarshes (Oost et al., 2020)

2.2 Processes that shape the Eastern Scheldt

This report focuses on the long-term morphological development of the Eastern Scheldt. The processes that shape the Eastern Scheldt on the long term are discussed below. The Eastern Scheldt is a tidal basin where tidal processes dominate over wind, wave, or river influences. This leads to the existence of flats, channels, and an ebb-tidal delta in the Eastern Scheldt. In Figure 2.3, the elements and their definitions are shown. The ebb-tidal delta is defined as the total excess sediment volume relative to the undisturbed bed profile in m^3. In a natural tidal basin, the channels, flats, and ebb-tidal delta are influenced by each other as a result of the hydrodynamic forcing (Q. J. Lodder et al., 2019).

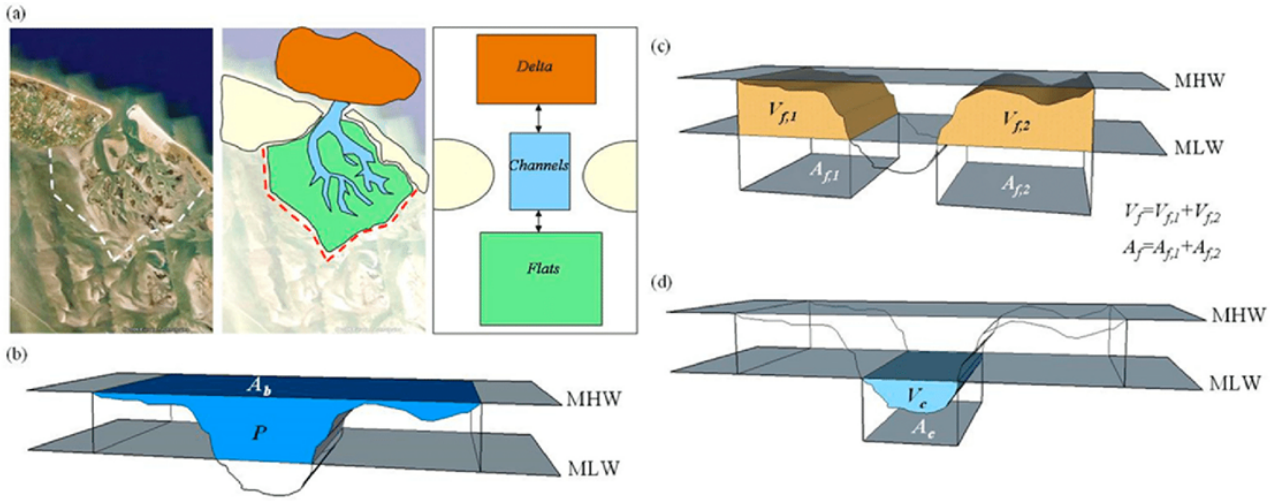

Figure 2.3: (a) The three-elements schematisation for a tidal inlet, (b) definitions parameters tidal prism P and basin area A_b, (c) area A_f and volume V_f of flats, (d) area A_c and volume V_c of channels. (Q. J. Lodder et al., 2019)

In general the hydrodynamic forcing in a tidal basin is characterized by the tidal prism (also indicated in Figure 2.3), the tidal range (difference between Mean Low Water (MLW) and Mean High Water (MHW)), tidal flow velocities, and wind waves. The tidal prism is the volume of water that flows in and out of a tidal basin. The volume of water entering the basin depends on the size of the inlet, the size of the basin, and the tidal range (Bosboom & Stive, 2021). The larger the tidal prism, the larger the cross-section of the channels become. The tidal prism influences the ebb-tidal delta, with a larger tidal prism transporting more sediment, resulting in a larger delta (Eelkema, 2013). Tidal flow velocities transport sediment to higher elevations, such as the flats and the ebb-tidal delta. Without sufficiently high tidal flow velocities, these areas do not receive sediment. Waves, particularly during storms, stir up sediment on the flats and in the ebb-tidal delta. The sediment is then transported by the tide and waves currents to lower elevations, leading to erosion of the flats and the shoals of the ebb-tidal delta (De Vet, 2020). The erosion and sedimentation mechanisms driven by waves and tides naturally develop toward a balance between these processes (Bosboom & Stive, 2021).

While hydrodynamic forcing shapes the tidal elements, the tidal elements also influence the hydrodynamic forcing. For example, if a storm enlarges an inlet, the flow velocities within the inlet decrease because the same volume of water flows through a larger opening. This reduction in flow velocity results in sedimentation, gradually filling the inlet. Sedimentation will continue until the flow velocities increase again, at which point erosion will begin to reopen the inlet channel. This process demonstrates how a tidal basin moves toward a balance between hydrodynamic forcing and the morphological response, also referred to as equilibrium (Bosboom & Stive, 2021).

In the long term, tides and waves exert a mean forcing, driving a tidal basin towards an equilibrium state. However, these waves and tides are influenced by climate change and human activities. For instance, SLR is a long-term trend that affects the equilibrium state of tidal basins like the Eastern Scheldt. An example of human interventions are the construction of barriers and dams, which alter the hydrodynamic forcing over time (Bosboom & Stive, 2021). The OSK is a perfect example of such an alteration. By reducing the inlet, the tidal prism in the Eastern Scheldt has decreased, influencing the equilibrium state toward which the basin is moving.

The changes that influence the development of the Eastern Scheldt are further elaborated below.

2.3 Development of the Eastern Scheldt

2.3.1 Historical development Eastern Scheldt till 1986

To predict future development of the Eastern Scheldt, it is useful to examine past developments. Major events with a large impact on the Eastern Scheldt were the St. Felix Flood in 1530, followed by the All Saints' Flood in 1532. Due to these floods the area called South Beveland (the south-eastern part of the Eastern Scheldt) remained submerged. South Beveland has an impermeable clay layer that is resistant to erosion, which has helped this area retain a relatively shallow depth. The inundation of South Beveland increased the tidal prism and created a larger, erosion-resistant intertidal area, which enhanced ebb dominance (Eelkema, 2013). This ebb dominance and the increase of the tidal prism led to erosion in the Zijpe channel. The Zijpe channel, located in the northern part of the Eastern Scheldt, connects the Eastern Scheldt with the Grevelingen estuary. As the Zijpe channel eroded, the tidal prism increased, shifting the tidal divide between the Grevelingen and the Eastern Scheldt further into the Grevelingen. This shift in the tidal divide further increased the tidal prism of the Eastern Scheldt towards the erosion of the Zijpe channel in a positive feedback loop (van den Berg, 1986).

In Figure 2.4, the Zijpe channel is visible, though still much smaller than just before the Delta Works were implemented. The Zijpe channel continued to erode after 1817, further increasing the tidal prism of the Eastern Scheldt into the Volkerak. This figure also shows that the Eastern Scheldt was still connected to the Western Scheldt. This connection was cut off by a railway embankment in 1871 (Geurts van Kessel et al., 2003).

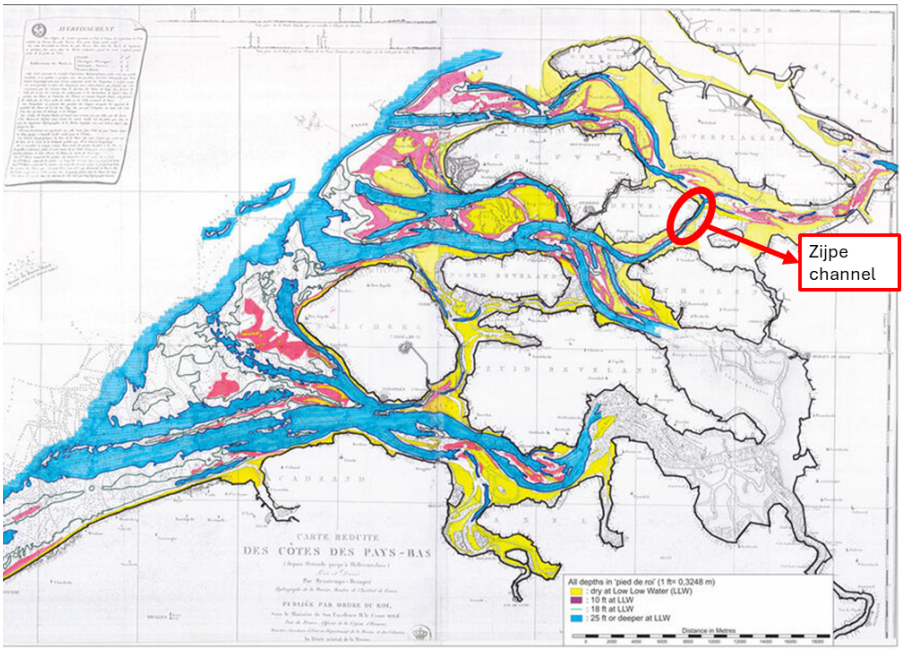

Figure 2.4: Bathymetry map of the Eastern Scheldt in 1817 (Elias et al., 2017)

The next major event was the North Sea Flood of 1953 and the subsequent Delta Plan. In 1961, the Veere inlet was closed off (see Figure 2.1 for location), which did not have a large impact on the Eastern Scheldt. The Grevelingen Dam was completed in 1965 and had also little influence on the Eastern Scheldt because it was built near the tidal divide. The dam with a more significant impact was the Volkerakdam, completed in 1967 (de Bok, 2001). By building this dam, the basin area was enlarged, leading to a 7% increase in the tidal prism (see also Figure 2.5). In the northern branch, the local tidal prism increased by 17%. This increase in the tidal prism led to channel erosion. The eroded sediment from the channels was partly exported to the ebb-tidal delta. It is estimated that, prior to the OSK, the Eastern Scheldt exported approximately $1.5 * 10^6\,m^3$/year of sediment through the ebb-tidal delta (Eelkema, 2013).

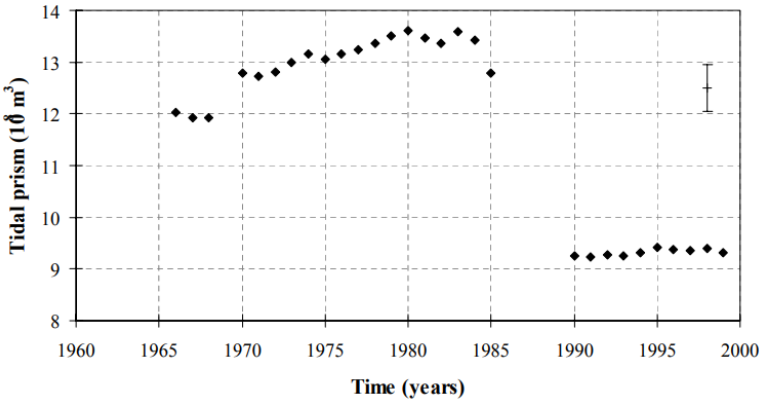

Figure 2.5: Trend of the tidal prism in the Eastern Scheldt from 1965 till 2000 calculated by de Bok (2001)

2.3.2 Impact of the storm surge barrier on the Eastern Scheldt

Due to the implementation of the OSK the tidal range and the tidal prism decreased and the sediment exchange between the basin and ebb-tidal delta (Huisman & Luijendijk, 2009) is blocked. In Table 2.1 an overview is given of the hydraulic changes in the Eastern Scheldt due to the delta works (Geurts van Kessel, 2004).

It was predicted that the tidal range would decrease. For this reason, the Philipsdam and the Oesterdam were built to maintain flat area, also know as the back barrier dams, for location of these dams see Figure 2.1. These dams reduce the basin area, which leads to tidal amplification in the Eastern Scheldt, resulting in a higher tidal range in the basin than would occur without these back-barrier dams (Rijkswaterstaat, 2024a). However, the tidal range is still smaller than before all deltaworks.

Table 2.1: Hydrodynamics and morphodynamic conditions before and after the Delta works (Geurts van Kessel, 2004).

	Before Delta works	After Delta works in 2004
Total basin area (km^2)	452	351
Average tidal range (m)	3.70	3.25
Cross-section tidal inlet channel (m^2)	80 000	17900
Maximum water velocity (m/s)	1.5	1.0
Residence time of water (days)	$5-25$ (west) $75-100$ (east)	$10-50$ (west) $150-200$ (east)
Mean tidal volume $(10^6 m^3)$	1230	880
Fresh water flow by rivers (m^3/s)	$50-100$	10
Salt concentration $(\%Cl^-)$	16.9(west) 15.4(east)	17.1 (west) 16.7(east)

The effect of the reduced tidal prism on the Eastern Scheldt is referred to as the sand demand of the channels. The cross-section of the channels in the current situation are too large for the amount of water that flows through them. In other words, the channels are not in equilibrium with the volume of water they convey. The tidal prism has been reduced by 30% which implies that the channels should also decrease in size by 30% to establish a new equilibrium. The channels need 400–600 million m^3 sediment is to establish an equilibrium (Kohsiek et al., 1987). For comparison, the Sand Motor, constructed on the Dutch coast, has a volume of 21.5 million m^3 of sand (Rijkswaterstaat, 2024b). Due to these large channels the tidal velocity in the Eastern Scheldt is reduced, see Table 2.1. Consequently, sediment transport by tides is reduced. Tidal-induced sediment

transport is responsible for the accretion of flats. In contrast, waves are the primary drivers of tidal flat erosion (De Vet, 2020). In storm condition waves stir up the sediments and transport it into the channels. With a decrease in accretion and the eroding mechanism still present, the flats are since the construction of the Delta works eroding. See Figure 2.6 for the erosion trend on the flats in the Eastern Scheldt. In this figure it is visible that the height (h), Area (A) and volume (V) of the flats is decreased after the completion of the OSK and back-barrier dams.

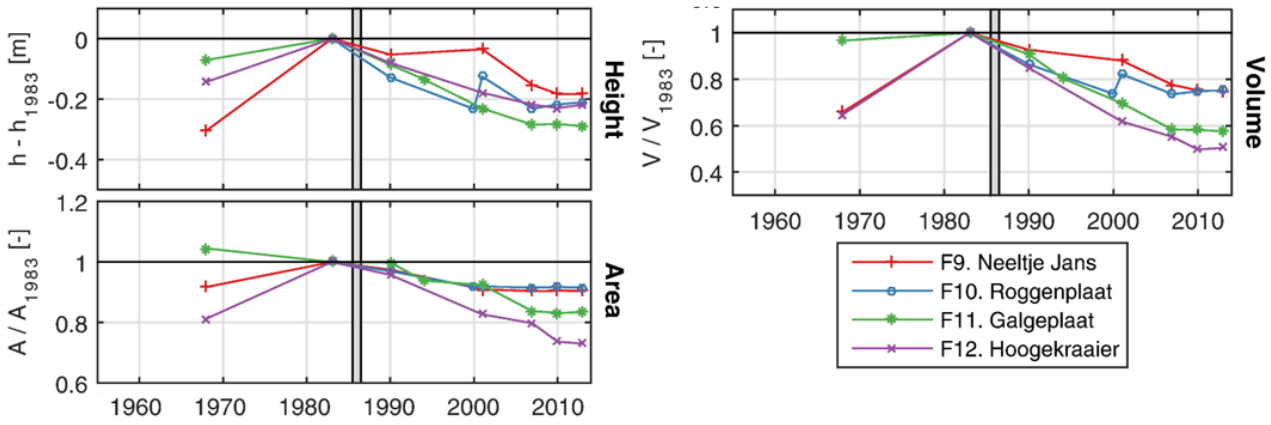

Figure 2.6: Development of the flats in height (h), area (A), and volume (v) in the Eastern Scheldt from 1960 to 2010, represented by the colored lines. The vertical grey line marks the completion of the OSK and the back-barrier dams (De Vet, 2020).

A study by Eelkema (2013) states that the ebb-tidal delta is also influenced by the implementation of the OSK. Due to the reduction of the tidal prism the ebb-tidal delta moves to a smaller equilibrium volume. The reduction of the tidal prism and the reduced tidal flow velocities lead to the same effect on the ebb-tidal delta as on the flats. In Figure 2.7, it is visible that the volume of the ebb-tidal delta above -10 is decreasing, while the sediment volume below -10 m is increasing. This indicates that sediment on the ebb-tidal delta is being transported from higher elevations to lower elevations.

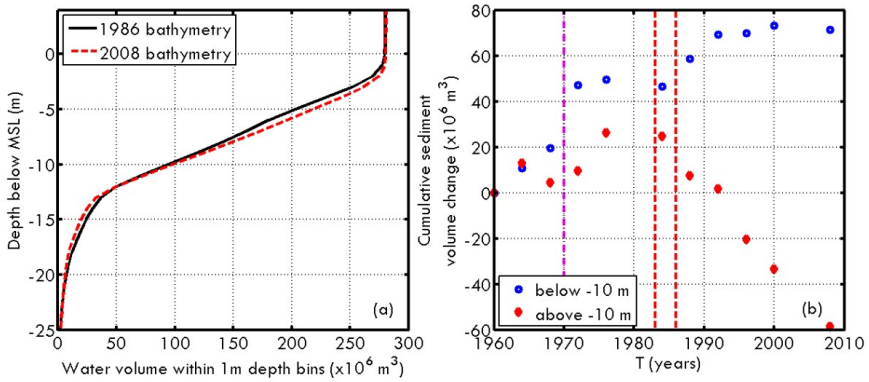

Figure 2.7: (a) Hypsometric curves of 1984 and 2008 of the ebb-tidal delta. (b) Cumulative sediment volume changes above (in red) and below (in blue) -10 m NAP on the ebb-tidal delta. Negative change means erosion (Eelkema, 2013)

What should be noted when looking at Figure 2.7 is that calculating volume differences involves subtracting bathymetry data from one another. However, small measurement errors in these data can cause significant inaccuracies over large spatial scales. For instance, a systematic error of just 1 cm across 100 km^2 results in a sediment volume error of 1 Mm^3, which is comparable to the natural variability. Despite this, thorough research by Eelkema (2013) concludes that the ebb-tidal delta was and is losing sediment at higher elevations.

The channels inside the basin face a similar issue concerning small measurement errors. Changes in channel cross-section are based on the assumption that only sediment from the flats enters the channels, as the OSK largely blocks all other sediment exchange. Consequently, the cross-section of the channels is decreasing since the implementation of the OSK and follows the same trend as the flats (de Vet et al., 2024).

2.3.3 Future prediction Eastern Scheldt

It is expected that the erosion trend of the flats will continue in the following years. However it is hard to determine the speed of this erosion trend. Apart from the issue of the channel 'demanding' sediment from the flats, SLR will enhance the erosion of the flats, by drowning them. From 0.5 meters of sea-level rise, the extent of these areas decreases significantly. With a rise of 1 meter or more, most of these areas will disappear, which means the current ecological functions, such as habitats for birds and other wildlife, will be heavily impacted (Zandvoort et al., 2019). Figure 2.8 presents a projection based on a SLR of 60 cm by 2100. In this scenario a large part of the flats will disappear and all current flat areas will have a shorter exposure time than now.

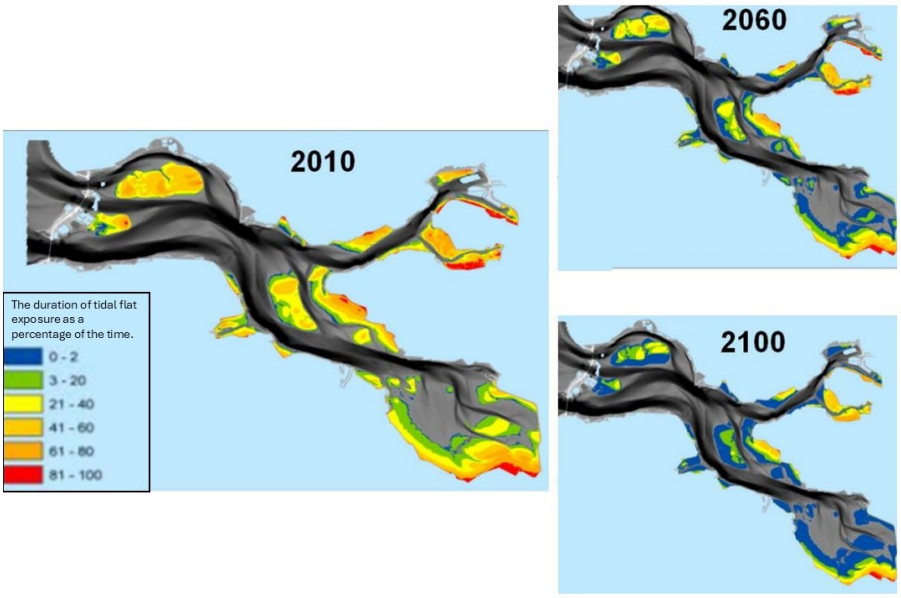

Figure 2.8: Prediction of the flats area and exposure time in 2060 and 2100 by a SLR of 60 cm in 2100 (de Ronde et al., 2013)

Research by de Vet et al. (2024) shows that the channels in the Eastern Scheldt will continue to 'demand' sediment from the flats. As a result of tidal flat erosion, the cross-sections of the channels will decrease in size and move to their equilibrium volume. Increasing SLR and the erosion of the flats will increase the tidal prism. This larger tidal prism will bring the channels closer to their equilibrium, reducing the sand demand of the channels. However, it is expected that if the sand demand of the channels is reduced to zero, the flats will already have drowned due to SLR.

Study by Eelkema (2013) shows that the measured trends of erosion at the shoals of the ebb-tidal delta have not yet shown signs of stabilizing. In the future, the ebb-tidal delta is expected to become smoother, with reduced depth differences between the shoals and channels. However, it remains unclear at what point in time or at what bed elevation the shoals will stop losing sediment. The primary gap in understanding lies in identifying the specific balance between wave and tidal forces required to make this prediction with a process based model.

2.4 Current and potential strategies for the Eastern Scheldt

2.4.1 Current strategies

Sand nourishment on the flats are the preferred strategy for now (Escaravage et al., 2024). In this method, sand from the Eastern Scheldt is sprayed onto the flats. This must be done directly on the flats, as otherwise the sediment would not end up in the right place. Using sediment from the Eastern Scheldt has the advantage of less disruption to the system, as the grain size of the sediment remains consistent. The nourishment process is labor-intensive due to tidal differences but so far this method appears to be effective. The benthos that are being buried by the sand nourishment can recover within a few years (Walles et al., 2021). These benthos are important for birds to forage. It remains necessary to monitor the nourishment's, as these are dynamic.

A report by Zandvoort et al. (2019) states that while the current approach to restoring the flats is effective, it does not offer a long-term solution if SLR exceeds 1 cm/year. Under such conditions, nourishment's would need to be applied more frequently, potentially preventing benthic species from adapting to the repeated burial. This will probably result in areas becoming unsuitable for birds to forage. If the SLR exceeeds 1 meter in 2100, it is expected that between 2070 and 2100 nourishment are not effective anymore at preserving the flats.

2.4.2 Potential measures in the Eastern Scheldt

The concept of sand demand in the channels and the erosion of the flats has been known for about 40 years. Much research has been done on the concept, the rate of erosion, and proposals to counteract the erosion of flats. Baptist et al. (2007) analyzed the entire southwest delta of the Netherlands, focusing on regaining dynamic conditions and restoring salt gradients to improve ecological values. This report did not investigate the removal of the OSK but instead considered removing compartment dams, such as the Philipsdam, creating inlets in seaside dams, or converting them into storm surge barriers. For this thesis, an important finding of that report is that removing compartment dams without removing the OSK negatively affects the flats, due to the tidal range decrease.

Van Der Cam (2021) also investigated whether infilling channels could support shoal buildup, concluding that accretion rates of 2% are helpful, but direct nourishment on the shoals are far more effective (Van Der Cam, 2021). Another suggestion was to decrease the barrier's friction by adjusting sluice gate openings, which would increase a little the tidal prism and reduce sand demand—beneficial for flats—but this option was costly and insufficient (Van Maldegem, 2004). De Bruijn (2012) investigated an extra inlet channel through Neeltje Jans, which would increase the tidal prism and flow velocities, bringing the system closer to morphodynamic equilibrium. However, most channels would remain oversized for the tidal volume, and sediment transport through the barrier would still be blocked, hindering sediment exchange.

The best option for restoring morphodynamic equilibrium remains the removal of the OSK. De Pater (2012) investigated the hydrodynamic response, concluding that removing the OSK would indeed increase the tidal prism, tidal range, and velocities, which could enhance shoal buildup. A study by Wisse (2022) used the process-based model Delft3D to study the long-term morphological development of the Eastern Scheldt without the OSK. However, this research encountered the same challenge as Eelkema (2013) on his research on the ebb-tidal delta, namely, the difficulty in accurately reproducing the balance between wave-driven and tide-driven sediment transports. As a result, there is still no reliable estimation of the long-term morphological development of the Eastern Scheldt.

2.5 Equilibrium relations for tidal elements

As explained in Section 2.2, a tidal basin develops toward a state of equilibrium in which it is in balance with the hydrodynamic forces such as waves, tides, and currents. Coastal engineers have used this equilibrium state to develop equilibrium relations by observing patterns in tidal basins worldwide (Bosboom & Stive, 2021). These equilibrium relations enable long-term morphological predictions, which is also the goal of this research. A process-based approach to the long-term morphological development of the Eastern Scheldt has already been investigated by Wisse (2022), as discussed in Section 2.4.2. Therefore, this research can use an alternative approach by focusing on the equilibrium concept. This section of the literature review describes equilibrium relations for the flats, channels, and ebb-tidal delta that are relevant to the Eastern Scheldt.

Equilibrium volume of the flats For determining the equilibrium volume of the flats the total basin area is an important factor. Renger and Partenscky (1980) found the relation between the tidal flat area to the tidal basin area, see Equation (1). Multiplying the tidal flat area with the flat height, leads to the equilibrium volume of the flats. A study by E. Eysink and Biegel (1992) found a relationship for the average level of flats above MLW and relative to the tidal range in the Wadden Sea. The definition for the average flat height is visible in Figure 2.9 and the relations presented in Equation (2). This relationship is also illustrated in Figure 2.10, where a significant spread in the data points is visible. This variability arises from the challenges of determining an average level for all flats within a tidal basin. Variations in tidal range and wave impact across the basin result in inconsistent water levels, making it difficult to calculate an accurate average flat level and causing the observed spread in the data points. Despite this variability, the relationship has been used in research on the Wadden Sea, including by (Q. J. Lodder et al., 2019). By multiplying the relative tidal flat height with the tidal flat area and tidal range, an equation for determining the tidal flat equilibrium volume is derived, as shown in Equation (3).

$$A_{f,eq} = A_b - 2.5 \times 10^{-5} * A_b^{1.5} \tag{1}$$

$$\alpha_{f,eq} = 0.41 - 0.24 \times 10^{-9} * A_b \tag{2}$$

$$V_{f,eq} = A_{f,eq} * H * \alpha_{f,eq} \tag{3}$$

Where:

$V_{f,eq}$	: equilibrium volume flats	$[m^3]$
$A_{f,eq}$	: equilibrium area of the flats	$[m^2]$
A_b	: total basin area	$[m^2]$
$\alpha_{f,eq}$	: average level of flats above MLW and relative to H	$[-]$
H	: tidal range	$[m]$

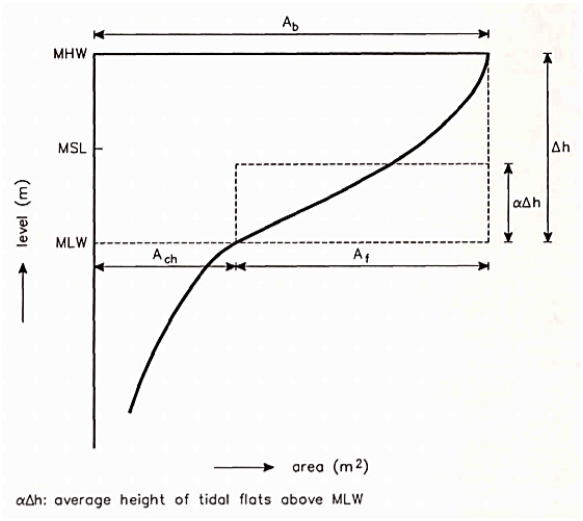

Figure 2.9: Definition for the average height of flats above MLW (E. Eysink & Biegel, 1992)

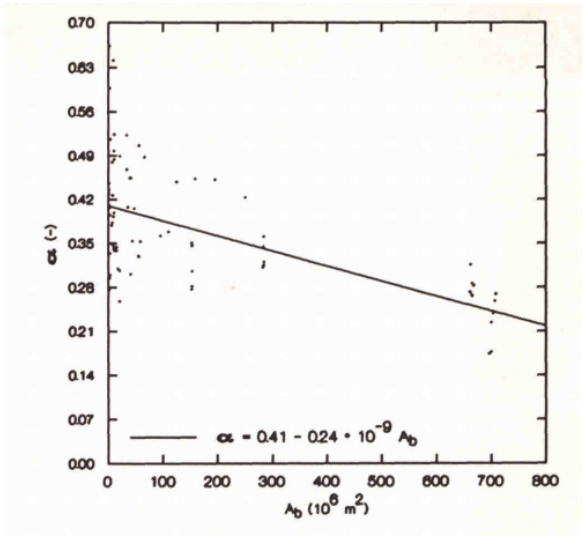

Figure 2.10: Relation for the average height of the flats above MLW in the Wadden Sea (E. Eysink & Biegel, 1992)

Equilibrium volume of the channels Research by W. D. Eysink (1991) established a relationship between the tidal prism and volume of channels. This equation is based on the observation that, along a channel, the local cross-section is directly proportional to the volume of water flowing through this cross-section. Integrating this relationship along the entire channel results in Equation (4). The empirical coefficient for the Eastern Scheldt is $\alpha_c = 73$ to $80 \times 10^{-6} m^{-3/2}$ and is derived from data on various sections of the Eastern Scheldt in 1959 and 1972 (W. D. Eysink, 1991). It is important to note that in this research, the channel volume is defined as the volume below MSL, rather than below MLW as shown in Figure 2.3.

$$V_{c,eq} = \alpha_c * P^{1.5} \tag{4}$$

Where:

$V_{c,eq}$: equilibrium volume of channels	$[m^3]$
P : tidal prism	$[m^3]$
α_c : empirical coefficient channels	$[m^{-3/2}]$

Equilibrium volume of the ebb-tidal delta Walton and Adams (1976) found relation for the volume of sand stored in the ebb-tidal delta, see Equation (5). These relations indicate that the ebb-tidal delta volume is larger for mildly exposed coasts than for highly exposed coasts. In other words, higher wave influence leads to a smaller ebb-tidal delta. To calculate the volume of sand in the ebb-tidal delta, first, an theoretically undisturbed coast should be constructed. This is done by selecting on both sides of the ebb-tidal delta an area where the ebb-tidal delta no longer has any influence on the bed level. Based on these depth lines, a reference coast is constructed. Then, the volume of the ebb-tidal delta is determined relative to the reference coast. The volume of sand is determined (which is above the reference coast), and the volume of the channels is determined (which is below the reference coast). The difference between these volumes is the volume of the ebb-tidal delta. These relations in Equation (5) are based on multiple ebb-tidal deltas along the American coast. The ebb-tidal dDeltas in the Wadden Sea also follow these relations (E. Eysink & Biegel, 1992).

$$\begin{array}{lll} \text{Highly exposed coasts} & \mathrm{V_{od,eq}} = 5.33 \times 10^{-3} \mathrm{P}^{1.23} & \text{, for } \mathrm{H^2T^2} > 28 \\ \text{Moderately exposed coasts} & \mathrm{V_{od,eq}} = 6.44 \times 10^{-3} \mathrm{P}^{1.23} & \text{, for } 2.8 < \mathrm{H^2T^2} < 28 \\ \text{Mildly exposed coasts} & \mathrm{V_{od,eq}} = 8.46 \times 10^{-3} \mathrm{P}^{1.23} & \text{, for } \mathrm{H^2T^2} < 2.8 \\ \text{All inlets} & \mathrm{V_{od,eq}} = 6.56 \times 10^{-3} \mathrm{P}^{1.23} & \end{array} \tag{5}$$

Where:

$V_{od,eq}$: equilibrium volume of ebb-tidal delta	$[m^3]$
P : tidal prism	$[m^3]$
H : significant wave height at the nearshore zone	$[m]$
T : significant wave period at the nearshore zone	$[s]$

2.6 Conclusion Literature review

In the past, the Eastern Scheldt could naturally developed towards an equilibrium state, where the flats were more balanced with the processes of erosion and sedimentation. Now this process has been disrupted by the construction of the OSK and the back-barrier dams. The OSK blocks sediment exchange between the channels and the ebb-tidal delta and has reduced the tidal prism resulting in the channels 'demanding' sediment from the tidal flats. This leads to erosion of the flats. These flats are critical for the ecosystem, supporting migrating birds that forage there, and play a crucial role in wave attenuation, reducing the wave load on dikes. Additionally, the ebb-tidal delta is becoming flatter, with sediment being transported from higher to lower elevations. Currently, the flats are maintained through sediment nourishment, but this approach is unsustainable when SLR increases. Several future scenarios have been explored to counteract the erosion of the flats. Removing the OSK is considered a potential solution because it addresses the root cause of the problem. Research suggest that the hydrodynamic changes resulting from the removal of the OSK could potentially restore the tidal flats. Other research highlight the challenges of using process-based models to accurately simulate the development the ebb-tidal delta and the flats for future scenarios. As a result, there is still no prediction for the long-term morphological response of the Eastern Scheldt with and without the OSK.

3 Methodology

3.1 Rationale and Overview of the Methodology

As described in Chapter 1, the goal of this research is to predict the morphological development of the Eastern Scheldt in a scenario that the OSK is removed, with a focus on the flats due to their ecological value. However, from the literature review (Section 2.2), it is known that sediment is transported between the flats, channels, and ebb-tidal delta. Therefore, the development of the flats is inherently linked to the development of the other tidal elements of the Eastern Scheldt. For this reason, the long-term morphological prediction also includes the development of the channels and ebb-tidal delta of the Eastern Scheldt.

From Section 2.4.1 it is known that challenges arise when using process-based models, such as Delft3D, to predict long-term morphological changes in the Eastern Scheldt. These models face difficulties in balancing wave erosion and tidal sedimentation on the flats and the ebb-tidal delta for long-term predictions in the Eastern Scheldt. To address these challenges, this research adopts the equilibrium concept for tidal basins, which states that a tidal basin develops toward a state in which the hydraulic forcing of waves, tides, and currents are balanced. This approach predicts aggregated volumes of the flats, channels, and ebb-tidal delta without providing spatial or depth-specific details. This long-term morphological prediction is divided into two parts.

In the first part the measured volumes of the flats, channels, and ebb-tidal delta are compared to equilibrium volumes, which are calculated using empirical equations from the literature, see Section 2.5. These equilibrium volumes represent the state toward the tidal basin should be moving. The comparison between the measured data and the equilibrium state provides an indication of whether the equilibrium volumes align with the observed data. Next, equilibrium volumes for the scenario without the OSK are calculated, offering insights into the volumes of the flats, channels and ebb-tidal delta of the Eastern Scheldt is likely to develop towards without the OSK. This analysis addresses sub-research question 2 and is referred to as the Data Analysis. Further details on this part including the data processing and comparison can be found in 3.2.

In the second part of the methodology the numerical model ASMITA is used. Since the calculation of equilibrium volumes and their comparison with historical and current volumes only provides a snapshot of the present situation and the final equilibrium state, predicting changes under dynamic factors such as SLR requires computational models. ASMITA is developed specifically for tidal basins and also employs the equilibrium concept, thereby avoiding the complexity of balancing wave erosion and tidal sedimentation processes. In this model, the Eastern Scheldt is also divided into three elements: flats, channels, and the ebb-tidal delta. ASMITA calculates sediment exchange between these three elements and provides an estimation of the morphological development trend over time. This development over time addresses sub-research questions 3 and 4. The second part of the methodology is referred to as ASMITA. Details about the ASMITA model scheme, how ASMITA is used in this thesis, as well as the scenarios that are run, can be found in 3.3.

3.2 Data Analysis

Since 1964, various measurements of parts of the Eastern Scheldt have been recorded, such as depth measurements. Using these depth measurements, the measured volumes are determined and compared with the calculated equilibrium volumes. This section explains how the measured volumes are defined, which data is used, and how the comparison between the measured and equilibrium volumes is done.

3.2.1 Calculation method for volumes of flats, channels, and ebb-tidal delta

Volume of the flats The volume of the flats is defined as the volume of sediment that lays between MLW and MHW, for visualization see Figure 2.3. The MLW and MHW are not constant, but change over the same period as the tidal prism, tidal range and basin area. So when using data of 1983 a different value for the MLW and MHW should be used than when calculating the volume of the flats in 2019. An estimation for the initial volume for the flats without the OSK can be calculated using the 2019 depth measurements, combined with the expected MLW and MHW levels in the Eastern Scheldt without the OSK. It is assumed that these calculated initial volume remain unchanged until the removal of the OSK.

Volume of the channels To compare the measured volume of the channels to its equilibrium volume, they need to have the same definition. The equilibrium volume is defined as the volume of water in the Eastern Scheldt below MSL, see Section 2.5. The MSL, MLW, and MHW are influenced by SLR. However, in this thesis, when calculating the volumes the effect of SLR is excluded to observe the morphological response of the channels and flats, following the approach also taken in the research by de Vet et al. (2024).

Volume of the ebb-tidal delta The ebb-tidal delta volume is defined as the total excess sediment relative to the undisturbed bed profile. The area of the ebb-tidal delta has the same boundaries as as research on the ebb-tidal delta by Eelkema (2013) and de Bok (2001). For this area the sediment volume is calculated using the method of Walton and Adams (1976) described in Section 2.5. First an undisturbed bed profile must be constructed to calculate the ebb-tidal delta volume. However, it is not possible to apply the method described in Section 2.5 because the north side of the Eastern Scheldt is influenced by the Grevelingen Lake (formerly the Grevelingen Estuary), while the south side is affected by the Western Scheldt. These factors significantly impact the coast, making it impossible to identify an undisturbed stretch of coast on either the north or south sides of the Eastern Scheldt. As a result, the measured volume is differently defined compared to its equilibrium volume, and therefore, differences can arise between these volumes. To still define a undisturbed bed profile the Bruun-rule is used (Bruun, 1954). The Bruun rule relates water depth to the distance from the coast, with water depth increasing as one moves further off shore. The degree of steepness of the bed profile depends on the shape parameter, with a larger shape parameter resulting in a steeper profile. See Equation (6) for the Bruun-rule.

$$h = Ax^{2/3} \tag{6}$$

h : waterdepth	$[m]$
x : offshore distance x= 0 is around the mean waterline	$[m]$
A : shape parameter	$[m^{1/3}]$

The steepness of the undisturbed bed profile is adjusted so that the -20 m depth level of the undisturbed bed matches the -20 m depth level of the measured bed level. This -20 m depth level is considered the depth of closure along the Dutch coast (Bosboom & Stive, 2021). Once the undisturbed bed profile is constructed, the channel volume of the ebb-tidal delta is defined as the measured bed profile below the undisturbed bed level, while the sand volume is defined as the measured volume above the undisturbed bed level, for visualization see Figure 4.4. By subtracting the total channel volume from the total sand volume, the ebb-tidal delta volume is calculated.

3.2.2 Description and overview of the used depth measurement

For the calculation of the volumes of the flats, channel and ebb-tidal delta depth measurements of the Eastern Scheldt are used. These depth measurements originate from the Vaklodingen dataset, which is collected by Rijkswaterstaat and dates back to 1964 in the Eastern Scheldt. Rijkswaterstaat typically takes new measurements every three years, although this has been less consistent in the past. The depth values in the Vaklodingen dataset are relative to MSL and have a resolution of a 20 m x 20 m.

Data from the Vaklodingen dataset is analyzed up to 2019, as a significant sediment nourishment was carried out on the flats in the Eastern Scheldt in that year (de Vet et al., 2024). Evaluating these supplemented volumes is beyond the scope of this thesis.

Furthermore, in years when measurements were taken, coverage of the total area of the Eastern Scheldt was not complete, leaving parts of the tidal elements unmeasured. These years are therefore not suitable for volume calculations. Only datasets are used from years with complete coverage. It is also important to note that measurement errors can occur. A systematic vertical measurement error of 1 cm across 100 km^2 results in a sediment volume error of 1 million m^3, which is comparable to the natural variability in the volume of tidal elements (Eelkema, 2013). These errors can influence the calculation of the channel volume and ebb-tidal delta volume. For the shallower water depths, the depth measurements also include LiDAR data from 2000, which are more precise and have smaller errors (de Vet et al., 2024). Therefore, for the flats, sediment volume errors are not significant after the year 2000. Taking into account the completeness and availability of data, the dataset used in this thesis is displayed in Figure 3.1.

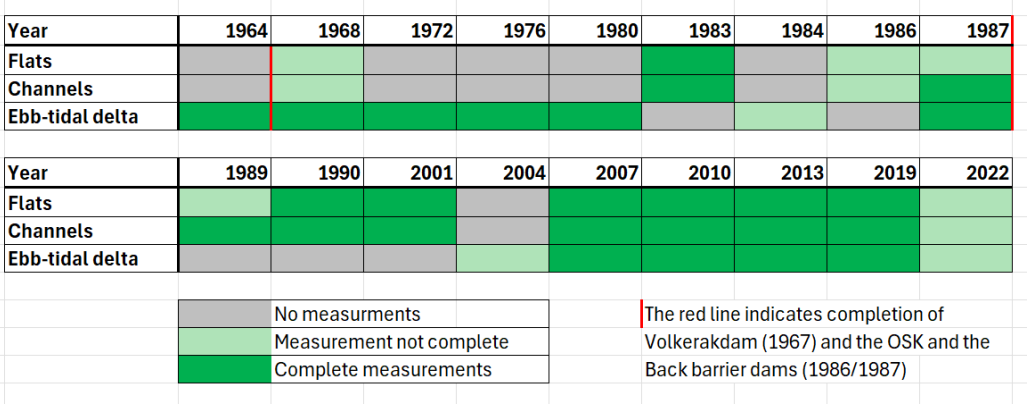

Figure 3.1: Overview of measurements which were available

It can be concluded that for the first time period (1967-1986), there is limited data available, with only one complete measurement for the channels and flats, while more measurements are available for the ebb-tidal delta.

3.2.3 Calculation of the equilibrium volumes with their time period

The relations used to calculate the equilibrium volumes are described in Section 2.5. The equilibrium volume of the flats depends on the basin area and the tidal range. The relation for the flats is based on observations from the Wadden Sea, but the Wadden Sea tidal basin has different characteristics, such as geometry and sediment particle sizes, compared to the Eastern Scheldt. Since there is no specific equilibrium relation for the flats in the Eastern Scheldt, the Wadden Sea relation is used. However, this may lead to an overestimation of the flat volume, as the flats in relation to the basin area in the Wadden Sea have a larger volume than those in the Eastern Scheldt (E. Eysink & Biegel, 1992). The equilibrium volume of the channels and the ebb-tidal delta is related to the tidal prism. The equilibrium volume for the channels has been specifically defined for the Eastern Scheldt. The relation for the ebb-tidal delta is based on tidal basins along the American coast (Walton & Adams, 1976). It is expected that the Eastern Scheldt's ebb-tidal delta follows this relation as well, as the relations can be modified to account for wave energy parameters, making them more specific to the Eastern Scheldt.

Changes in the tidal prism, basin area, or tidal range directly affect the equilibrium volumes of the flats, channels, and ebb-tidal delta. Significant historical or future changes in these parameters are important for understanding the equilibrium volumes toward which each tidal element has been moving in the past and will continue to move in the future. To appropriately use the equilibrium equations, the time period during which the tidal prism, tidal range, and basin area remain fairly constant must be identified to calculate the equilibrium volumes. From literature it is know that from the year 1967 the big changes in tidal prism, basin area and tidal range in the Eastern Scheldt are due to the construction of the delta works. This thesis will not go further back in time, due to the lack of data before 1967. From 1967, three distinct time periods can be identified in which the tidal prism, tidal range, and basin area remained fairly constant. The first period spans from the construction of the Volkerakdam (1967) to the completion of the OSK and back-barrier dams (1986). The second period represents the current situation, from 1987 to the present. The third period explores a scenario in which the tidal prism and tidal range would change in the Eastern Scheldt due to removal of the OSK. For these three time periods the tidal prism, tidal range and basin area should be determined by reviewing earlier research on the Eastern Scheldt.

By having established three time period in which the tidal prism, tidal range and basin area are constant the equilibrium volumes for these time periods can be calculated. Calculating these equilibrium volumes will help answering sub-research question 2 which is about the equilibrium state of the Eastern Scheldt through time.

3.3 ASMITA

In this section, the second part of the methodology is explained. First, how the ASMITA model operates is described in Section 3.3.1. Then, the restrictions on using the ASMITA model in this thesis are outlined in Section 3.3.2, followed by the parameter definitions and model runs, as detailed in Section 3.3.3.

3.3.1 Description of the ASMITA model

In this section, a summary of the ASMITA model is provided. For a comprehensive description and further background on the ASMITA model, refer to Z. Wang and Lodder (2019), Bonenkamp (2023) or Huismans et al. (2024).

The ASMITA model describes the morphodynamics of tidal basins on an aggregated temporal and spatial scale, using the equilibrium concept. The underlying assumption of the ASMITA model is that the morphological system will always tend to develop towards its equilibrium state. This equilibrium state is defined by empirical equilibrium relations, such as described in the first part of this methodology (Z. B. Wang et al., 2018). In the ASMITA schematization, the basin is divided into three elements: the flats, the channels, and the ebb-tidal delta. These elements are defined similarly to the volume calculation and equilibrium volumes as described in Section 3.2.1. For a visualization of these elements see Figure 3.2, with the distinction that the channels are now defined as the total water volume below MLW.

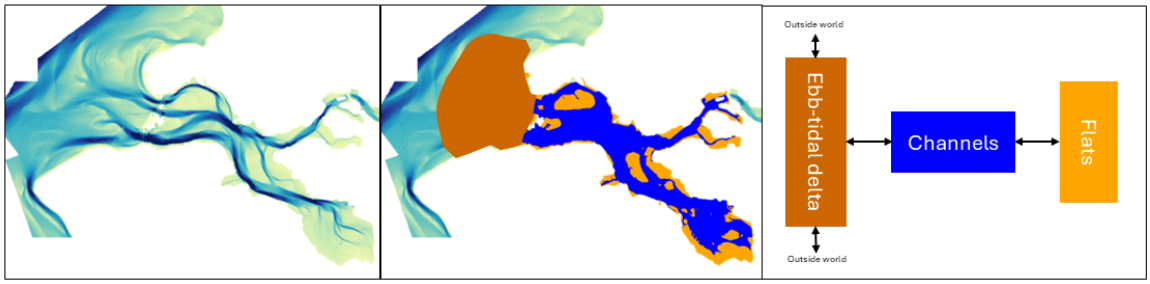

Figure 3.2: Schematization of the Eastern Scheldt used in ASMITA

The hydrodynamics in ASMITA are also schematized. Detailed information about the hydrodynamics is not required due to the high level of aggregation of the tidal elements (Z. Wang & Lodder, 2019). The following formula describes the hydrodynamics:

$$P = A_b * H - V_f \tag{7}$$

In which H is the tidal range, A_b is the area of the basin and V_f the volume of the flats. A_b and H are kept constant in this research, so the tidal prism changes due to changes in V_f. With the prescribed hydrodynamics, the equilibrium state of each element can be calculated. The equilibrium volume for flats in ASMITA follows the same formulation as in the Data Analysis, see Equation (3) in Section 2.5. For the channels, Equation (8) is used to calculate the equilibrium volume. ASMITA defines the channel volume as the water volume below MLW rather than below MSL. The channel volume has a linear relationship with the tidal prism if the basin area does not change (Z. B. Wang et al., 2024). The equilibrium volume of the ebb-tidal delta is calculated using the same relationship applied in the Data Analysis, as proposed by Walton and Adams (1976), see Equation (9). The empirical coefficients for the channels and ebb-tidal delta should be determined by identifying a volume in combination with a tidal prism where the basin was in equilibrium.

$$V_{c,eq} = \alpha_c P \tag{8}$$

$$V_{od,eq} = \alpha_{od} P^{1.23} \tag{9}$$

where:

$V_{c,eq}$: equilibrium volume of the channel, defined as the water volume below MLW [m^3]

α_c : empirical coefficient for channels [m^{-1}]

$V_{od,eq}$: equilibrium volume of the ebb-tidal delta, [m^3],
defined as the total excess sediment relative to the undisturbed bed level

α_{od} : empirical coefficient for ebb-tidal delta [$m^{-0.69}$]

P : tidal prism [m^3]

With the equilibrium state now defined, the equilibrium sediment concentration for each element can be calculated. This sediment concentration is defined as the concentration that each element would have if it were in equilibrium (Huismans et al., 2024). Formulas for semi-empirical sediment movement are employed in process-based models like Delft3D. Sediment properties that affect sediment transport in these models include flow velocity, bed shear stress, and the median sediment particle size (D_{50}). However, because ASMITA is aggregated, it does not provide complete local flow information. Instead, the element's equilibrium concentration is calculated as (Huismans et al., 2024):

$$c_e = c_E(V_e/V)^n \tag{10}$$

In this formulation V is the volume of the element, with its equilibrium value V_e and c_E is the global equilibrium concentration, which is equal to the concentration outside the system and n is a power. The ratio V_e/V reflects the flow strength in the element compared to the equilibrium state. It indicates whether the system tends toward erosion or accretion. This formulation is analogous to power-law sediment transport equations of sand or/and mud (Z. Wang & Lodder, 2019). For coarse sand particles, the Engelund-Hansen approach is used, where n equals 5. For finer sediments like mud or silt, the Partheniades-Krone formulations apply, with n equal to 3 (Bonenkamp, 2023).

To calculate the actual sediment concentration, the sediment mass balance is used. This mass balance in ASMITA is also aggregated, as shown in the resulting equation (Huismans et al., 2024):

$$\sum_{\mathrm{i}} S_i + F_b = 0 \tag{11}$$

This formula shows that the sediment flux between the bed and the water column within a tidal element, given by F_b, is equal to the sediment transport at each open boundary of the element, represented by S_i. When sediment is being carried into the flats, channels, or ebb-tidal delta, S_i is positive in this context, and F_b is positive if sedimentation takes place. (Huismans et al., 2024).

Writing this balance in more detail leads to the following formula:

$$w_s A(c_e - c) = \delta(c - c_E) \tag{12}$$

With this balance, c, the actual sediment concentration, can be calculated. The horizontal exchange rate, denoted as δ, represents the extent to which neighboring elements exchange sediment. The sediment exchange between the bed and the water column is described by the vertical exchange rate, denoted as w_s. Additionally, c_e represents the element equilibrium concentration, c_E denotes the global equilibrium concentration, and A is the plan area of the element (Bonenkamp, 2023).

To the calculate the morphological change, the volume change of each element is calculated using the sediment concentration which defines the sediment exchange between the water and the bed.

$$\frac{\mathrm{d}V}{\mathrm{d}t} = -F_b = -w_s A\,(c_e - c) \tag{13}$$

With this morphological change, the new volumes of the elements are defined and the hydrodynamics, equilibrium state, equilibrium concentration and concentration field are recalculated. These steps are then repeated. This leads to the modeling scheme visible in Figure 3.3. In this scheme, the equations explained in this section are made specific for each tidal element. The corresponding equations are denoted in the modeling scheme.

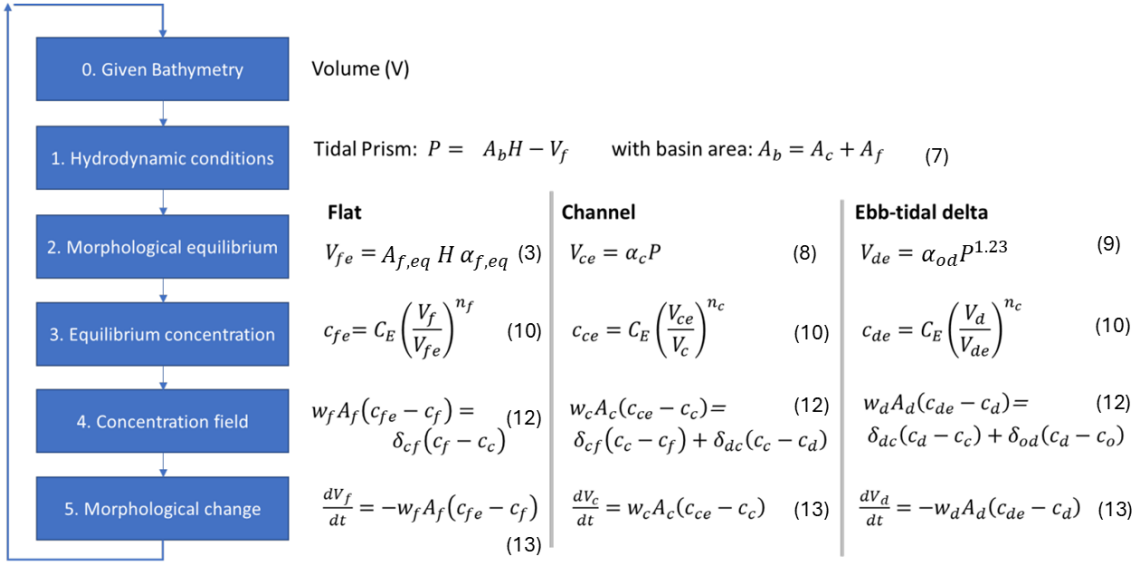

Figure 3.3: Flowchart of the computational scheme of ASMITA (Huismans et al., 2024), with the equations specified for each element. The equation numbers are indicated as (#).

Parameters of ASMITA

An overview of the ASMITA model parameters wich are mentioned in the text above is provided into three categories:

1. **Initial values**: These include the areas and starting volumes of flats, channels, and ebb-tidal deltas, as well as the tidal range.
2. **Equilibrium parameters**: These parameters define the equilibrium volumes toward which each element develops. These include the equilbrium volume of the flats V_{fe}, empirical coefficient for channels α_c and the ebb-tidal delta α_{od}. In which larger equilibrium parameters lead to a larger defined equilibrium volume.
3. **Morphological timescale parameters**: Determine the pace at which an element moves towards its equilibrium volume. These parameters include the local equilibrium sediment concentration power n, the vertical exchange coefficient w_s, the horizontal exchange coefficient δ, and the global equilibrium concentration c_E. A larger w_s, δ and c_E will lead to a faster pace of an element towards its equilibrium.

The initial values and equilibrium parameters can be determined, the morphological timescale parameters require some calibration to accurately reflect the dynamics in a tidal basin (Z. Wang & Lodder, 2019).

3.3.2 Restrictions of ASMITA for the situation in the Eastern Scheldt without the OSK

To predict the situation without the OSK, models are typically calibrated and validated based on current and past data. However, in the ASMITA model, a tidal basin is schematized into distinct elements: flats, channels, and the ebb-tidal delta. The model estimates amongs others sediment exchange between these elements to predict volume changes over time. In the current situation with the OSK, sediment exchange is limited to the flats and channels, making it effectively a two-element model. Without the OSK, the tidal basin would need to be schematized into three elements—the flats, channels, and ebb-tidal delta—because sediment exchange between all three components would then occur. This fundamental difference means that the two scenarios cannot be directly compared. Before the construction of the OSK, the Eastern Scheldt should also be schematized into 3-element, but limited data is available for calibration from that time. Consequently, the parameters for the ebb-tidal delta can not be validated. For the current situation, the two-element model can be used to validate the parameters linked to the flats and the channels in the three-element model. However, in this research, the

two-element model was not successfully calibrated. This was primarily due to the difficulty in determining a value for the equilibrium volume of the flats in the current situation. More information on why this is challenging can be found in Section 5.1. The consequence for the scenario of interest in this thesis—modeling the situation without the OSK—is that the 3-element model is not calibrated. As a result, the output of the model should be considered as a likely result, where the trends are not a precise quantitative prediction, but rather an indication of the general trend.

The ASMITA model used in this research has a constant tidal range during simulations. This is a key parameter, as it defines the tidal prism, which is used to calculate the equilibrium volumes of the channels and ebb-tidal delta. The tidal range also plays a role in calculating the equilibrium volume of the flats and the volume of both the flats and the channels. However, in reality, the tidal range changes due to morphological changes and SLR (Z. B. Wang et al., 2024). It is predicted that SLR could lead to an increase in the tidal range in the current situation (Jiang et al., 2020), whether this is also the case in the situation without the OSK is unknown. For that reason the tidal range is kept constant, however this means that this assumption limits the model's ability to reflect real-world dynamics, particularly those influenced by SLR. The consequence is that the output of the model should be considered as a indication of the general trend, rather than a precise quantitative prediction. For more discussion on the tidal range see Section 5.2.4

3.3.3 Choice of model parameters and model runs of ASMITA

This section explains how the parameters required to run ASMITA are defined in the absence of calibration. Followed by the definitions for the different scenarios which are used in the model runs of ASMITA.

The initial parameters are defined based the depth measurements of 2019 and the assumption that bed level does not change till the OSK is removed. For the sea level rise rate a constant value of 2.3 mm/year is used which is based on the rate observed over the last 50 years along the dutch coast (Overbeek & van Dorland, 2023).

The equilibrium volume of the flats, used as input in ASMITA, is calculated using Equation (3) (see Section 2.5). Since no specific relation exists for flats in the Eastern Scheldt, the applied relation is based on flats in the Wadden Sea. This could result in an overestimation of the equilibrium volume because, on average, flats in the Wadden Sea in relation to their basin area are larger (E. Eysink & Biegel, 1992). To assess whether this overestimation influences the results, a sensitivity analysis is conducted on the equilibrium volume of the flats. The empirical equilibrium parameters α_c and α_{od} are based on the assumption that the Eastern Scheldt was in equilibrium before the construction of the OSK. The empirical equilibrium coefficient α_{od} is based on the measured volume of the ebb-tidal delta. It is defined as the division of the ebb-tidal delta volume by the tidal prism raised to the power of 1.23, see Equation (9). To determine the volume of the ebb-tidal delta, the Bruun rule, as explained in Section 3.2.1, is applied. Using this rule, the undisturbed bed level is constructed, with the shape parameter A controlling the steepness of the undisturbed bed level. The shape parameter A is chosen such that the -20 m depth of the measured bed level aligns with the -20 m depth of the undisturbed bed level. Although achieving a perfect match is not possible, values of A between 0.035 and 0.040 provide a reasonable fit. A steeper undisturbed bed level (larger A) results in a larger volume for the ebb-tidal delta. This occurs because the distance between the measured bed level and the undisturbed bed level increases with a larger A, leading to a higher calculated volume. To understand the influence of the shape parameter A on the empirical coefficient α_{od}, and consequently on the development of the flats, a sensitivity analysis is conducted.

The morphological timescale parameters n and w_s have clear physical meanings and are directly related to sediment transport dynamics. The local equilibrium sediment concentration power n is determined by matching the velocity exponent used in sediment transport formulas, while the vertical exchange coefficient w_s is linked to the fall velocity of sediment particles. Since both of these parameters are based on physical principles, it is assumed in this thesis that for this reason no additional verifications are necessary.

The global equilibrium concentration (c_E) is a boundary condition in ASMITA, defining the amount of sediment available in the basin. The model which is used in this thesis has a two-fraction sediment system, consisting of fine (mud) and coarse (sand) sediments, this provides a more realistic model then using one sediment fraction (Z. Wang & Lodder, 2019). While measurements for the fine fraction are available, the coarse fraction's concentration is difficult to measure directly and is treated as a parameter with an established range based on research in the Wadden Sea. This range is also applied to the Eastern Scheldt, due to lack of data. Currently, the flats in the Eastern Scheldt contain only 1% mud (Rios-Yunes et al., 2023). In the Eastern Scheldt, no mud is found in the ebb-tidal delta (Kohsiek et al., 1987). This could be due to wave impacts preventing settlement of mud (Huismans et al., 2024). In this thesis it is assumed that after the removal of the OSK, mud will be

imported into the channels and flats. As a result, the mud fraction on the flats is expected to increase to 10%, and the global equilibrium concentration of both the fine and coarse fractions is adjusted accordingly. Because the global equilibrium concentration of the coarse fraction is purely a calibration parameter, a sensitivity analysis is also conducted to assess the influence of the 10% mud assumption on the flats.

The horizontal exchange coefficient (δ) describes the exchange between elements such as the flats and the channels. Due to the high level of aggregation in ASMITA, determining this parameter requires estimating the averaging distances between the elements. For instance, the average distance between the flats and the channels could range from 1 km to 3 km. Given this uncertainty, a sensitivity analysis is conducted to assess the minimum and maximum values of the horizontal exchange coefficient and investigate the impact on the models output.

An additional verification on the global equilibrium concentration (c_E) and horizontal exchange coefficient (δ) involves calculating the critical sea-level rise for the flats (R_c). R_c is interpreted as the threshold SLR rate above which the flats cannot keep up and will eventually drown. The critical SLR for the flats, using ASMITA parameters, is calculated based on the global equilibrium concentration, horizontal exchange coefficients, settling velocities, and the area of the tidal elements. For the full calculation, refer to Equation (24) in Appendix B.

Once R_c is calculated, it can be compared to basins with comparable areas in the Wadden Sea. In the Wadden Sea, basins with areas similar to that of the Eastern Scheldt have a critical sea-level rise for the flats ranging from 6.4 to 10 mm/year (Huismans et al., 2022). If the critical sea-level rise calculated for the Eastern Scheldt falls within this range, it provides additional evidence that the chosen parameters for δ are physically reasonable.

Model Runs ASMITA
With the ASMITA model parameters defined and sensitivity runs completed, the trends of the flats, channels, and ebb-tidal delta towards their equilibrium volumes can be visualized. This run is referred to as the reference run. However, when SLR increases or the flats have a smaller initial volume, the predicted trends are likely to change. To assess the influence of scenarios with higher SLR rates or smaller flat volumes, scenario runs are done. For scenarios with higher SLR rates, values exceeding the historical rate of 2.3 mm/year observed over the last 50 years are chosen. Similarly, to evaluate the impact of scenarios where the flat volume is smaller, reduced initial volumes of the flats are selected.

Table 3.1 gives an overview of all models runs which will be done with the ASMITA model. Details on the values of the parameters used in each run are visble in Section 4.2.

Reference scenario	Model outcome with most likely parameters
Sensitivity runs	Influence of larger and smaller horizontal exchange parameters on model outcome
Sensitivity runs	Influence of larger and smaller shape parameter of the Bruun profile on model outcome
Sensitivity runs	Influence of using smaller equilibrium volumes of the flats on the model outcome
Sensitivity runs	Influence of values of different values within the range of the global equilibrium concentration of the coarse fraction on model outcome
Scenario runs	Influence of larger SLR-rate on model outcome compared to Reference scenario
Scenario runs	Influence of smaller initial flat volume on model outcome compared to Reference scenario

Table 3.1: Overview of all model runs with ASMITA

3.4 Conclusion methodology

The methodology of this thesis first defines the MLW, MHW and tidal basin per time period with an almost constant equilibrium state. Then with these values the volumes of the flats, channels and ebb-tidal delta are determined based on depth measurements. These volumes are then compared to the equilibrium volumes of that time period, to assess if the Eastern Scheldt was, is and will be developing towards it equilibrium volumes. This answers sub-research question 2. To understand the rate at which the Eastern Scheldt develops towards equilibrium and how factors, such as SLR are influencing these trends, the numerical model ASMITA is utilized. Defining appropriate model parameters is crucial for the effective application of ASMITA, as it enables accurate prediction of trends. However, determining this parameter set is challenging because the ASMITA model used in this thesis lacks a calibration process. To derive the model parameters, a sensitivity analysis is conducted, and comparisons are made with parameters used for the Wadden Sea. Based on this analysis, the parameter set is established, and several scenarios are plotted to examine the results. The outcomes of the ASMITA simulations help answer sub-research questions 3 and 4.

4 Results

In this chapter, the results derived from the methodology outlined in Chapter 3 are presented. The results are divided into two parts: the data analysis (Section 4.1) and the outcomes from the ASMITA model (Section 4.2). The first part focuses on comparing the measured volumes with the equilibrium volumes, detailing the steps required to perform this comparison. The second part presents the results obtained from the ASMITA model, beginning with the sensitivity analysis. This is followed by the reference scenario and an exploration of the impacts of various scenarios, including SLR, on the observed trends.

4.1 Data analysis

This section aims to compare the measured volumes of the flats, channels, and ebb-tidal delta of the Eastern Scheldt with their corresponding equilibrium values. First, the hydraulic parameters required to calculate both the measured and equilibrium volumes are defined (Section 4.1.1). Next, the measured volumes are computed (Section 4.1.2), followed by the calculation of the equilibrium volumes (Section 4.1.3). Finally, the measured volumes are compared with the equilibrium volumes (Section 4.1.4).

4.1.1 Parameters defined per time period

As described in Section 3.2.2, the upcoming calculations, including the volume and ASMITA computations require model parameters. The historic dataset is divided in periods for which these parameters were approximately constant. These tree time periods are visible in Table 4.1 and determined in Section 3.2.3.

These parameters include the MLW and MHW, to determine the tidal range H and the volumes of the flats and the channels. Additionally, the basin area A_b is also needed, defined as the combined area of the flats and the channels. The MLW, MHW, and tidal range are treated as constant values for the entire Eastern Scheldt across all time periods. A constant approach ensures consistency, as spatially varying MLW and MHW values are unavailable for the future scenario (after the removal of the Eastern Scheldt barrier). Furthermore the ASMITA model also uses one constant value. Although spatially varying values exist for the present, a single constant MLW and MHW value is used for all periods to calculate the flat volumes. The basin area for each time period is determined based on using the depth measurements in the Vaklodingen dataset. The tidal prism P is derived from earlier research.

First time period: 1967-1986: Before completion of the OSK and back barrier dams
For the first time period the values of the parameters are collected from research by de Bok (2001). In this report measurements dating back to 1961 are evaluated including the calculation of the tidal prism, see Figure 2.5 and the MLW and MHW. The mean values in time and space of the MLW, MHW, and the tidal range and the mean value of the tidal prism in time for this period are shown in Table 4.1. The basin area is determined from using the depth measurements of 1983.

Second time period: 1987-2025: After completion of the OSK and back barrier dams
For the MLW and MHW values, data from De Vet (2020) is utilized. This dataset provides MLW and MHW values for the entire basin, calculated using a calibrated Delft3D model. The mean value for the basin from this dataset is used. De Vet (2020) calculated a value of 908 million m^3 for the tidal prism just after the completion of the OSK and the back barrier dams with his Delft3D model. de Bok (2001) also derived values for the MLW, MHW, and tidal prism. However, in his method, the Eastern Scheldt was divided into seven sections, whereas the Delft3D model from De Vet (2020) is considered more precise. It calculates MLW and MHW on a 20×20 meter grid, offering a higher resolution. These values for this time period are shown in Table 4.1. The area of the basin is calculated using the depth measurements for this time period.

Third time period: future scenario removal OSK
The third time period is a possible future scenario in which the OSK is removed. For this, estimations must be made for the hydraulic parameters. De Pater (2012) investigated the hydrodynamic response in the Eastern Scheldt after removing the barrier. In this research, the response was analyzed using an analytical model and a Delft3D model. In his study, the removal of the OSK refers to the removal of only the sluice gates, while the bathymetry (including the sills and scour holes) remained unchanged.

Appendix A present calculations performed using the same analytical equation as in research from De Pater (2012), but with a slightly different application. In this thesis the Eastern Scheldt is schematized by a rectangular shape and research of the De Pater (2012) schematized the Eastern Scheldt into more sections. Calculations in Appendix A indicate that removing the OSK leads to a 13% increase in the tidal prism and a 14% increase in

the tidal range at the end of the basin. The research by De Pater (2012), using his analytical method, suggests an increase in the tidal range between 10% and 20% and an increase in the tidal prism of 8%. His Delft3D model results show increases of 10-20% in the tidal range and 16% in the tidal prism without the OSK. The ratio between the MLW and MHW levels in the situation without the OSK stays approximately the same as in the current situation.

Based on these findings, this research assumes that the MLW and MHW will increase by 15% in the future scenario. Futhermore, it is assumed that the tidal prism will increase by 16% if the OSK, as estimated using Delft3D by De Pater (2012). These estimates are assumed more precise than those from the analytical model. The values from the second time period are multiplied by the corresponding percentages and presented in Table 4.1 for the future scenario. The basin area stays the same for the situation without the OSK.

		1967-1986	**1987-2025**	**future scenario: removal of OSK**
MHW	$[m]$	1.97	1.67	1.92
MLW	$[m]$	-1.71	-1.25	-1.43
Tidal range (H)	$[m]$	3.68	2.92	3.36
Tidal prism (P)	$[m^3]$	$1360 \cdot 10^6$	$908 \cdot 10^6$	$1053 \cdot 10^6$
Basin area (A_b)	$[km^2]$	402	355	355

Table 4.1: Tidal and basin parameters per time period (de Bok, 2001), (de Vet et al., 2024) and (De Pater, 2012).

4.1.2 Volume trend of the tidal elements

The volumes of the flats, channels and ebb-tidal delta are calculated using available depth measurements and the parameters from the previous section. First the volume of the flats and channels are computed, followed by the volume of the ebb-tidal delta. For more information see Section 3.2.1.

Flats and Channels In Figure 4.1, the bed level of 1983 is shown. The Eastern Scheldt area was larger than it is today because the Philipsdam and the Oesterdam had not yet been constructed, see also Figure 2.1. Within this figure the contour lines at MLW and MHW are also shown. The area in between the MLW and MHW defines the area of the flat. Note that the color visualization of the depth measurements may be misleading when determining flats and channels. Areas that have shallow depth may still be considered channels using the definition above. This can for instance be seen in the south east part where a large part of channel is quite shallow.

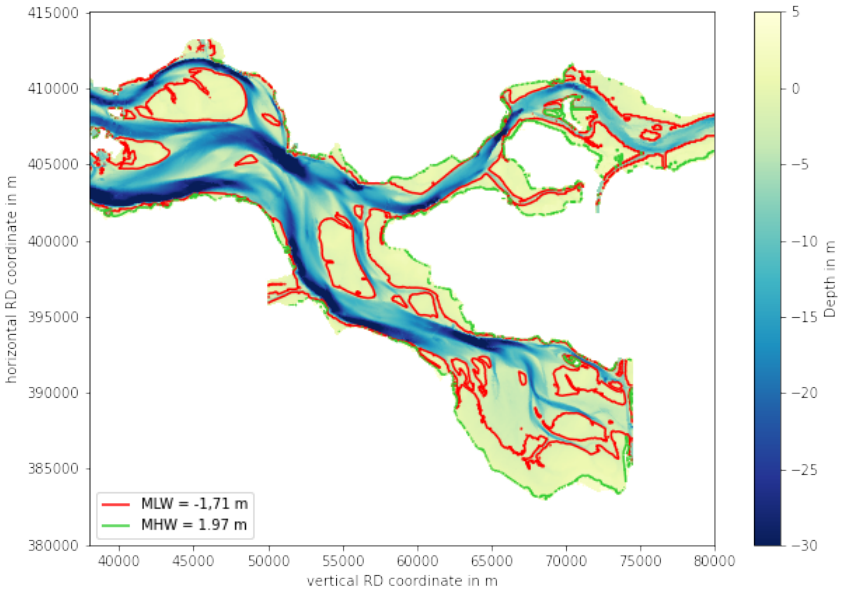

Figure 4.1: The Eastern Scheldt in 1983 with the contour lines of the MHW and MLW in red en green at that time

The sediment volume of the flats and channels are calculated using the only the complete datasets, see Figure 3.1. The sediment volumes between MLW and MHW (which are defined in Table 4.1) are calculated for the flats. For the channels the water volume below MSL is calculated. The calculated values are plotted in Figure 4.2

This figure illustates the erosion trend of the tidal flats, as explained in Section 2.3.2. However, for the channels, the expected trend of volume decrease after the completion of the OSK is not observed. This could be explained by increased measurement errors in deeper waters in the depth data, which would lead to errors in sediment volume that exhibit the same variability as the natural trend, see also Section 3.2.2. From this point onward, it is assumed that the channels experience the same decrease in volume as the flats. This assumption is justified by the observation that almost no sediment enters the basin (Huisman & Luijendijk, 2009), meaning the only way the channel volume could decrease is through the erosion of flats within the channels which is the same assumption as in research from de Vet et al. (2024). See Figure 4.2 the blue dotted line for this trend.

Figure 4.2 also shows that the flat and channel volumes were significantly larger before the completion of the OSK and the back-barrier dams than they are today. The increased channel volume can be attributed to the greater size of the basin prior to construction of the Philipsdam (one of the back-barrier dams, see Figure 2.1). This resulted in more channel area in the Eastern Scheldt, leading to an increased total channel volume. For the flats, in addition to the larger basin area, the tidal range was also higher before the completion of the OSK and back-barrier dams (see Table 4.1). This higher tidal range resulted in more sediment between the MLW and MHW boundaries. This led to a larger computed volume of the flats during that period.

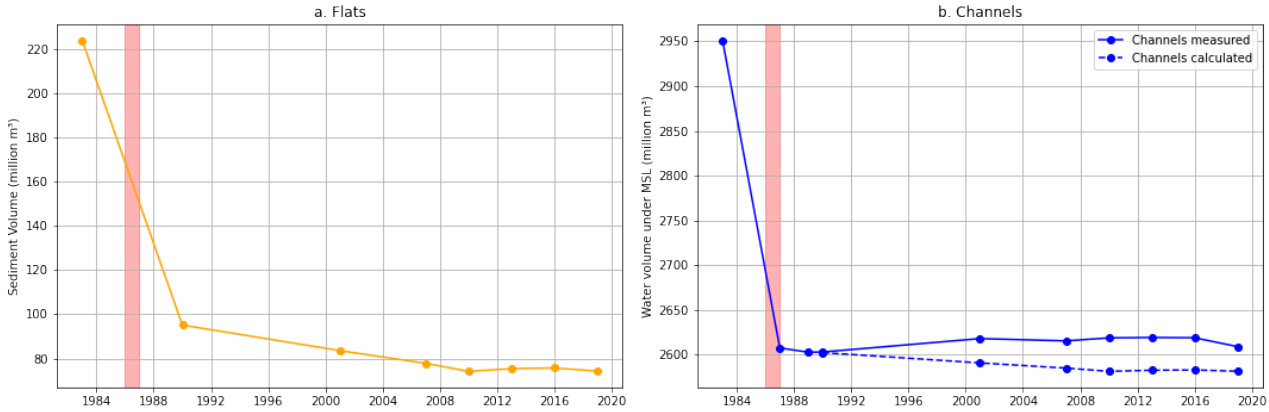

Figure 4.2: The trend of the volumes of (a) the flats and (b) channels. The calculated channels (dotted line) is based on the assumption that they lose volume as they receive sediment from the tidal flats, following a similar trend as the flats. The vertical red boxes on the background indicate completion of the OSK and the back barrier dams

Using the depth measurements, an initial volume of the flats in the situation if the OSK is removed is calculated based on the 2019 data, along with the MLW and MHW values for the situation without the OSK. The calculated volume of the flats is 91 $\cdot 10^6$ m^3.

Ebb-tidal delta

The volume of the ebb-tidal delta is calculated by first constructing an undisturbed bedlevel profile. The measured depth below this undisturbed bed level profile is classified as channels and above is classified as sand volumes. This undisturbed bed level profile is constructed with the Bruun-rule, which relates the distance from the coast to a bed level, read Section 3.2.1 for more information of the Bruun-rule. Values for shape parameter A between 0.035 and 0.040 provide a reasonable fit for aligning the -20 m depth line of the undisturbed bed profile with the -20 m depth line of the measurements. A value of $A = 0.038$, the mean of this range, is used. The shape of the undisturbed bed level,with $A = 0.038$, is shown in Figure 4.3, next to the depth measurements in 2019. This figure shows that at a depth of -20 m, the undisturbed bed profile almost aligns with the bed level in 2019, which was the goal by determining the undisturbed bed profile.

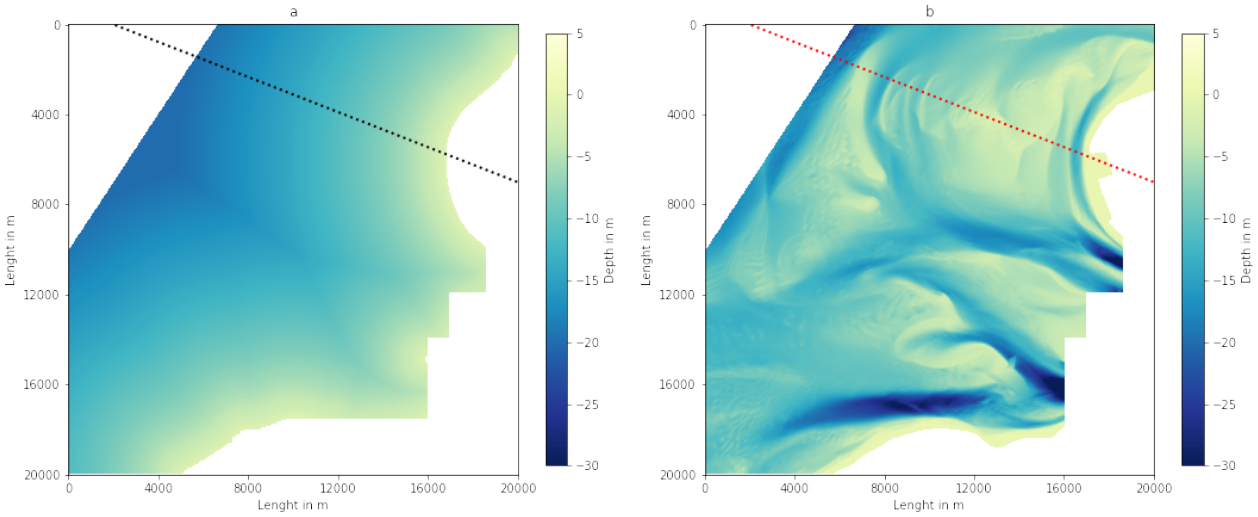

Figure 4.3: (a) The constructed undisturbed bed level with formula from bruun (b) the bed level of the ebb tidal delta in 2019. In both figures a diagonal line used in Figure 4.4 is indicated with a dotted line

Figure 4.4 shows a cross-section of the undisturbed bed profile and the bed level in 2019. The channel volume below the undisturbed bed profile is highlighted in blue, while the sand volume above the undisturbed bed profile is shown in brown. By subtracting the total channel volume from the total sand volume, the ebb-tidal delta volume is determined.

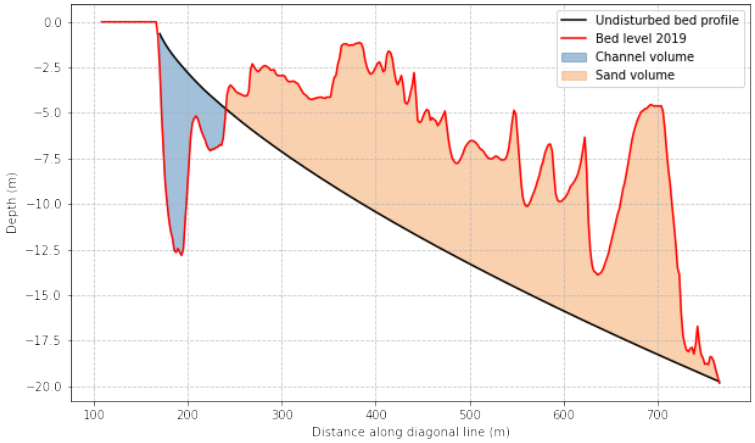

Figure 4.4: Cross-section of the undisturbed bed profile (in black) and measured bed level in 2019 (in red). In blue the channel volume is visible and in brown the sand volume. See Figure 4.3 for the location of the cross-section

With the undisturbed bed profile constructed, the volumes of the ebb-tidal delta are calculated and visualized, as shown in Figure 4.4. A comparison of the ebb-tidal delta for the first and last years of available data is shown in Figure 4.5, where the depth values are expressed relative to the undisturbed bed profile. This figure highlights that a significant portion of the sand volume is located farther from the coastline, whereas the channels are predominantly situated closer to the coast. This is because shallows further away from the shoreline contribute more to the sediment volume due to the deeper Bruun profile there.

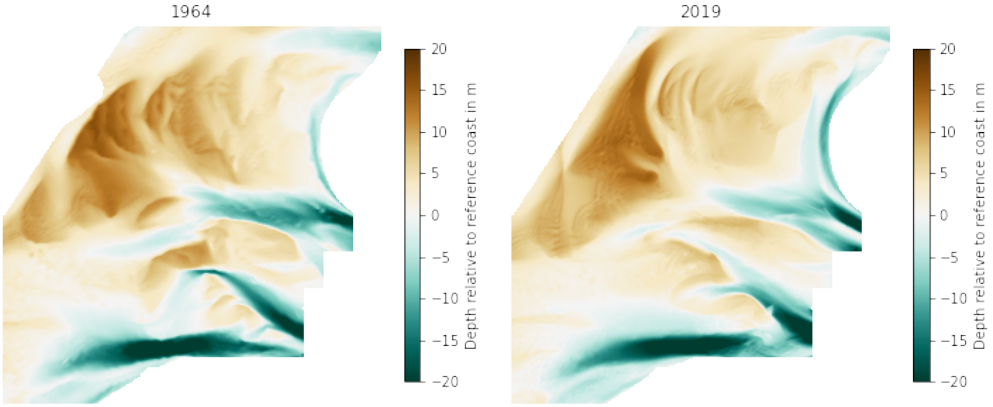

Figure 4.5: The ebb-tidal delta volumes relative to the undisturbed bed profile are shown, with the sand volume represented in brown and the channels in blue for the years 1964 and 2019.

In Figure 4.6, the trend of the cumulative volume of the ebb-tidal delta, as well as the trends of the separate volumes of the channels and sand, are visualized. This figure indicates that prior the completion of the OSK and the back barrier dams, the ebb-tidal delta was growing. After the completion of the OSK and the back-barrier dams the volume of the ebb-tidal delta is decreasing. However, the decreasing trend following the construction of the OSK and back-barrier dams is not clearly documented due to a gap of nearly 27 years in the measurement data. A study from Eelkema (2013) als concludes a decrease in volume of the ebb-tidal delta in the current situation.

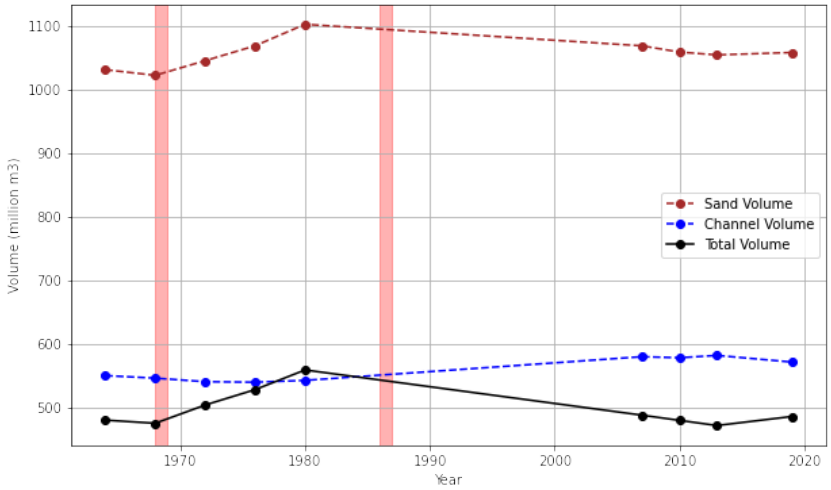

Figure 4.6: The channel volume, the sand volume and the total volume of the ebb-tidal delta per year. The vertical red boxes on the background indicate completion of the Volkerakdam and of the OSK and the back barrier dams

4.1.3 Calculation of equilibrium volumes

The equilibrium volumes of the flats, channels and ebb-tidal delta per time period are calculated using Equation (3), Equation (4) and Equation (5), which are described in Section 2.5 and Section 3.2.3.

As seen in Section 2.5 the calculations of the equilibrium volume of the ebb-tidal delta, depend on the 'level of exposure of the coast'. This classification is a function of the average wave height and wave period at the ebb-tidal delta. According to research by Eelkema (2013), the average wave height at the sea-side edge of the ebb-tidal delta is $1.1m$, with an average wave period of 4 seconds. These values yield $H^2T^2 = 19.4$ $\mathbf{m^2}$ $\mathbf{s^2}$, classifying the Eastern Scheldt ebb-tidal delta as a moderately exposed coast. Consequently, the relationship specific to moderately exposed coasts should be used to calculate the equilibrium volume of the ebb-tidal delta.

The actual calculations for the equilibrium volumes are computed using the parameters defined in Table 4.1. The result of this calculation are the equilibrium volumes of the flats, channels and ebb-tidal delta are $V_{f,eq}V_{c,eq}$ and $V_{od,eq}$ in Table 4.2.

As evident from Table 4.2, all computed equilibrium volumes for the time period before the completion of the OSK are larger than current equilibrium volumes. This is because the tidal prism, tidal range, and basin area were all greater prior to the OSK's construction. The equilibrium volumes of the channels and the ebb-tidal delta are primarily related to the tidal prism, while the equilibrium volume of the flats is influenced by both the basin area and the tidal range. Since these factors were larger before the OSK was completed, the resulting equilibrium volumes were also greater. If the OSK were to be removed, it is estimated that the tidal range and tidal prism would increase, leading to larger equilibrium volumes for the flats, channels, and ebb-tidal delta in that scenario. To see the effect of these changing equilibrium volumes on the Eastern Scheldt, an comparison with the measured volumes is made in Section 4.1.4.

	1967-1986	**1987-2025**	**future scenario: removal of OSK**
Equilibrium volume flats $[m^3]$ ($V_{f,eq}$)	$231 \cdot 10^6$	$178 \cdot 10^6$	$205 \cdot 10^6$
Equilibrium volume channels $[m^3]$ ($V_{c,eq}$)	$3660 \cdot 10^6$ to $4010 \cdot 10^6$	$1997 \cdot 10^6$ to $2189 \cdot 10^6$	$2495 \cdot 10^6$ to $2735 \cdot 10^6$
Equilibrium volume ebb-tidal delta $[m^3]$ ($V_{od,eq}$)	$1100 \cdot 10^6$	$672 \cdot 10^6$	$807 \cdot 10^6$

Table 4.2: The calculated equilibrium volumes of the flats, channels and ebb-tidal delta of the Eastern Scheldt for different time periods.

4.1.4 Comparison equilibrium volumes with measured volumes

In Figure 4.7, the equilibrium volumes from Table 4.3 are plotted alongside the measured values from Figure 4.2 and Figure 4.6. Additionally, the estimated volumes of the flats, channels, and ebb-tidal delta in the scenario where the OSK is removed are visualized as: *estimated initial volume without the OSK* in Figure 4.7. For the flats, the volume without the OSK is calculated using the 2019 depth measurements and the water levels in the situation without the OSK. The flats than have a larger volume compared to 2019, namely $91 \cdot 10^6$ m^3; see also Section 4.1.2. The volumes of the channels and ebb-tidal delta are assumed to remain the same as in 2019.

It is important to note that the equilibrium volumes, shown in Figure 4.7, were calculated for only three periods in which all hydraulic parameters were assumed to be constant. In reality, the tidal prism and tidal range constantly change due to factors such as SLR and changing bathymetry (see Section 2.2). Consequently, the equilibrium volumes would actually change as a continuous function over time with. The effect of the influence of SLR is included in the ASMIT calculations, visible in Section 4.2.

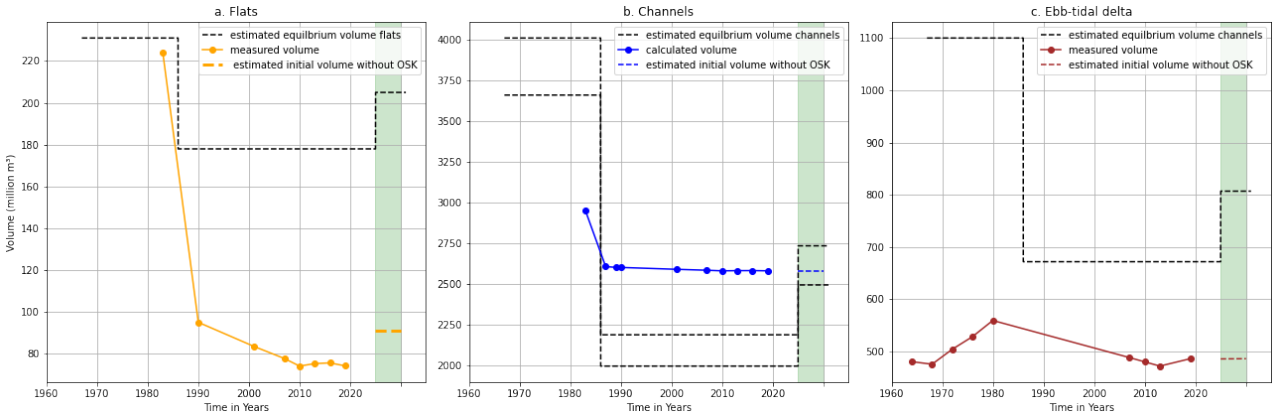

Figure 4.7: For the flats (a), channels (b), and ebb-tidal delta (c), the equilibrium volumes for each time period are shown in black. The solid colored line represents the volumes, while the dashed colored line indicates an estimation for the initial volume in the scenario without the OSK. The vertical green line marks the scenario in which the OSK is removed.

In Table 4.3, the equilibrium volumes, calculated in the previous section, are compared with the actual measured volumes. This is done for four moments in time.

- 1980/1983: Representing the period before the construction of the OSK and back-barrier dams. Measurements from both years are needed to have all necessary data.
- 1990: The first year with an available data point for the flats following the completion of the OSK and back-barrier dams.
- 2019: This year represents the most recent measurement unaffected by the influence of sediment nourishment's in the Eastern Scheldt, allowing a comparison for each tidal element.
- Future Scenario: the initial volumes for the scenario without the OSK for the flats, channels, and ebb-tidal delta are compared with their respective equilibrium volumes. For the channels and ebb-tidal delta, the initial volumes are assumed to remain the same as in 2019. For the flats, the initial volume is calculated based on the expected MLW and MHW levels without the OSK and the 2019 bed level, as detailed in Section 4.1.2.

		1980/1983: Before completion of the OSK and back barrier dams	**1990: Just after completion of the OSK and back barrier dams**	**2019: Most recent measurement without nourishments**	**future scenario: removal of OSK**
Measured volume flats V_f	$[m^3]$	224 $\cdot 10^6$ (1983)	95 $\cdot 10^6$	74 $\cdot 10^6$	91 $\cdot 10^6$ (estimated volume)
Measured volume channels V_c	$[m^3]$	2950 $\cdot 10^6$ (1983)	2602 $\cdot 10^6$	2581 $\cdot 10^6$	2581$\cdot 10^6$ (estimated volume)
Measured volume ebb-tidal delta V_{od}	$[m^3]$	560 $\cdot 10^6$ (1980)	-	486 $\cdot 10^6$	486$\cdot 10^6$ (estimated volume)
V_f difference	[%]	-3	-46	-58	-56
V_c difference	[%]	-20 to -26	+30 to +19	+29 to +18	+1 to -2
V_{od} difference	[%]	-49	-	-28	-40

Table 4.3: Comparison equilibrium volumes, visible in Table 4.2 and measured volumes with the percent difference in which minus % means that the volume measured is smaller that the equilibrium volume and plus means that the measured volume is larger than the equilibrium volume.

Insights from the comparison Table 4.3 and Figure 4.7 shows that volume of the flats before the completion of the OSK is close to its computed equilibrium volume. After the construction of the OSK and the back-barrier dams, both the equilibrium volumes and the measured volumes were expected to be smaller due to the reduced basin area and tidal range. However, the measured volume is significantly smaller than the equilibrium volume after 1986. This discrepancy could be attributed to the construction of the Philipsdam, which excluded a large portion of the flat area from the Eastern Scheldt basin. Consequently, this flat area no longer contributes to the measured flat volume. Additionally, in the current situation, the flat volume is not developing toward its equilibrium volume. This could be explained by the greater influence of the sand demand from the channels compared to the sand demand from the flats. While the flats are 'attempting' to develop toward their equilibrium volume, the channels demand more sediment, thereby preventing the flats from reaching their equilibrium volume. This explanation is further elaborated on in Section 5.1.1.

Regarding the water volume of the channels, it becomes evident in Figure 4.7 that the measured volume was smaller than its computed equilibrium volume before the completion of the OSK and the back-barrier dams. This aligns with expectations, as the channels were eroding at that time and thus developing toward a larger equilibrium volume. After the construction of the OSK and the back-barrier dams, the measured water volume in the channels is larger than the equilibrium volume, indicating that the channels 'want to develop' toward a smaller equilibrium volume and are therefore importing sediment. This align with its sand demand as described in Section 2.3.2. For the future scenario, the comparison shows that removing the OSK leads to an increase in the equilibrium volume due to the larger expected tidal prism without the OSK. This results in that a water volume in the channels is much closer to the expected equilibrium volume. A full elaboration of these results is provided in Section 5.1.2.

For all time periods, the volume of the ebb-tidal delta is much smaller than its equilibrium volume. This was not expected, possible explanations are discussed in Section 5.1.3.

4.2 ASMITA Results

In this section, the results obtained with the ASMITA model are presented. First, the parameters required for the model are derived, forming the basis for all model runs with ASMITA (Section 4.2.1). Next, a reference scenario is presented, representing a likely scenario and using the defined parameters (Section 4.2.2). The a sensitivity analysis is then conducted by varying some parameters to assess their influence (Section 4.2.3). Finally, various scenarios are explored to evaluate the impact of different SLR rates and smaller flat volumes (Section 4.2.4).

4.2.1 Parameter set ASMITA

In Table 4.4, all parameters required for the ASMITA model are listed. A brief explanation of their derivation is provided below, while the complete derivation can be found in Appendix B. The parameters defined form the base of each ASMITA run.

The initial parameters are derived from the depth measurements taken in 2019. Using this bed level, the volumes of the flats, channels, and the ebb-tidal delta are calculated, and these values are consistent with those presented in Table 4.3. However, in the ASMITA model, the water volume for the channels is defined as the volume of water below MLW, so this volume is calculated separately. The hydraulic values used in these calculations matches the one presented in Table 4.2.

The equilibrium parameters are based on the assumption that the Eastern Scheldt was in equilibrium before the construction of the OSK, derivation of the values can be found in Appendix B. For the flats the equilibrium volume calculated for the scenario without the OSK is used, see Table 4.2. To assess the influence of a smaller equilibrium volume on the model outcome, a sensitivity analysis for this parameter is conducted. The empirical equilibrium parameter for the channels α_c is defined using the assumption that the channels are in equilibrium if the tidal prism was not decreased due to the OSK and the back barrier dams with 30%, see also Section 3.3.1. The empirical coefficient for the ebb-tidal delta (α_{od}), as discussed in Section 3.3.3, is sensitive to the calculation of the ebb-tidal delta volume and thus sensitive to the shape parameter A. The value of α_{od} in Table 4.4 is calculated using the mean value of the shape parameter A.

The parameters related to the morphological timescale are derived and also visible in Table 4.4. The values for the parameters n and w_s have clear physical meanings and are directly related to sediment transport dynamics, the derivation of the values can be read in Appendix B. The global equilibrium concentration c_E of the fine fraction is based on measurements (see Appendix B), while concentrations of the coarse fraction at the edge of the ebb-tidal delta were not available for the Eastern Scheldt. However, in the Wadden Sea, concentration measurements of the coarse fraction show a range of 100 mg/L and 200 mg/L (Postma, 1961), corresponding to a global equilibrium concentration of $c_{E,\text{coarse}} = 0.5 \times 10^{-4}$ to $c_{E,\text{coarse}} = 1.3 \times 10^{-4}$. In ASMITA studies with two sediment fractions conducted by Bonenkamp (2023) and Huismans et al. (2024), the global equilibrium value was chosen in these studies as $c_{E,\text{coarse}} = 4 \times 10^{-4}$, corresponding to a concentration of 636 mg/L. In this study, a range between 0.5×10^{-4} and 4×10^{-4} is considered for the global equilibrium concentration of the coarse fraction. As explained in Section 3.3.3, the global equilibrium concentration within this range is chosen to ensure that the mud fraction on the flats is approximately 10%. This is for a value of $c_{E,\text{coarse}} = 4 \times 10^{-4}$, wich is also stated in Table 4.4. The horizontal exchange parameter δ values are also defined in this table, for the full definition see Table B.2 in Appendix B.

A constant sea level rise rate of 2.3 mm/year is used in all model runs, which is based on the rate observed over the last 50 years along the dutch coast (Overbeek & van Dorland, 2023).

As mentioned in Section 3.3.3 an additional check on the the horizontal exchange parameters (δ) and the global equilibrium concentration (c_E) is done by calculating the critical sea-level rise (R_c) for the flats using Equation (24) (see Appendix B). For the parameters values which are stated in Table 4.4 a $R_c = 4.0$ mm/year is calculated. This value is lower than the critical sea-level rise for flats in the Wadden Sea with basins of similar size. However, due to differences in system charateristics of the Eastern Scheldt and the Wadden Sea this R_c value is still suggested to be acceptable, for a full explanation see Section 5.2. To further evaluate the uncertainty regarding the horizontal exchange parameters (δ) and the global equilibrium concentration (c_E) sensitivity analysis are done, see Section 4.2.3.

Initial parameters: Tidal range H, horizontal area A and initial volumes V of the three elements. The subscripts indicate the elements, i.e. f = flat, c = channel, od = ebb tidal delta, which also apply to the following groups of parameters.			
H	(m)	3.36	
A_f	(km^2)	117	
A_c	(km^2)	239	
A_{od}	(km^2)	280	
$V_{f,0}$	(m^3)	$91 \cdot 10^6$	
$V_{c,0}$	(m^3)	$2346 \cdot 10^6$	
$V_{od,0}$	(m^3)	$486 \cdot 10^6$	
SLR	(mm/year)	2.3	
Parameters influencing morphological timescale: n = power in the relation for the local equilibrium sediment concentration, C_E = global equilibrium concentration, w_s = vertical exchange coefficient in the element indicated by the second subscript, δ = horizontal exchange coefficient between the two elements indicated by the two subscripts (o = outside world)			
		$\downarrow (s)$ sand sediment fraction	$\downarrow (m)$ mud sediment fraction
n	$(-)$	$n_s = 5$	$n_m = 3$
c_E	$(-)$	$c_{E,s} = 4 * 10^{-4}$	$c_{E,m} = 7 * 10^{-6}$
$w_{s,f}$	(m/s)	$w_{s,f,s} = 0.006$	$w_{s,f,m} = 0.001$
$w_{s,c}$	(m/s)	$w_{s,c,s} = 0.015$	$w_{s,c,m} = 0.001$
$w_{s,od}$	(m/s)	$w_{s,od,s} = 0.015$	$w_{s,od,m} = 1 * 10^{-5}$
δ_{c-f}	(m^3/s)	$\delta_{c-f,s} = 205$	$\delta_{c-f,m} = 1234$
δ_{c-od}	(m^3/s)	$\delta_{c-od,s} = 163$	$\delta_{c-od,m} = 2451$
δ_{o-od}	(m^3/s)	$\delta_{o-od,s} = 466$	$\delta_{od-o,m} = 7502041$
Parameters for defining the morphological equilibrium: V_{fe} = equilibrium volume of the flat element, α = coefficient in the relation between the equilibrium volume (V) of the element indicated by the subscript and the tidal prism (P): $V_{c,eq} = \alpha_c P, \quad V_{od,eq} = \alpha_{od} P^{1.23}$			
V_{fe}	(m^3)	$205 \cdot 10^6$	
α_c	(m^{-1})	1.76	
α_{od}	$(10^{-3} m^{-0.69})$	3.27	

Table 4.4: Overview of all model parameters used in ASMITA for the scenario without OSK

4.2.2 Reference run

Using the parameter set presented in Table 4.4, a likely development of the Eastern Scheldt without the OSK was modeled with ASMITA and will be referred to as the reference scenario. In Figure 4.8 the development trends of the reference scenario are visible. The flats are increasing in volume, the channels do not change much in volume and ebb-tidal delta decreasing and the tidal prism is increasing. The tidal prism is decreasing due to the fact that the flats are increasing.

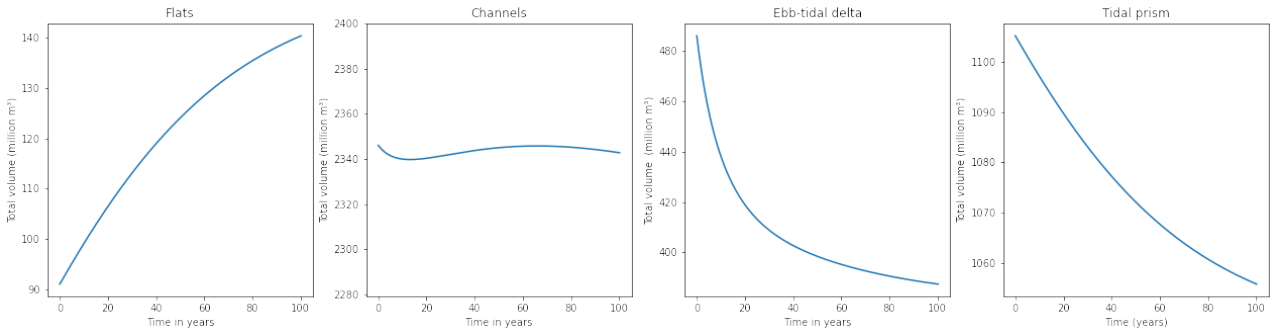

Figure 4.8: A likely development of the flats, channels, ebb-tidal delta and tidal prism of the Eastern Scheldt in the absence of the OSK, analyzed in terms of volume. The development trends are modeled using ASMITA with the parameter set shown in Table 4.4

In Figure 4.9, the mud, sand, and sea-level rise fractions that influence the volumes of the flats, channels, and ebb-tidal delta are visualized. The black lines represent the sum of the mud, sand, and SLR fractions. For the flats, it shows that the mud fraction is about 10% of the total sediment, which was the goal when determining the coarse equilibrium concentration (Section 3.3.3). Additionally, the flats are accumulating sediment and growing. However, due to SLR this growth is slowed down. When examining the development of the channels, SLR is responsible for increasing the channel volume - reminder, measured as water volume. The channels are moving towards a smaller equilibrium volume and are thus infilling with sediment. For the ebb-tidal delta, the volume decreases over time. At a certain point, when the sand fraction (yellow line) and the SLR fraction cross each other, the equilibrium volume is reached. This indicates that the ebb-tidal delta is decreasing in response to SLR. To counteract this decrease, the ebb-tidal delta imports sediment to adjust to the effects of SLR.

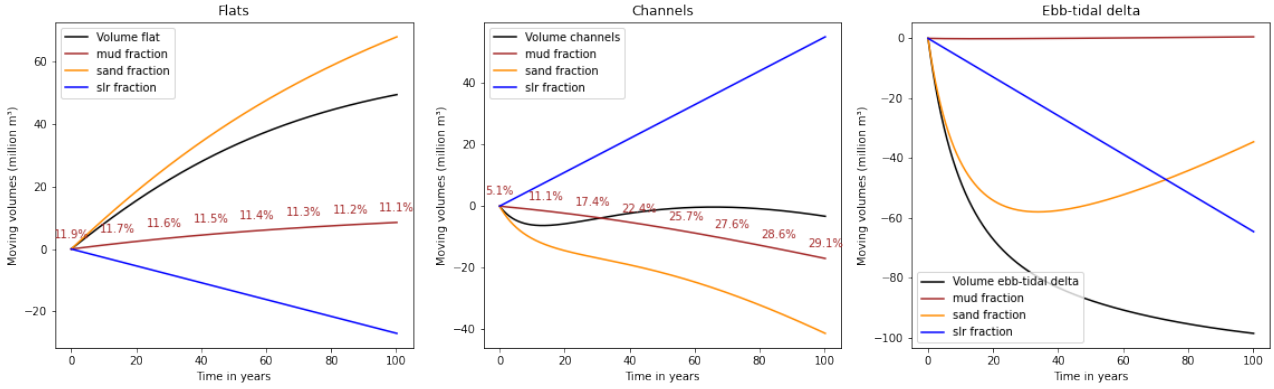

Figure 4.9: A likely development of the flats, channels, ebb-tidal delta, and tidal prism of the Eastern Scheldt in the absence of the OSK, analyzed in terms of the volume of mud (brown), sand (orange), SLR (blue), and the total increase or decrease of the flats, channels, and ebb-tidal delta. The development trends are modeled using ASMITA with the parameter set shown in Table 4.4

In Figure 4.10, the equilibrium volumes of the flats, channels, and ebb-tidal delta over time are visualized. As described in Section 3.3.1, the equilibrium volume of the flats depends on the tidal range and tidal basin area, which are constant in these calculations. The equilibrium volume of the channels and ebb-tidal delta depends on the tidal prism, which is not constant. As shown, the development of the equilibrium volume of the channels and ebb-tidal delta follow (almost) the same trajectory as the tidal prism in Figure 4.8

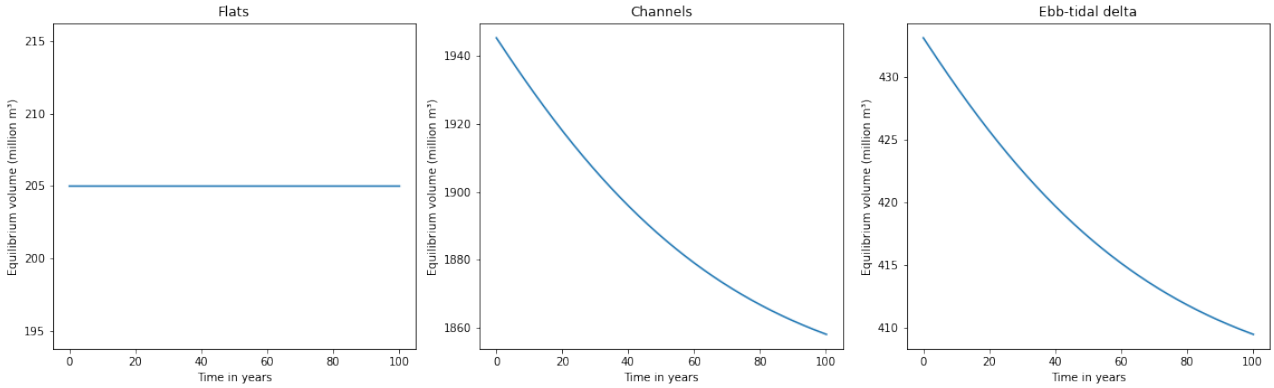

Figure 4.10: A likely development of the equilibrium volumes of the flats, channels, ebb-tidal delta, and tidal prism of the Eastern Scheldt in the absence of the OSK. The development trends are modeled using ASMITA with the parameter set shown in Table 4.4

The results from this reference scenario should be interpreted with caution, as the parameter set used is derived from parameter definitions but lacks proper calibration, as explained in Section 3.3.2. Consequently, the modeled scenario serves as an approximation rather than an exact prediction. To understand the uncertainties associated with this prediction, a sensitivity analysis is done in Section 4.2.3.

4.2.3 Sensitivity analysis

The sensitivity analysis focuses on the horizontal exchange parameter (δ), the shape parameter (A), the equilibrium volume of the flats ($V_{f,eq}$) and the global equilibrium concentration of the coarse fraction ($c_{E,\text{coarse}}$). A sensitivity analysis is performed for these parameters because they are challenging to derive from measurements; see also Section 3.3.3. These parameters are adjusted, while the remaining parameters retain the values listed in Table 4.4. The development trends of the flats, channels, and ebb-tidal delta are analyzed and compared, along with the critical sea-level rise of the flats for each sensitivity run. The sensitivity analysis evaluates the robustness of the outcomes to the reference run and explores investigate the impact of the parameter uncertainity.

Horizontal exchange parameter (δ)
The horizontal exchange parameter has a physical interpretation, representing the amount of sediment transported between the elements. It is based on the average distances and lengths between and of the tidal elements in the Eastern Scheldt. To asses how sensitive the output of the reference scenario is to defining these averaged distances, each distance is adjusted to reflect a range 15% higher and lower than their values in Table 4.4. With these adjusted values a minimum and a maximum horizontal exchange parameter δ is calculated. The values of the averaged distances and the calculation of maximum and minimum horizontal exchange parameters are detailed in Appendix B.4 and used as input in ASMITA.

The results of these computations are shown in Figure 4.11. For the minimum values of the horizontal exchange parameters, less sediment is transported between the elements and it takes longer to reach the equilibrium volumes. This is also evident in the figure, where the results for the flats a minimum horizontal exchange values (blue lines) show a gentler slope compared to the maximum horizontal exchange values (red line). For the channels, when the horizontal exchange parameter (δ) is set to a minimum value, the channel volume increases. This occurs because, in this scenario, SLR has a greater influence than sediment infill, causing the channel volume to grow. Conversely, when the horizontal exchange parameter is set to a maximum value, the opposite occurs: sediment infill becomes the dominant factor, outweighing the influence of SLR, and the channel volume decreases. The development of the ebb-tidal delta is not significantly influenced by variations in the horizontal exchange parameter.

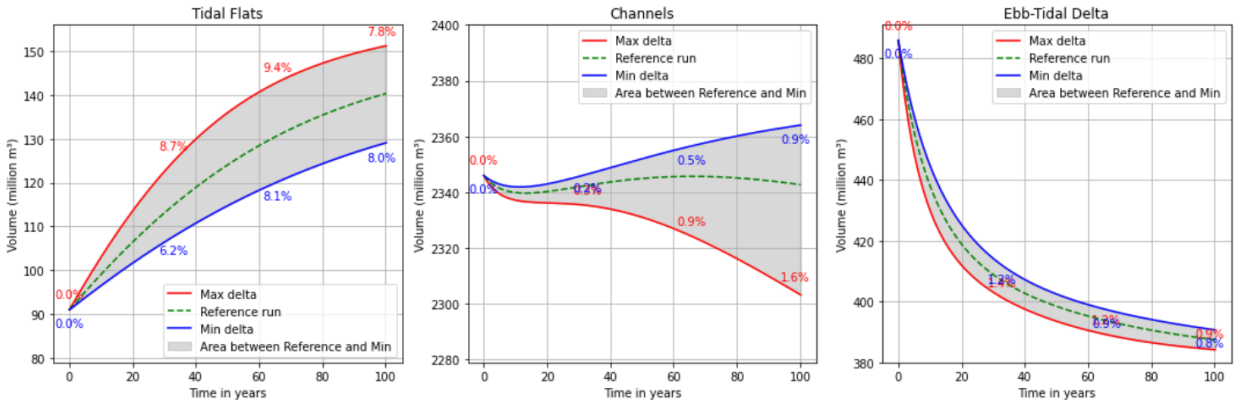

Figure 4.11: Development trends of the flats, channels, and ebb-tidal delta in the Eastern Scheldt without the OSK, with varying horizontal exchange parameter δ for distances within the expected geometric range. The percentage difference between the minimum (blue) and maximum (red) values relative to the reference run is shown.

Also the critical sea level rise R_c for the minimum and maximum exchange parameters are calculated using Equation (24). For the minimum exchange parameters $R_c = 3.0$ $mm/year$ and for the maximum $R_c = 5.5$ $mm/year$. The fact that the critical sea level rise is lower for the minimum values of the horizontal exchange parameter is quite logical. With less sediment transported between tidal elements, it takes longer for them to reach equilibrium. This results in the tidal flats being less able to keep up with sediment import when sea level rise rates are higher.

It can be stated that the development trend, meaning the increase or decrease in volume of the channels, is sensitive to the horizontal exchange parameter. The development trend of the flats and the ebb-tidal delta change in pace but do not reverse from an increase to a decrease or vice versa.

Shape parameter Bruun profile

As explained in Section 3.2.1 and Section 3.3.3, the volume of the ebb-tidal delta is calculated using a Bruun profile. This introduces some uncertainty due to the choice of the shape parameter A, which determines the steepness of the undisturbed bed profile and thus the volumes of the ebb-tidal delta. Parameters in the range of $A = 0.35$ to $A = 0.40$ provided a reasonable fit, as discussed in Section 4.1.2. For the sensitivity analysis, values of $A = 0.35$ and $A = 0.40$ are used to assess its sensitivity. For these values, the empirical equilibrium parameter and the initial volume of the ebb-tidal delta are calculated (see Appendix B.5 for detailed calculations). These values are then incorporated into the sensitivity analysis of the shape parameter A. The results are presented in Figure 4.12.

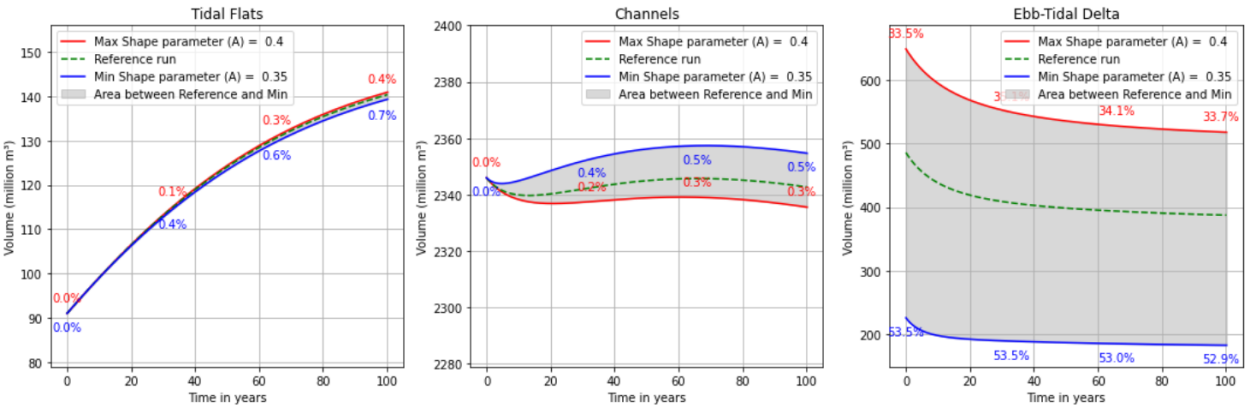

Figure 4.12: Development trends of the flats, channels, and ebb-tidal delta in the Eastern Scheldt without the OSK, with varying the shape parameter (A), see for the used values Table B.5. The percentage difference between the minimum (blue) and maximum (red) values relative to the reference run is shown.

Figure 4.12 shows that the trends for the flats, channels, and ebb-tidal delta follow similar trajectories. The flats and channels show almost no sensitivity to the shape parameter A in the corresponding development trends. For the ebb-tidal delta, the minimum and maximum deviations from the mean volume are relatively large, which is expected, as a steeper Bruun profile classifies more sediment as ebb-tidal delta. However the volume changes per sensitivity run are approximately the same. Therefore it can be said that the development trends of the flats, channels and ebb-tidal delta in the Eastern Scheldt are not sensitive for the shape parameter A.

Equilibrium volume of the flats

The equilibrium volume of the flats used in the reference run is $205 \cdot 10^6\,\mathrm{m}^3$, calculated using a relation based on flats in the Wadden Sea. This may lead to an overestimation of the equilibrium volume. To address this, a sensitivity analysis is performed by reducing the equilibrium volume of the flats by 30% and 15%, resulting in volumes of $144 \cdot 10^6\,\mathrm{m}^3$ and $174 \cdot 10^6\,\mathrm{m}^3$, respectively.

Using these adjusted values as input produces the results shown in Figure 4.13. The figure illustrates that the development pace of the flats is sensitive to a smaller equilibrium volume. For smaller equilibrium volumes the development of the flats slows down. However, the trend does not change to a decrease. The channels and the ebb-tidal delta exhibit minimal differences in response.

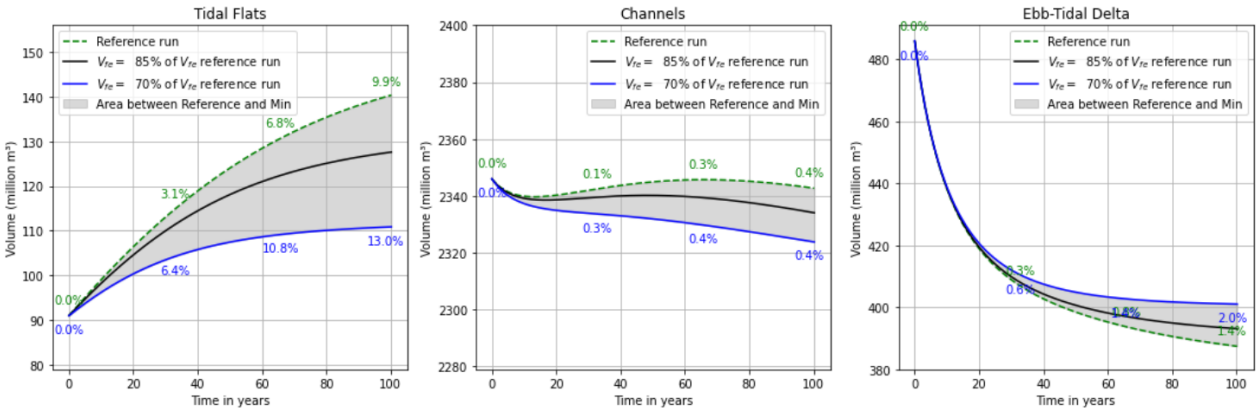

Figure 4.13: Development trends of the flats, channels, and ebb-tidal delta in the Eastern Scheldt without the OSK, with varying the equilibrium volume of the flats. The percentage difference between the minimum (blue) and reference run (green) values relative to the $V_{f,eq} = 174 * 10^6\mathrm{m}^3$ is shown.

Global equilibrium concentration of the coarse fraction

As shown in the reference run (Figure 4.9), a value of $c_{E,\mathrm{coarse}} = 4 \times 10^{-4}$ within the range of 0.5×10^{-4} till 4×10^{-4} is selected such that the mud fraction on the flats in the Eastern Scheldt without the OSK is approximately 10%. This assumption is based on the expectation that removing the Eastern Scheldt barrier would lead to increased suspended sediment deposition on the flats, as explained in Section 3.3.3. In the current situation, the flats have a mud fraction of approximately 1%.

To assess how sensitive the output of ASMITA is to the equilibrium concentration, a sensitivity analysis is conducted. In this analysis, 0.5×10^{-4} and 2.5×10^{-4} are selected to examine their effects on the developments. The results of this sensitivity analysis are shown in Figure 4.14. As shown for the minimum value the flats do not increase in volume (blue line). This is because lowering $c_{E,\mathrm{coarse}}$ results in less available sediment, leading to slower development in the Eastern Scheldt. When $c_{E,\mathrm{coarse}}$ increases, more sediment becomes available (e.g., on the flats), resulting in greater volume increases, as seen in the reference run and black line.

Additionally, the critical sea level rise for the different values of $c_{E,\mathrm{coarse}}$ is calculated using Equation (24). For $c_{E,\mathrm{coarse}} = 0.5 \times 10^{-4}$, $R_c = 1.3\,\mathrm{mm/year}$; for $c_{E,\mathrm{coarse}} = 2.5 \times 10^{-4}$, $R_c = 2.6\,\mathrm{mm/year}$; and for $c_{E,\mathrm{coarse}} = 4 \times 10^{-4}$, R_c was previously calculated as $4.0\,\mathrm{mm/year}$. It can be observed that for the minimum value of $c_{E,\mathrm{coarse}}$, the critical sea level rise is low and the flats do not increase in volume anymore. This means that the development of the flats and channels is sensitive to the global equilibrium concentration of the coarse fraction, more information can be found in Section 5.2.2.

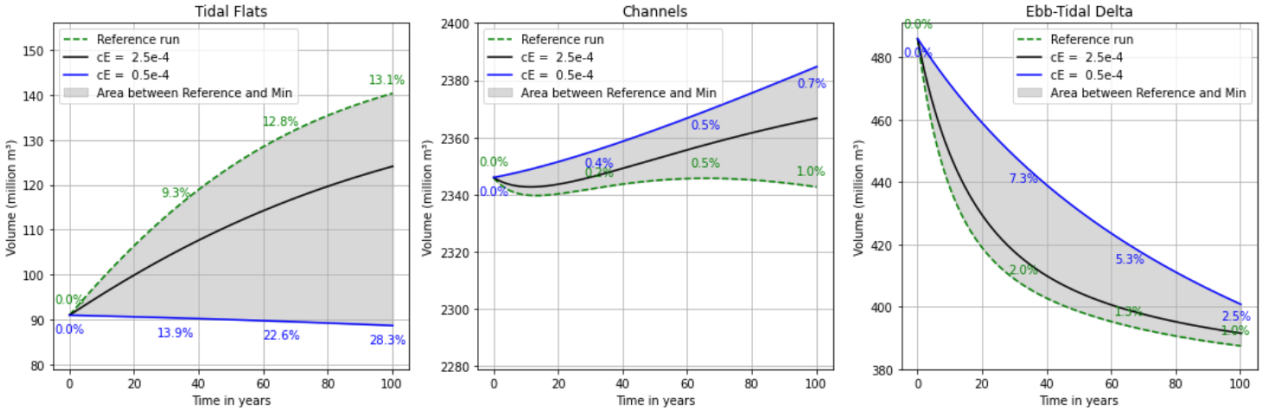

Figure 4.14: Development trends of the flats, channels, and ebb-tidal delta in the Eastern Scheldt without the OSK, with varying the global equilibrium concentration of the coarse fraction. The percentage difference between the minimum (blue) and reference run (green) values relative to the $c_{E,\text{coarse}} = 2.5 \times 10^{-5}$ is shown.

4.2.4 Scenarios influencing the development of the Eastern Scheldt in the absence of the OSK

The reference scenario was modeled in which the SLR rate was based on historical data. This SLR could potentially increase in the future (Overbeek & van Dorland, 2023). The effect of increasing SLR rates is analyzed in this section. Additionally, the starting volume of the flats in ASMITA is derived from 2019 depth measurements and the expected tidal range if the OSK were removed. However, what the starting volume of the flats would be in the future remains uncertain due to SLR, erosion, and sediment nourishment, see Section 2.3.3 and Section 2.4.1. To explore the effects of reduced flat volume, additional runs are carried out with ASMITA.

SLR-rate scenarios

To account for an increased SLR, two additional SLR scenarios are investigated. Research from KNMI outlines two scenarios: a low-emission scenario and a high-emission scenario for greenhouse gases. For the period up to 2050, a sea level rise of 5 mm/year is expected (with a certain margin of uncertainty) for the high-emission scenario. For the period up to 2100, this could increase to 11 mm/year (also with a margin of uncertainty) for the high-emission scenario (Overbeek & van Dorland, 2023). These two values are used as constant SLR rates in this analysis to investigate their potential impact on the Eastern Scheldt. The results of these scenarios are shown in Figure 4.15. When interpreting this figure, it is important to note that for SLR rates of 5 and 11 mm/year, it is uncertain whether the flat volume will indeed continue to increase during a 5 mm/year SLR rate (orange line). Due to the lack of calibration, it is not possible to confirm that the flats will still increase in volume at specific absolute SLR rates. What can be observed is that for the higher SLR rates the flats increase less in volume or even decrease in volume because they cannot keep up with the SLR. The channels increase in volume due to the higher SLR-rates. For the ebb-tidal delta, as modeled in ASMITA, the trend do not show a big difference in its response to high or low SLR rates.

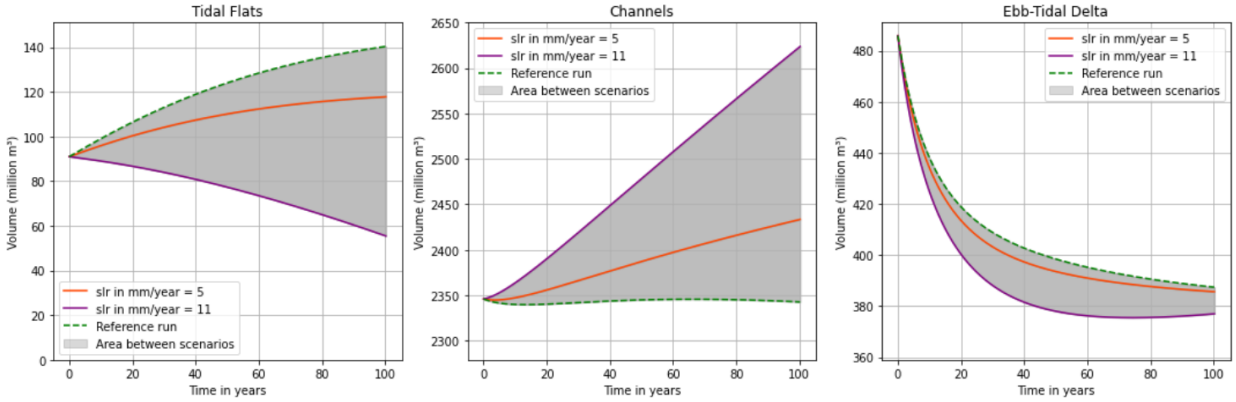

Figure 4.15: A likely development of the volumes of the flats, channels, ebb-tidal delta, and tidal prism of the Eastern Scheldt in the absence of the OSK under different SLR-rate scenarios. The development trends are modeled using ASMITA with the parameter set shown in Table 4.4

Initial volumes scenarios

The initial volume of the flats in ASMITA is based on the volume calculated using the 2019 depth measurements and the expected tidal range if the OSK were removed. However, if the OSK is removed, this flat volume could decrease (Section 2.3.3). Currently, sediment nourishments are also being carried out on the flats in the Eastern Scheldt (Section 2.4.1). As such, predicting the future volume of the flats is challenging. To investigate the impact of smaller initial volumes of the flats and channels, two scenarios are analyzed. In the first scenario, the initial volume of the flats is set to 90% of the volume derived from the 2019 depth measurements. It is assumed that if the flats decrease in sediment volume, this volume would be deposited in the channels, resulting in a 10% increase in the channels' volume. In the second scenario, the initial volume of the flats is set to 80%, with the channels decreasing by 20% of the flats' volume. The outcomes of these scenarios are shown in Figure 4.16. As visible, these changes in starting volumes mainly influence the first part of the development. The tidal flats with a smaller initial volume experience a delay in reaching a larger volume compared to tidal flats with a larger initial volume.

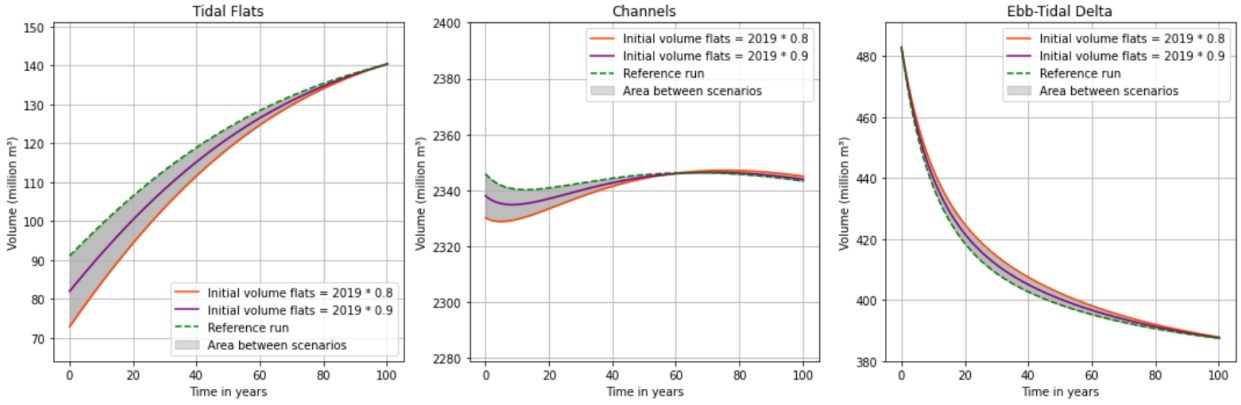

Figure 4.16: A likely development of the equilibrium volumes of the flats, channels, ebb-tidal delta, and tidal prism of the Eastern Scheldt in the absence of the OSK under different scenarios for the initial volume of the flats and channels. The development trends are modeled using ASMITA with the parameter set shown in Table 4.4

5 Discussion

The goal of this thesis is to provide an estimation of how the morphology of the Eastern Scheldt will develop in the long term if the OSK is removed. The emphasis in this long-term prediction is on the development of the flats. In this chapter, the results are interpreted, in the first section: Data Analysis, examines the comparison between the measured volumes and the calculated equilibrium volumes. The second part: ASMITA focuses on interpreting the results modeled using ASMITA.

5.1 Discussion Data Analysis

This section discusses the measured volume trends of the flats, channels and flats in comparison with calculated equilibrium volumes, it ends with a synthesis stating the key findings. For further details on how the comparison is made in this research, refer to Section 3.2.

5.1.1 Flats

Before completion of the OSK and Back Barrier Dams Figure 4.7 indicates that in 1983, prior to the completion of the OSK and the back-barrier dams, the volume of the flats was close to the calculated equilibrium volume. At that time the basin could still exchange sediment between its elements (Kohsiek et al., 1987). So the flats could gain sediment which makes it reasonable that the flats were indeed close to their equilibrium in 1983.

Current State In the current situation, two discrepancies exist between the measured and equilibrium volumes of the flats. As shown in Figure 4.7, the difference between the equilibrium and measured volumes in 1990 is significant. By this time, the back-barrier dams and OSK had not been in place long enough to substantially affect sediment dynamics, so the flats were expected to remain closer to their equilibrium volume. However, this is not evident in the data. Secondly, the current development trend of the flats does not show movement toward the equilibrium volume.

Several factors can explain why in 1990, the measured flat volumes deviated as much from the equilibrium volumes. First, it could be attributed to the calculation method of the flats' volume, which uses spatially constant MLW and MHW values, as discussed in Section 4.1.1. Using constant MLW and MHW values leads to a calculated flats volume of $74 \cdot 10^6\,\mathrm{m}^3$ in 2019 (see Table 4.3). However, research by de Vet et al. (2024) indicates that using spatially varying MLW and MHW values results in a flat volume of $98 \cdot 10^6\,\mathrm{m}^3$ for 2019. This difference in volume is expected across all other years, including 1990. Additionally, part of the basin containing a significant flat area was cut off by the Philipsdam and Oesterdam and is no longer part of the Eastern Scheldt, see Figure 2.1 for an indication of this area. This could further explain why the measured volume is much smaller than the equilibrium volume. Furthermore the equilibrium volume is calculated using the empirical relation for the average relative flat height, which is based on data that exhibits considerable variability, as shown in Figure 2.10 in Section 2.5. This variability arises due to the difficulty of defining a single relationship for the average relative flat height that applies to all flats in a basin (E. Eysink & Biegel, 1992). Finally, an important explanation could lie in calculation of the equilibrium volume of the flats, as described in Section 3.2.3, which are based on flats in the Wadden Sea. However the system characteristics of the Eastern Scheldt are different of the Wadden Sea. For example, the Eastern Scheldt is oriented in the prevailing wind direction (SW) (Eelkema, 2013), the channels have much larger cross-sections, and the Eastern Scheldt basin is more rectangular compared to the Wadden Sea basins, which are more square (E. Eysink & Biegel, 1992). All these factors could result in higher wave impact and thus more erosive forces on the flats in the Eastern Scheldt (E. Eysink & Biegel, 1992). Consequently, it is possible that a lower equilibrium volume should be calculated for the flats in the Eastern Scheldt, for example, by using a lower average equilibrium height for the flats. Adjusting this parameter has also been done by Huismans et al. (2024) in research on the Zoutkamperlaag basin in the Wadden Sea, where the equilibrium height was increased to achieve a better estimation of the equilibrium volume of the flats.

The second discrepancy lies in the fact that the flats in the current situation are not developing towards their equilibrium volume, see Figure 4.7. In Figure 4.7, it is evident that both channels and flats are currently out of equilibrium and should "demand" sediment. However, in the Eastern Scheldt, the flats are eroding rather than gaining sediment (Walles et al., 2021). This can be explained by that the channels have a greater sediment demand compared to the flats, which prevents the flats from developing towards their equilibrium state. A similar situation arises under high SLR scenarios, as shown in Figure 4.15, where the flats cannot cope with larger SLR rates and also fail to reach equilibrium. So it can be reasoned that in the current situation, the high sand demand of the channels, combined with minimal sediment import from outside the basin, similarly hinders the flats' development. While this situation can be modeled using an ASMITA model, uncertainties in the equilibrium volume of the flats and the morphological timescale parameters prevented this research from accurately capturing these developments. If the equilibrium volume for the flats in the Eastern Scheldt basin is defined, it would be possible to develop this 2-element model.

Future Scenario Without the OSK Looking ahead, comparing the values of 2019 with the equilibrium values for a future scenario without the OSK, the volume of the flats is expected to increase, as the removal of the OSK will also induce a larger tidal range. However, this initial increase does not necessarily bring the flats closer to their equilibrium, as the equilibrium volume also increases with the increasing tidal range (see Table 4.3).

5.1.2 Channels

Before completion of the OSK and Back Barrier Dams Before the completion of the OSK and the back-barrier dams, the channels were eroding due to the significant increase in basin area and tidal prism caused by the construction of the Volkerakdam (Eelkema, 2013). This erosion resulted in an increasing channel volume. The equilibrium volume of the channels in 1983 is calculated to be larger than the measured channel volume, see Table 4.3, which aligns with the erosion trend as the channels developed toward their equilibrium.

Current State In the present situation, as shown in Figure 4.7 and Table 4.3, the channels are larger than their equilibrium volume. This is expected, as the sand demand of the channels is estimated to be between $400 \cdot 10^6$ and $600 \cdot 10^6$ m^3 (Kohsiek et al., 1987). The difference between the equilibrium volume and the measured volume is of a similar magnitude (see Table 4.3).

Future Scenario Without the OSK Figure 4.7 and Table 4.3 show that the estimated initial channel volume in the scenario without the OSK has a very small difference to its equilibrium volume. The sand demand was calculated using a tidal prism decrease of 30% (Kohsiek et al., 1987). If the OSK were removed, the tidal prism is expected to increase by 16% (De Pater, 2012). To reach its pre-OSK and back-barrier dam levels, the tidal prism would need to increase by $(1/0.7 = 1.43)$ 43%. However, the basin area and thus the channel volume are now smaller due to the back-barrier dams, so the tidal prism does not need to increase by 42% to achieve balance with the water volume in the channels. As the results indicate, it is reasonable to conclude that the channels would be very close to their equilibrium state even if the tidal prism does not increase by 42%. Additionally, with the OSK removed, the sand supply to the channels will no longer be limited to the flats but will also include the ebb-tidal delta. This is because the sediment blockage by the OSK between the channels and the ebb-tidal delta is expected to decrease.

5.1.3 Ebb-tidal delta

Discrepancy Between Measured and Equilibrium Volumes The comparison in Figure 4.7 and Table 4.3 show that the calculated equilibrium volume is significantly larger than the measured volumes. These equilibrium volumes were derived using Walton and Adams (1976) method. The considerable difference between the measured and equilibrium volumes may partly result from using a different method when constructing the undisturbed bed level for calculating the ebb-tidal delta volume, see for more information Section 4.1.2. However, the fact that the calculated equilibrium volumes are nearly twice the measured volumes raises questions about the applicability of this empirical equation to the Eastern Scheldt's ebb-tidal delta. Potential factors contributing to this discrepancy include differences in tidal environment, sediment supply, and coastline morphology between the American tidal basins and the Eastern Scheldt.

Before completion of the OSK and Back Barrier Dams Before the completion of the OSK and back-barrier dams, the ebb-tidal delta experienced sediment gain, visible in Figure 4.6. At that time, the channels were eroding due to the increased tidal prism caused by the completion of the Volkerak Dam. Sediment from the channels was partly transported to the ebb-tidal delta, leading to its sediment gain (Eelkema, 2013). So the measurement align with earlier research.

Current State Following the completion of the OSK and the back-barrier dams, the ebb-tidal delta began to lose sediment volume, see Figure 4.6. Due to a lack of usable data for 27 years after the OSK's completion, the post-construction trend is difficult to observe in detail. Nonetheless, it is evident that the ebb-tidal delta volume has decreased. This decrease is attributed to the OSK causing the ebb-tidal delta to flatten, significantly contributing to the reduction in volume (Eelkema, 2013).

5.1.4 Synthesis Data Analysis

The key findings from the comparison for the flats indicate that more research is needed on how the equilibrium volume for the Eastern Scheldt should be calculated. It is expected that the equilibrium volume will be smaller than calculated in this research due to differences in system characteristics between the Wadden Sea and the Eastern Scheldt. One potential approach could involve redefining the equilibrium height of the flats in the Eastern Scheldt. However, a more detailed comparison between the Eastern Scheldt and the Wadden Sea is required, as will be discussed in the recommendation section. This equilibrium volume can then also be applied to the 2-element ASMITA model for the current situation, see also the recommendation section. Nevertheless, it can still be stated that if the OSK were to be removed, the flats would experience an immediate increase in volume due to the tidal range increase.

Comparing the equilibrium volume and the measured volume of the flats indicate a sand demand in the channels under the current situation. If the OSK is removed in the future, the channels are expected to be closer to their increased equilibrium volume. As a result, the sand required to fill the channels will decrease. Additionally, without the OSK, the source of this sand demand will not be limited to the flats but can also include the ebb-tidal delta, as the sediment blockage between the channels and the ebb-tidal delta is expected to decrease significantly.

The measured volumes of the ebb-tidal delta in this thesis aligns with developments described in earlier research. However, the significant difference between the measured and equilibrium volumes prevents drawing final conclusions and raises doubts about the applicability of the empirical relationship of the ebb-tidal volume of Walton and Adams (1976) to the Eastern Scheldt.

5.2 Discussion on results modeled with ASMITA

The ASMITA model was employed in this thesis to estimate the development trends of the flats, channels, and ebb-tidal delta of the Eastern Scheldt in the scenario where the OSK is removed. However, this research did not succeed in calibrating parameters within ASMITA due to difficulties in using the 2-element model for the current situation (Section 3.3.2). As a result, a reference scenario was defined to show the most likely development of the Eastern Scheldt without the OSK. Due to the lack of calibration, conclusions focus on identifying parameters with high influence and determining whether an erosion or sedimentation trend is present, rather than providing precise quantitative predictions.

First, the results provided by the reference scenario will be discussed (Section 5.2.1). Then, the sensitivity of the model output to various parameters will be analyzed (Section 5.2.2), followed by an examination of how different SLR scenarios and initial flat volume scenarios influence the development (Section 5.2.3). Finally, some limitations of the ASMITA model will be highlighted (Section 5.2.4), and the section will conclude with a synthesis summarizing the key findings of the results modeled with ASMITA (Section 5.2.5).

5.2.1 Reference scenario

The reference scenario, as presented in Section 4.2.2, represents the most likely scenario based on available data. From Figure 4.8, it is shown that if the OSK is removed, the flats increase in volume, the channels do not change much in volume, and the ebb-tidal delta decreases. Additionally, the tidal prism decreases in volume due to the growth of the flats. Furthermore, Figure 4.9 illustrates the impact of different sediment fractions. For the channels it is visible that the volume trend for a large part is influenced by the SLR. The channels have a large area, and thus the SLR has a large influence.

As explained in the methodology (see Section 3.3.3), to provide an additional verification on $c_{E,coarse}$ and δ, the critical sea level rise (R_c) was calculated and compared with R_c values of basins with similar basin areas in the Wadden Sea. These basins in the Wadden Sea have R_c values ranging from 6.4 to 10 mm/year (Huismans et al., 2022). However, the reference scenario has a critical sea level rise of 4 mm/year. This value is still considered physically logical, even though it is lower. As explained in Section 5.1.1, the volume of the flats in the Eastern Scheldt compared to its basin area is expected to be lower than that of the flats in the Wadden Sea, which suggests that the R_c value could also be lower than 6.4 mm/year. However further research is required to confirm this assumption.

5.2.2 Sensitivity analysis

Horizontal Exchange Parameter The sensitivity analysis (Section 4.2.3), Figure 4.11 shows that different values for the horizontal exchange parameter affect the pace at which elements develop towards their equilibrium and influence the critical sea level rise of the flats but do not alter the overall erosion or sedimentation trends. The horizontal exchange parameter is adjusted to define a range based on the average distance needed, within which the maximum and minimum values are determined. A higher horizontal exchange parameter means more sediment transport between the flats, resulting in a higher critical sea level rise and faster development pace. This is also visible in Figure 4.11.

Bruun's Shape Parameter From Figure 4.12, where the shape parameter of the Bruun (A) is varied, it can be concluded that A minimally influences the trends of all tidal elements. Notably, the tidal flats remain unaffected. While the ebb-tidal delta shows variation in absolute values, its relative trend follows the same developmental pattern. This is due to the empirical equilibrium factor α_{od} scaling equally with changes in measured volumes of the ebb-tidal delta, ensuring that the development trends of the flats and channels remain largely unaffected.

Equilibrium volume of the flats Figure 4.13 illustrates that for smaller equilibrium volumes of the flats, the volume increase is both lower and slower. Nevertheless, the flats continue to grow, even with smaller equilibrium volumes. This behavior is expected because the equilibrium volume of the flats remains larger than the initial volume, meaning the flats will still "want" to increase to reach their equilibrium state. This demonstrates that, as discussed in Section 5.1.1, if the equilibrium volume in this thesis is overestimated, it does not affect whether the flats will import sediment, only the rate at which sediment is transported to the flats. Additionally, Figure 4.13 shows that the channels and the ebb-tidal delta are not significantly impacted by smaller equilibrium volumes of the flats.

Global Equilibrium Concentration Figure 4.14 shows that different values of the global equilibrium concentration of the coarse fraction ($c_{E,coarse}$) result in varying development trends for the flats. For the minimum value of $c_{E,coarse} = 0.5 \times 10^{-4}$ which relates to a concentration of 100 mg/L, the flats no longer increase in volume. This means that the model output is highly sensitive to $c_{E,coarse}$. For this minimum value, there is less sediment available, and the SLR of 2.3 mm/year counteracts this small sediment increase, causing no total volume increase of the flats. The channels increase in water volume due to SLR increase is not counteracted by sediment infill and the ebb-tidal delta develops slower to its equilibrium volume for smaller values of $c_{E,coarse}$.

When calculating the critical sea level rise of the flats with $c_{E,coarse} = 0.5 \times 10^{-4}$, a value of 1.4 mm/year was calculated. This value is considered unlikely because R_c is very low, making $c_{E,coarse} = 0.5 \times 10^{-4}$ an unrealistic value. However further research is required to confirm this.

5.2.3 Modelled scenarios

SLR-rate scenario Using the parameter set of the reference scenario, the impact of SLR on the development of the flats, channels, and ebb-tidal delta in the Eastern Scheldt is analyzed. As shown in Figure 4.15, even with the removal of the OSK, high SLR rates result in a decrease in the volume of the flats and an increase in the volume of the channels. In high SLR scenarios, the flats are unable to keep up with the rising sea levels and will eventually drown. As is also the case for flats in the Western Scheldt (Elmilady et al., 2022). The development trend of the ebb-tidal delta is not significantly influenced by the SLR rates. This could be explained by ebb-tidal delta already being close to its equilibrium, making it better equipped to cope with SLR.

Initial volume of flats scenarios Two additional scenarios were conducted to investigate whether further erosion of the flats into the channels would significantly influence the development trend of the flats, channels, and ebb-tidal delta if the OSK is removed. As shown in Figure 4.16, a smaller starting volume for the flats and channels does not change the overall trend. However, with a smaller starting volume, the flats need more time to reach their equilibrium volume. The channels, decreasing in volume, reach their equilibrium volume sooner when starting with a lower initial volume. Meanwhile the ebb-tidal delta is almost unaffected by this change.

5.2.4 Model uncertainties

Apart from the uncertainties regarding the lack of calibration, the ASMITA model itself also has model uncertainties:

- **Constant tidal range assumption:** ASMITA assumes a tidal range constant throughout time. However, it is known that the tidal range changes due to SLR and the morphodynamic response. A study by Jiang et al. (2020) shows that the tidal range increases in the Eastern Scheldt with SLR. Excluding this effect can lead to an underestimation of the flat volume. Adjusting the tidal range would have multiple effects: it would influence the tidal prism, which in turn affects the equilibrium volumes, including the equilibrium volume of the flats. A study on the Wadden Sea using ASMITA indicates that accounting for tidal range changes has significance influence and results in less sediment demand when the tidal range is adjusted (Z. B. Wang et al., 2024).
- **Fixed tidal element areas:** ASMITA assumes that the areas of all tidal elements remain constant, so volume changes occur solely in height. In reality, the areas of tidal elements also increase or decrease in response to volume changes.
- **Exclusion of wave effects:** The ASMITA model does not explicitly consider waves as a driving force for morphological development. Instead, the effects of waves are implicitly accounted for through the relationships used for morphodynamic equilibrium and the parameters that determine morphological time scales (Q. Lodder et al., 2022). However, this simplification may become a source of uncertainty if wave climates in the Eastern Scheldt area significantly change in the future.

5.2.5 Synthesis ASMITA

Combining all the results modeled with ASMITA, the findings indicate that the flats will import sediment if the OSK is removed. The rate and magnitude of sediment import depend on various parameters, as demonstrated by the sensitivity analysis. For larger horizontal exchange parameters (δ), equilibrium volumes of the flats (V_{eq}), or global equilibrium concentrations of the coarse fraction ($c_{E,\text{coarse}}$), more sediment will be imported to the flats. In which the development trend of the flats is highly sensitive to $c_{E,\text{coarse}}$, which describes the sediment availability in the Eastern Scheldt. The model outcomes show almost no sensitivity to the shape parameter of the Bruun rule (A).

The total increase (or decrease) in the volume of the flats in the Eastern Scheldt without the OSK depends on balancing the total sediment import and the rate of SLR. If the sediment import is insufficient relative to the SLR, the flats will no longer increase in total volume. For the channels, the situation is reversed, as the SLR leads to an increase in the water volume of the channels. The ebb-tidal delta generally shows low sensitivity to changes in these parameters. An additional interesting result is that, with smaller initial flat volumes, the flats will still import sediment if the OSK is removed. However, the total flat volume exhibits a time lag compared to scenarios with larger initial flat volumes.

With all the results interpreted and the model uncertainties addressed, a conclusion and recommendation will be provided in following chapter.

6 Conclusion and recommendations

6.1 Conclusion

This study aimed to predict the morphodynamic changes in the Eastern Scheldt without the storm surge barrier (OSK). The research question that is answered in this Chapter is: *What is the long term morphological development of the Eastern Scheldt, focusing on the tidal flats, when removing the storm surge barrier and under the influence of sea level rise?.*

The literature review indicates that prior to the construction of the OSK and the back-barrier dams, hydrodynamic changes of the system led to undisturbed sediment exchange between the tidal elements - the flats, channels, and ebb-tidal delta. However, the implementation of the OSK and back-barrier dams has blocked sediment exchange and reduced the tidal prism by 30%, which caused the channels to draw sediment from the flats. As a result, the tidal flats are now eroding, unable to adapt to rising sea levels, and are at risk of drowning. The OSK and the back-barrier dams have fundamentally altered the natural dynamics that typically govern the evolution of a tidal basin.

Results from this research, when comparing the theoretical equilibrium volumes and measured volumes, show that due to this alteration of natural dynamics, the flats in the Eastern Scheldt are not developing towards their larger equilibrium volume. Additionally, the significant difference between the equilibrium volume and measured volume of the flats suggests that the relation used in this research to calculate the equilibrium volume should be refined. In this research, the equilibrium volume of the flats was calculated using relations based on flats in the Wadden Sea. Future research should investigate if and how this equilibrium volume should be adjusted (see Recommendations). A proper calibration of the equilibrium volume in the 2-element model of ASMITA for the current situation, would lead to greater confidence in the parameters of the ASMITA model of the 3-element model for the future scenario without the OSK (see also the Recommendations section). The initial hydrodynamic response to removing the OSK is an expected increased tidal range, which would immediately result in a larger flat area. The comparison between the equilibrium volumes and the measured volumes also shows that the current volume of the channels is very close to their equilibrium volume in the scenario without the OSK. This can be explained by the applied 16% expected increase in tidal prism, which is based on earlier research. With the removal of the OSK, it is expected that the sediment exchange between the channels and the ebb-tidal delta will no longer be obstructed by the OSK. The channels being closer to their equilibrium volume and not relying solely on the flats as a sediment source will result in significantly less sediment being drawn from the flats. The measured volume of the ebb-tidal delta is almost twice as small as the equilibrium volume. This raises doubts about the applicability of the empirical relationship for the ebb-tidal volume proposed by Walton and Adams (1976) to the Eastern Scheldt.

Results modeled with ASMITA indicate that the flats will import sediment. Sensitivity analysis on these results show that the rate and magnitude of this sediment import largely depend on the sediment concentration entering the basin without the OSK. A reliable estimation of this sediment concentration requires further research (see Recommendations). The ASMITA results also show that the increase in flat volume depends on the balance between sediment import and sea-level rise. Most scenarios indicate an increase in total flat volume. However, for scenarios with extreme SLR rates, the flats in the Eastern Scheldt may eventually drown, even with the OSK removed.

In summary, the results indicate that removing the OSK leads to sediment importation to the flats, explained by the disappearance of the sediment blockage and the current volume of the channels matching the new equilibrium volume, therefore demanding significantly less sediment of the flats. The total increase in the volume of the flats depends on the balance between sediment import and sea-level rise. The current model enables predictions for trends of the tidal elements but requires calibration for absolute quantities.

6.2 Recommendations

More research is needed to make predictions about absolute volume changes of the tidal elements, if the OSK is removed. The following recommendations for future research are proposed:

1. **Equilibrium volumes comparing with basin characteristics:** As shown in the comparison, the difference between the measured and equilibrium volumes of the flats is quite large. This could be due to the fact that the relation for the equilibrium volume used in this thesis is based on flats in the Wadden Sea. Due to differences in system characteristics, such as the orientation of the basin to its prevailing wind direction, sediment particle size, or the level of branching of the channels in a basin, it is expected that these relations are not directly applicable to the Eastern Scheldt. Further research should investigate to what extend these system characteristics differ between the Wadden Sea basin and the Eastern Scheldt and how they influence the calculations of the equilibrium volume of the flats. This analysis could also be extended beyond the Wadden Sea basin and the Eastern Scheldt to include other systems, to identify a more robust trend in flat volume relative to system characteristics. The same goes for the ebb-tidal delta, where differing system characteristics might explain the large difference between the equilibrium volume and the measured volume observed in these results.

2. **2-Element model ASMITA:** This research did not include the 2-element model of the Eastern Scheldt for the current situation. This was primarily due to uncertainties regarding the equilibrium volume of the flats. If the equilibrium volume of the flats is refined with the recommendations above, this would lead to morphological time scale parameters being the only parameters requiring calibration. This calibration would lead to greater confidence in the model parameters used for predictions without the OSK.

3. **Sediment availability:** The ASMITA results indicate that the volume of sediment transported to the flats is highly depended on the sediment concentration in the Eastern Scheldt. However, due to the lack of measurements and uncertainties about how the removal of the OSK would impact sediment exchange, further research is needed to investigate this. If the OSK were to be removed, it remains unclear how much sediment would enter the basin and how much would ultimately reach the flats. Exploring the dynamics of sediment exchange in this context could provide valuable insights. Additionally, it may be worth considering different approaches to OSK removal, such as focusing on the barrier itself or addressing related features like bed protection and scour holes. These aspects could play a key role in sediment distribution and availability for the flats.

This research has solely focused on the development of the tidal elements, in case of the removal of the OSK. But without the OSK, the Eastern Scheldt will lose the coastal protection of the barrier. If the OSK is removed, plans must be developed for protecting the surrounding land area. It is important to note that it should be able to protect the Eastern Scheldt without a storm surge barrier, as demonstrated by the Western Scheldt, which remains protected without the need for a storm surge barrier. Investigations into dyke reinforcements and alternative coastal protection measures for the Eastern Scheldt should be done to accomplish this.

References

Baptist, M. J., De Mesel, I., Stuyt, L. C. P. M., Henkes, R., De Molenaar, H., Wijsman, J., ... Kimmel, V. (2007). *Herstel van estuariene dynamiek in de zuidwestelijke Delta* (Tech. Rep.).

Bonenkamp, M. (2023). *Long-Term Morphological Modelling of Tidal Inlet Systems: Implementing Salt Marshes in ASMITA.* Retrieved from `http://repository.tudelft.nl/.`

Bosboom, J., & Stive, M. (2021). *Coastal Dynamics.* TU Delft Open. doi: 10.5074/T.2021.001

Brand, N., Kothuis, B., & van Prooijen, B. (2016). *The Eastern Scheldt Survey* (Tech. Rep.).

Bruun, P. (1954). *Coast erosion and the development of beach profiles* (Tech. Rep.).

de Bok, C. (2001). *Long Term Morphology of The Eastern Scheldt.* Delft University of Technology.

De Bruijn, R. A. (2012). *The future of the Oosterschelde with a new inlet channel.* Delft University of Technology.

De Pater, P. (2012). *Effect of removal of the Oosterschelde storm surge barrier.* Delft University of Technology.

de Ronde, J., Mulder, J., van Duren, L., & Ysebeart, T. (2013). *Eindadvies ANT Oosterschelde* (Tech. Rep.).

de Vet, P., van Prooijen, B., Herman, P., Bouma, T., van Maren, D., Walles, B., ... Wang, Z. (2024, 12). Response of estuarine morphology to storm surge barriers, closure dams and sea level rise. *Geomorphology*, *467*, 109462. Retrieved from `https://linkinghub.elsevier.com/retrieve/pii/S0169555X24004148` doi: 10.1016/J.GEOMORPH.2024.109462

De Vet, P. L. M. (2020). *Intertidal Flats in Engineered Estuaries On the Hydrodynamics, Morphodynamics, and Implications for Ecology and System Management* (Doctoral dissertation, Delft University of Technology). doi: 10.4233/uuid:2b392951-3781-4aed-b093-547c70cc581d

Eelkema, M. (2013). *Eastern Scheldt Inlet Morphodynamics* (Doctoral dissertation, Technische universiteitDelft, Delft). Retrieved from `https://resolver.tudelft.nl/uuid:72bfaa03-6359-4d21-95f3-e3676915213c`

Elias, E. P., Van Der Spek, A. J., & Lazar, M. (2017, 9). The 'Voordelta', the contiguous ebb-tidal deltas in the SW Netherlands: Large-scale morphological changes and sediment budget 1965-2013; Impacts of large-scale engineering. *Geologie en Mijnbouw/Netherlands Journal of Geosciences*, *96*(3), 233–259. doi: 10.1017/njg.2016.37

Elmilady, H., van der Wegen, M., Roelvink, D., & van der Spek, A. (2022, 1). Modeling the Morphodynamic Response of Estuarine Intertidal Shoals to Sea-Level Rise. *Journal of Geophysical Research: Earth Surface*, *127*(1). doi: 10.1029/2021JF006152

Escaravage, V., Donk, S. v., Vet, L. d., Vermeer, N., Bakker, A. d., Werf, J. v. d., & Belzen, J. v. (2024, 2). *Roggenplaatsuppletie (Oosterschelde): morfologische en ecologische ontwikkelingen over de eerste drie jaren (2020T1-2021T2-2022T3) na aanleg* (Tech. Rep.). Wageningen Marine Research.

Eysink, E., & Biegel, E. (1992). Impact of sea level rise on the morphology of the Wadden Sea in the scope of its ecological function.

Eysink, W. D. (1991, 5). Morphologic Response of Tidal Basins to Changes. In *Coastal engineering 1990* (pp. 1948–1961). New York, NY: American Society of Civil Engineers. doi: 10.1061/9780872627765.149

Fitzgerald, D. M., & Hughes, Z. (2019). Marsh processes and their response to climate change and sea-level rise.
doi: 10.1146/annurev-earth-082517

Geurts van Kessel, A. J. M. (2004). *Verlopend tij. Oosterschelde, een veranderend natuurmonument* (Tech. Rep.).

Geurts van Kessel, A. J. M., Kater, B. J., & Prins, T. C. (2003). *Veranderende draagkracht van de Oosterschelde voor kokkels* (Tech. Rep.).

Haasnoot, M., Bouwer, L., Diermanse, F., Kwadijk, J., van der Spek, A., Oude Essink, G., ... Mosselman, E. (2018, 4). *Mogelijke gevolgen van versnelde zeespiegelstijging voor het Deltaprogramma. Een verkenning* (Vol. 12; Tech. Rep. No. 4). doi: 10.1088/1748-9326/aa6512

Huisman, B., & Luijendijk, A. (2009). *Sand demand of the Eastern Scheldt : morphology around the barrier* (Tech. Rep.). Deltares.

Huismans, Y., van der Spek, A., Lodder, Q., Zijlstra, R., Elias, E., & Wang, Z. B. (2022, 2). Development of intertidal flats in the Dutch Wadden Sea in response to a rising sea level: Spatial differentiation and sensitivity to the rate of sea level rise. *Ocean and Coastal Management*, *216*. doi: 10.1016/j.ocecoaman.2021.105969

Huismans, Y., Wang, Z., Alonso, A. C., & Harlequin, D. (2024, 12). *Hindcast evolution of Zoutkamperlaag tidal basin with ASMITA* (No. 11210366-001-ZKS-0001). Delft: Deltares.

Jiang, L., Gerkema, T., Idier, D., Slangen, A. B. A., & Soetaert, K. (2020, 3). Effects of sea-level rise on tides and sediment dynamics in a Dutch tidal bay. *Ocean Science*, *16*(2), 307–321. doi: 10.5194/os-16-307-2020

Kohsiek, L., Mulder, J., Louters, T., & Berben, F. (1987). *De Oosterschelde naar een nieuw onderwaterlandschap* (Tech. Rep.). Goes: RWS dienst getijdewateren.

Lodder, Q., Huismans, Y., Elias, E., de Looff, H., & Wang, Z. B. (2022, 3). Future sediment exchange between the Dutch Wadden Sea and North Sea Coast - Insights based on ASMITA modelling. *Ocean and Coastal Management*, *219*. doi: 10.1016/j.ocecoaman.2022.106067

Lodder, Q. J., Wang, Z. B., Elias, E. P., van der Spek, A. J., de Looff, H., & Townend, I. H. (2019, 10). Future response of thewadden sea tidal basins to relative sea-level rise-an aggregated modelling approach. *Water (Switzerland)*, *11*(10). doi: 10.3390/w11102198

Oost, A., Cleveringa, J., & Taal, M. (2020, 10). *Kombergingsrapport Friesche Zeegat Pinkegat en Zoutkamperlaag* (Tech. Rep.). Deltares.

Overbeek, B., & van Dorland, R. (2023, 10). *KNMI'23 klimaat scenario's voor Nederland* (Tech. Rep.). Koninklijk Nederlands Meteorologisch Instituut.

Postma, H. (1961, 4). Transport and accumulation of suspended matter in the Dutch Wadden Sea. *Netherlands Journal of Sea Research*, *1*(1-2), 148–190. doi: 10.1016/0077-7579(61)90004-7

Renger, E., & Partenscky, H. (1980, 1). SEDIMENTATION PROCESSES IN TIDAL CHANNELS AND TIDAL BASINS CAUSED BY ARTIFICIAL CONSTRUCTIONS. *Coastal Engineering Proceedings*(17), 146. doi: 10.9753/icce.v17.146

Rijkswaterstaat. (2024a). *De Deltawerken.* Retrieved from `https://www.rijkswaterstaat.nl/water/waterbeheer/bescherming-tegen-het-water/waterkeringen/deltawerken`

Rijkswaterstaat. (2024b, 12). *Over de Zandmotor.* Retrieved from `https://dezandmotor.nl/over-de-zandmotor/`

Rios-Yunes, D., Tiano, J. C., van Rijswijk, P., De Borger, E., van Oevelen, D., & Soetaert, K. (2023, 2). Long-term changes in ecosystem functioning of a coastal bay expected from a shifting balance between intertidal and subtidal habitats. *Continental Shelf Research*, *254*, 104904. doi: 10.1016/j.csr.2022.104904

Suijlen, J., & Duin, R. (2002). *Atlas of near-surface total suspended matter concentrations in the Dutch coastal zone of the North Sea* (Tech. Rep.). National Institute for Coastal and Marine Management/RIKZ.

van den Berg, J. H. (1986). *Aspects of sediment- and morphodynamics of subtidal deposits of the Oosterschelde (Netherlands)* (Doctoral dissertation, Rijkswaterstaat, The Hague). Retrieved from `https://resolver.tudelft.nl/uuid:b0b1ec46-a82c-49a0-9dcd-8f8ffd235646`

Van Der Cam, Q. (2021). *Channel nourishments to feed the eroding flats in the Eastern Scheldt.* Retrieved from `https://resolver.tudelft.nl/uuid:49cc8f31-d69f-41bc-8b7e-55e23f1735ce`

van der Werf, J., Reinders, J., van Rooijen, A., Holzhauer, H., & Ysebaert, T. (2015, 9). Evaluation of a tidal flat sediment nourishment as estuarine management measure. *Ocean & Coastal Management*, *114*, 77–87. doi: 10.1016/j.ocecoaman.2015.06.006

Van Maldegem, D. (2004). *"Oplossingsrichtingen" maatregelen voor reductie-en compensatie effecten zandhonger Oosterschelde Achtergrondinformatie workshop 1 december 2005* (Tech. Rep.).

Van Maren, D. S., & Winterwerp, J. C. (2013, 6). The role of flow asymmetry and mud properties on tidal flat sedimentation. *Continental Shelf Research*, *60*, S71-S84. doi: 10.1016/J.CSR.2012.07.010

van Zanten, E., & Adriaanse, L. (2008). *Verminderd getij* (Tech. Rep.). Rijkswaterstaat.

Walles, B., van Donk, S., Hamer, A., Wijsman, J., Ysebaert, T., Rurangwa, E., ... Slager, A. (2021, 3). *Roggenplaatsuppletie (Oosterschelde): ontwikkelingen voor (T0: 2015-2019) en het eerste jaar na aanleg (T1: 2020) van de suppleties* (Tech. Rep.). Wageningen Marine Research. Retrieved from `https://research.wur.nl/en/publications/142b19af-5c2b-4aeb-bdd2-a228b66ac355` doi: 10.18174/544639

Walton, T. L., & Adams, W. D. (1976, 1). Capacity Of Inlet Outer Ears To Store Sand. *Coastal Engineering Proceedings*(15), 111. doi: 10.9753/icce.v15.111

Wang, Z., & Lodder, Q. (2019). *Sediment exchange between the Wadden Sea and North Sea Coast Modelling based on ASMITA* (Tech. Rep.).

Wang, Z. B., Elias, E. P., van der Spek, A. J., & Lodder, Q. J. (2018, 9). Sediment budget and morphological development of the Dutch Wadden Sea: impact of accelerated sea-level rise and subsidence until 2100. *Netherlands Journal of Geosciences*, *97*(3), 183–214. doi: 10.1017/njg.2018.8

Wang, Z. B., Lodder, Q. J., Townend, I. H., & Zhu, Y. (2024, 12). Future sediment transport to the Dutch Wadden Sea under severe sea level rise and tidal range change. *Anthropocene Coasts*, *7*(1). doi: 10.1007/s44218-024-00044-y

Wisse, J. (2022). *Sea level rise in the Oosterschelde estuary.* Retrieved from `https://resolver.tudelft.nl/uuid:fd97af2a-8c81-49c9-a46b-817d015388eb`

Zandvoort, M., van der Zee, E., & Vuik, V. (2019). *De effecten van Zeespiegelstijging en Zandhonger op de Oosterschelde* (Tech. Rep.).

Appendices

Appendix A Harmoninc method

The analystical method is used to give an estimation on the waterlevels in the Eastern Scheldt and discharge trough the inlet with and without the OSK. The analytical method used is called the harmonic method.

A.1 Approach

In this method the Eastern Scheldt is schematized as visible in Figure A.1.

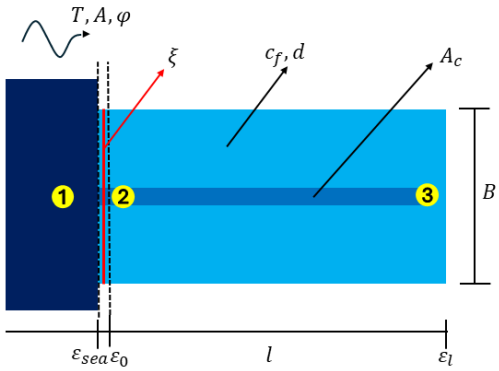

Figure A.1: Schematization of the Eastern Scheldt used for the Harmoninc method, with in red the OSK and in yellow used observation points

The shallow water equations are used by linearizing the the inertia and resistance. For a closed basin such as the Eastern Scheldt, this lead to the following equations.

$$\tilde{\zeta}_\ell = \frac{\tilde{\zeta}_0}{\cosh p\ell} \tag{14}$$

$$\tilde{Q}_0 = \frac{\mathrm{i}\omega B}{p}\tilde{\zeta}_0 \tanh p\ell \tag{15}$$

where:

$$p = \mathrm{i}k_0\sqrt{1-\mathrm{i}\sigma}$$
$$k_0 = \frac{\omega}{c_0} \quad \text{and} \quad c_0 = \sqrt{\frac{gA_c}{B}}$$
$$\sigma = \frac{\kappa}{\omega}$$
$$\kappa = \frac{8}{3\pi}c_f\hat{Q}_{\mathrm{rep}}/(A_c R)$$
$$\hat{Q}_{\mathrm{rep}} \approx 0.63\hat{Q}_0 \quad \text{(for a one-sided closed estuary)}$$

Taking into account the OSK this leads to the following equations.

$$\tilde{\zeta}_0 = \tilde{\zeta}_{\mathrm{sea}} - \beta\tilde{Q}_0 \tag{16}$$

where β is the linear resistance factor of the barrier, defined by $\beta = \frac{8}{3\pi}\xi\hat{Q}_0/\left(2gA_c^2\right)$. In the loss coefficient of the barrier ξ is described by $\xi = (1-\frac{1}{\mu})^2$ and μ is the ratio between the net discharge area of the opening of the

barrier and the flow-conveying area of the channels. Substituting the expression for $\hat{Q}_0$ leads to the following equations.

$$\tilde{\zeta}_0 = \frac{\tilde{\zeta}_{\text{sea}}}{1 + \beta(\mathrm{i}\omega B/p)\tanh p\ell} \tag{17}$$

$$\tilde{\zeta}_\ell = \frac{\tilde{\zeta}_{\text{sea}}}{\cosh p\ell + \beta(\mathrm{i}\omega B/p)\sinh p\ell} \tag{18}$$

To correctly use the above equations, several steps need to be followed. The first step is to describe the tidal wave entering the Eastern Scheldt, which can be done using the following equation: $\tilde{\zeta} = A \cdot \sin\left(\frac{2\pi}{T} + \phi\right)$. Where A is the amplitude of the M2 tidal constituent, T is the period, and ϕ is the phase shift of the wave. Next, the Eastern Scheldt needs to be schematized by determining the parameters shown in Figure A.1. This can be done by using observation points 2 and 3 (also shown in Figure A.1) and selecting the parameters so that the water levels obtained from the harmonic method closely match the measured values at these observation points. Once parameters that describe the Eastern Scheldt are known, the loss coefficient ξ can be calibrated using observation points 1 and 2. The last step is to chose a ξ value that represents the situation without the barrier and then the water levels can be assed in the Eastern Scheldt for this situations.

A.2 Calibration of parameters

The first step in the harmonic method involves assessing the current water levels at three key points: Point 1, Point 2, and Point 3. These points correspond to the measurement locations Roompot Buiten, Roompot Binnen, and Marollegat. The observed water levels at these locations are shown in Figure A.2. At the closed end of the basin (Marollegat), the water levels are highest due to wave amplification. Moving towards the Oosterscheldekering (OSK), water levels just before the barrier (Roompot Binnen) are also lowest, whereas the water levels just beyond the barrier (Roompot Buiten) are mediate. To analyze the tidal basin, the measured water levels can be represented by the following expression: $\tilde{\zeta} = A_{M2} \cdot \sin\left(\frac{2\pi}{T_{M2}} + \phi\right)$. This representation is achieved by approximating the amplitude and phase shift at each location, using the Python package U-Tide, which extracts tidal constituents from measurements. The wave amplitudes within the basin, from the open sea to just behind the barrier and finally to the closed end, are approximately 1.6 m, 1.3 m, and 1.8 m. These resulting wave approximations are shown in Figure A.3. As illustrated, there is a slight phase shift between the waves because the tidal wave takes some time to travel through the Oosterschelde basin, a pattern that is also visible in the observational data.

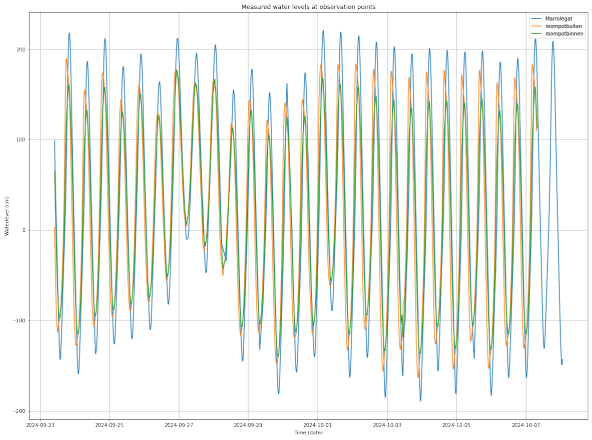

Figure A.2: Measured water levels at observation points

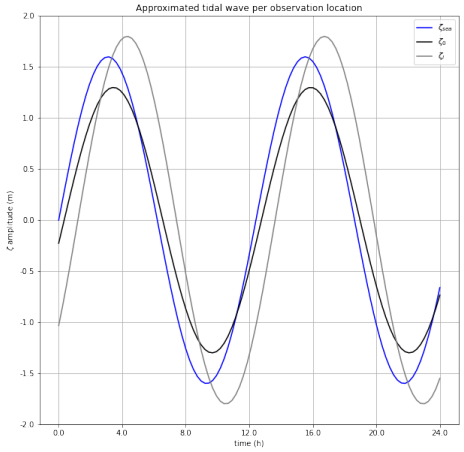

Figure A.3: Approximated water levels per observation point

When determining the parameters that describe the simplified Eastern Scheldt, these should relate to the Eastern Scheldt itself. In total, the Eastern Scheldt has an area of 350 km^2. The length is approximately 45 km, and

the width is around 8 km. The bottom friction factor (c_f) for natural conditions is about 0.004. Regarding the depth of the basin, it varies between +2 m and -50 m. In the simplification, one representative value should be chosen. The conveyance area of the tidal channels is calculated as the width of the tidal channel multiplied by the depth, which should be approximately 40,000 m^2 (20 m depth times 2,000 m width). Additionally, the tidal prism can be checked. As stated in Table 2.1, this is 880 $\times 10^6$ m^3. Knowing these parameter values, they can be varied slightly to match the approximated water levels and tidal prism.

In Figure A.4 and Table A.1, the approximated water levels and the water levels with the harmonic method are displayed. It can be observed that the water levels at the closed end (ζ_l) and and just behind the barrier (ζ_0) of the harmonic method match the approximated water levels. Additionally, the tidal prism is calculated with the harmonic method is in the same range as it is currently. The parameters used for these waves are presented in Table A.2.

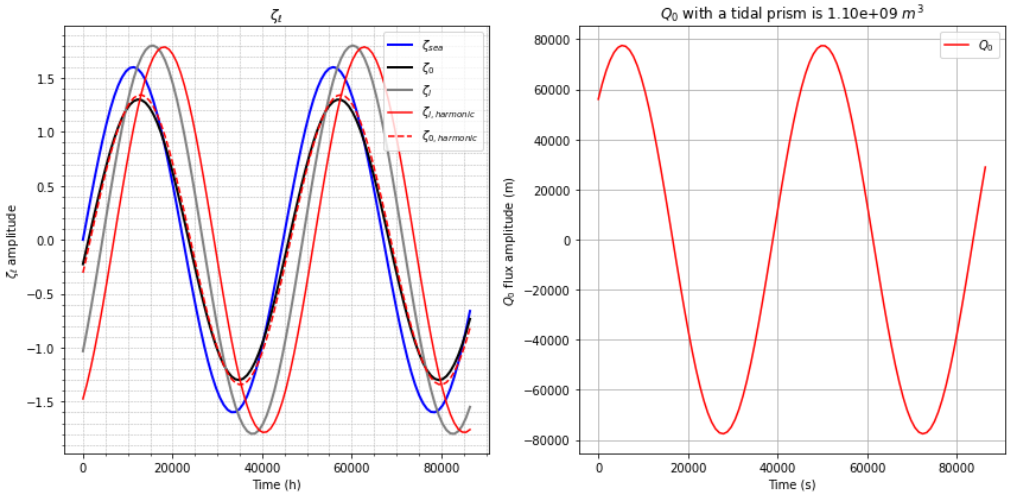

Figure A.4: Water levels constructed with the harmonic method

Table A.1: Values of the MHW and MLW from Figure A.4

	ζ_{sea}	ζ_0	ζ_l	$\zeta_{l,harmonic}$	$\zeta_{0,harmonic}$
MHW in m	1.6	1.3	1.8	1.79	1.34
MLW in m	-1.6	-1.3	-1.8	-1.79	-1.34

Table A.2: Parameters for the Eastern Scheldt

Parameter	Value
A_c (Conveyance area of the channel in m^2)	44000
d (Depth in m)	12
B (Width of the basin in m)	6800
l_b (Length of the basin in m)	52000
c_f (Friction factor)	0.0025
ξ (friction factor barrier)	5

A.3 Removal of the OSK

Now the harmonic method is calibrated, the model can be adjusted to see the effect of the removal of the OSK. The removal of this OSK in this model is done by setting the friction factor of the barrier to zero. The result of the harmonic method is then visualized in Figure A.5 with the water level values in Table A.3

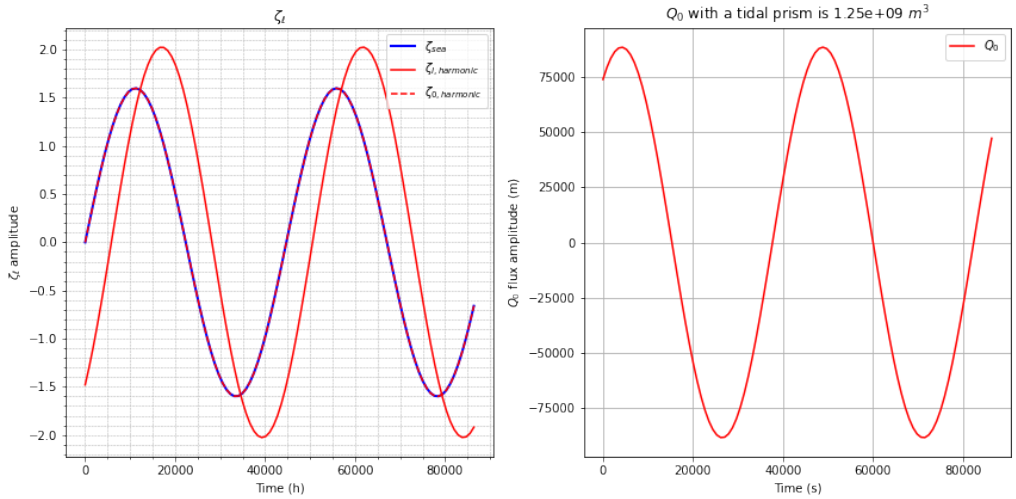

Figure A.5: Water levels constructed with the harmonic method without the OSK

Table A.3: Values of the MHW and MLW from Figure A.4

	ζ_{sea}	$\zeta_{l,harmonic}$	$\zeta_{0,harmonic}$
MHW in m	1.6	2.03	1.6
MLW in m	-1.6	-2.03	-1.6

Comparing with and without the OSK the tidal prism has an increase of 13% and the tidal range at the end of the basin has an increase of 14%.

Appendix B Definition of Parameters for ASMITA in the Scenario Without OSK

The ASMITA requires various parameters as inputs. this section gives an overview how the parameters for the Eastern Scheldt are derived for the ASMITA model. These parameters are divided in three groups: the initial values, the equilibrium parameters and the morphological timescale parameters. The initial values determine the state of the Eastern Scheldt from which the model begins running. The equilibrium parameters are used to calculate the equilibrium state, the morphological timescale parameters determine the pace at which the system moves to its equilibrium.

B.1 Initial values

The initial values are a set of parameters which include the tidal range (H), the area (A) and volume (V) of the flats, channels and ebb-tidal delta of the Eastern Scheldt.

The tidal range for the situation without the OSK is stated Table 4.1, which is 3.36 meter. This value is based on on calculations in Appendix A and research of De Pater (2012). For more explaination on this value read Section 4.1.1.

The volumes of the flats, channels, and ebb-tidal delta are based on the 2019 depth measurements. In ASMITA, the flats volume is defined as the sediment volume between MLW and MHW. This volume, calculated in Section 4.1.2, is 91 m^3. The channel volume in ASMITA is defined as the water volume below MLW. It is important to note that this channel volume is smaller than the channel volume used for comparing the measured channel volume with the equilibrium channel volume. This difference arises because the equilibrium volume is calculated as the water volume below MSL. The initial water volume of the channels below MLW, in the scenario without the OSK, is calculated to be 2346 million m^3. The volume of the ebb-tidal delta is identical to the volume used in the equilibrium volume calculations, as it follows the same definition in ASMITA. This volume is 486 million m^3 as stated in Table 4.3. The areas for the flats and channels are calculated using the MLW an MHW as boundaries. For the ebb-tidal delta the same area is used as in research on the ebb-tidal delta by Eelkema (2013) and de Bok (2001). These area together with the initial volumes and the tidal range are visible in Table B.1

Tidal range	H	(m)	3.36
Area of the flats	A_f	(km^2)	117
Area of the channels	A_c	(km^2)	239
Area of the ebb-tidal delta	A_{od}	(km^2)	280
Initial volume of the flats	$V_{f,0}$	(million m^3)	91
Initial volume of the channels	$V_{c,0}$	(million m^3)	2346
Initial volume of the ebb-tidal delta	$V_{od,0}$	(million m^3)	486

Table B.1: Initial values used as parameters in ASMITA for the Eastern Scheldt without OSK

B.2 Equilibrium parameters

The equilibrium parameters in ASMITA define to which equilibrium volume each element is moving. The equilibrium parameter consist of the equilibrium volume of the flats ($V_{f,eq}$), the empirical equilibrium parameter for the channels (α_c) and the empirical equilibrium parameter for the ebb-tidal delta (α_{od}).

The equilibrium volume of the flats is calculated using the method as described in Section 2.5. This volume is calculated for the situation without the OSK, see Table 4.2 and is 205 million m^3 sediment.

For calculating the equilibrium volume of the channels, a different relation as described in Section 2.5 is used, see Equation (19) (Z. B. Wang et al., 2024). In ASMITA, the channels are defined as the volume of water below MLW, rather than MSL. As stated in Section 2.3.2, sand demand is calculated under the assumption that the channels would be in equilibrium if the tidal prism was not decreased with 30%. This assumption is also used in defining the empirical equilibrium parameter for the channels. The channel volume below MLW just after the completion the OSK in 1990 is calculated and divided by the tidal prism at that time.

The channel volume below MLW in 1990 is 2278 million m^3, calculated with the depth measurement in 1990 and the MLW value of -1.25 meter. The MLW value is stated in Table 4.1. The tidal prism in 1990 is 905 million m^3 water, see also Table 4.1. The tidal prism that would lead to no sand demand would than be $P = 905 * 10^6/0,7 = 1293 * 10^6 m^3$ This leads to a empirical equilibrium parameter for the channels of $\alpha_c = (2278 * 10^6)/(1293 * 10^6) = 1.76$

$$V_{c,eq} = \alpha_c P \tag{19}$$

where:

$V_{c,eq}$	: equilibrium volume of the channels below MLW	$[m]$
α_c	: empirical equilibrium parameter for channels	$[-]$
P	: Tidal prism	$[m]$

For calculating the equilibrium volume of the ebb-tidal delta, the same relation as described in Section 2.5 is used, but with a different empirical equilibrium parameter, see Equation (20). This is done because the equilibrium volumes calculated with the relation in Section 2.5 is expected to overestimate the equilibrium volume of the ebb-tidal delta, read Section 5.1. For this reason the same assumption is used as for the channels, that the ebb-tidal delta was in equilibrium before the completion of the OSK. For the ebb-tidal delta there is an data point before the completion of the volkerakdam in 1964. This data point is chosen for the equilibrium volume because at this time the Eastern Scheldt was not yet influenced by the delta works. The sediment volume of the ebb tidal delta was in 1964 480 million m^3, see Figure 4.6. The tidal prism at that time had a volume 1200 million m^3 water (de Bok, 2001). This leads to empirical equilibrium parameter for the ebb-tidal delta of $\alpha_{od} = (480 * 10^6)/(1200 * 10^6)^{1.23} = 3.27 * 10^{-3}$

$$V_{od,eq} = \alpha_{od} P^{1.23} \tag{20}$$

where:

$V_{od,eq}$	: equilibrium volume of ebb-tidal delta	$[m]$
α_{od}	: empirical equilibrium parameter for ebb-tidal delta	$[-]$
P	: tidal prism	$[m]$

B.3 Morphological timescale parameters

The parameters for the morphological timescale are the following: Local equilibrium sediment concentration power n, Vertical exchange coefficient w_s, Horizontal exchange coefficient δ and Global equilibrium concentration c_E, which should be defined for the coarse (sand) and the fine (mud) fraction. This is because previous research on the Wadden Sea shows that it's important to include both sand and mud fractions when the parameters are theoretically derived, which is the case in this thesis. Also models that include both sand and mud give are more realistic result (Z. Wang & Lodder, 2019). Currently, the flats in the Eastern Scheldt contain only 1% mud (Rios-Yunes et al., 2023), but it is expected that after the removal of the OSK, mud will be imported into the basin on channels and flats. As a result, the mud fraction on the flats is expected to increase to 10%. In the Wadden Sea, no mud is found in the ebb-tidal delta due to wave impacts preventing its settlement (Huismans et al., 2024). It is assumed that the same condition applies to the Eastern Scheldt's ebb-tidal delta.

Local equilibrium sediment concentration power n
The exponent n in the local equilibrium sediment concentration should match the velocity exponent used in sediment transport formulas. For coarse sand particles, the Engelund-Hansen approach is used, where n equals 5. For finer sediments like mud or silt, the Partheniades-Krone formulations apply, with n equal to 3 (Bonenkamp, 2023).

Vertical exchange coefficient w_s
The parameter w_s represents the vertical movement of sediment between the water column and the bed. It is related to the fall velocity of the sediment particles and should be in the same range. In the Eastern Scheldt, the grain size varies throughout the basin, with coarser sediment found in the channels and finer sediment on the flats. Additionally, the grain size becomes smaller further inland (Kohsiek et al., 1987). For the flats, the median grain size of sand is 100 μm (Rios-Yunes et al., 2023). For the channels and the ebb-tidal delta, the median grain size is 200 μm (Kohsiek et al., 1987) (Eelkema, 2013). Using the estimated fall velocities for quartz spheres (based on Rouse's equations) and Stokes' law, the fall velocities are approximately, 0.006 m/s for the flats and 0.015 m/s for both the channels and the ebb-tidal delta. For mud with diameters smaller than 62 μm the fall velocities vary between 0.0001 and 0.002 m/s (Van Maren & Winterwerp, 2013). In this thesis an fall velocity of 0.001 m/s is used for the mud fraction.

Global equilibrium concentration c_E
The global equilibrium concentration c_E is an boundary condition in ASMITA. These concentrations are using Equation (21) (Bonenkamp, 2023).

$$c_E = \frac{c}{(1-\rho_s)n} \tag{21}$$

where:

c_E	: global equilibrium concentration fine fraction	[−]
c	: measured sediment concentration fine fraction	[g/l]
ρ_s	: sediment density	[kg/m^3]
n	: porosity	[−]

The mean suspended sediment concentration near the Eastern Scheldt variates between 10 and 40 mg/l. The higher value relates tot the winter in which more waves are present an the sediment is easier in suspension (Suijlen & Duin, 2002). With a porosity of 0.4 and a sediment density of 2650 kg/m^3 this leads to a range of $c_{E,fine} = 6.3 \times 10^-6$ to 2.5×10^-5. For the coarse fraction, there is no data available for the sediment concentrations in the water column. As a result, $c_{E,coarse}$ is a calibration parameter without specified range.

Measurements from the Wadden Sea show that the concentration of coarse sediment is highest during peak tidal velocity, with values between 100 mg/L and 200 mg/L (Postma, 1961), corresponding to a global equilibrium concentration of $c_{E,\text{coarse}} = 0.6 \times 10^{-4}$ to $c_{E,\text{coarse}} = 1.3 \times 10^{-4}$. However, in ASMITA studies with two sediment fractions conducted by Bonenkamp (2023) and Huismans et al. (2024), the global equilibrium value was chosen as $c_{E,\text{coarse}} = 4 \times 10^{-4}$, which corresponds to a concentration of 636 mg/L. In this study, a range between 0.5×10^{-4} and 4×10^{-4} is taken for the global equilibrium concentration. This range is based on measurements and values from earlier research using a two-fraction ASMITA model.

Both the global equilibrium concentrations of the fine and the coarse fraction are adjusted so that the he mud fraction on the flats is around to 10%. This is for values of $C_{E,f} = 7 \times 10^-6$ and $C_{E,c} = 4.0 \times 10^-4$

Horizontal exchange coefficient δ
The horizontal exchange coefficient δ describes the diffusive movement of water and sediment between the tidal elements. Its value is influenced by factors such as the size of the elements, the intertidal dispersion coefficient, and the distance between two elements, as shown in Equation (22). The dispersion coefficient D is directly related to tidal flow velocity, water depth, and fall velocity, as shown in Equation (23). For the ebb-tidal delta, it is assumed that no mud is present due to the high wave impact. For this reason, the fall velocity of the mud fraction on the ebb-tidal delta is set to 1×10^{-6} m/s, which ensures that mud particles will never settle on the ebb-tidal delta.

$$\delta = \frac{DS}{L} \tag{22}$$

$$D = \varepsilon \frac{u^2 H}{w_s} \tag{23}$$

where:

δ	: horizontal exchange coefficient	$[m^3/s]$
D	: Intertidal dispersion coefficient	$[m^2/s]$
S	: Flow cross sectional area between two elements	$[m^2]$
L	: Characteristic length scale for horizontal sediment transport	$[m]$
u	: Typical tidal flow velocity	$[m/s]$
H	: Average depth at the border between two elements	$[m]$
w_s	: Fall velocity	$[m/s]$
ε	: dimensionless parameter	$[-]$

To give an overview how exactly each horizontal exchange parameter is calculated the definitions of the parameters used to determine the horizontal exchange for each element are provided in Table B.2. The dimensionless parameters ϵ and α are used to obtain logical values for velocity and the horizontal exchange parameter. α is chosen such that the velocity does not exceed 1 m/s, which represents a typical maximum velocity under for tidal basin under normal conditions (Bosboom & Stive, 2021). ϵ is chosen such that the horizontal exchange parameters for the coarse fraction are of the order 100 and for the fine fraction around the order 1000, which is the same order as research on the Wadden Sea (Huismans et al., 2024).

To verify whether the horizontal exchange parameters are reasonable, the critical sea-level rise for the flats will be calculated using Equation (24) (Huismans et al., 2024). In the Wadden Sea, basins with areas comparable to the Eastern Scheldt have a critical sea-level rise for the flats of 6.4 to 10 mm/year (Huismans et al., 2022). If the critical sea-level rise calculated for the Eastern Scheldt aligns with this values, it provides further evidence that the chosen parameters for δ are physically reasonable.

$$R_{\mathrm{c}} = \frac{c_{\mathrm{E,fine}}}{\frac{1}{w_{\mathrm{s,f,fine}}} + \frac{A_{\mathrm{f}}+A_{\mathrm{c}}+A_{\mathrm{d}}}{\delta_{\mathrm{o-od,fine}}} + \frac{A_{\mathrm{f}}+A_{\mathrm{c}}}{\delta_{\mathrm{od-c,fine}}} + \frac{A_{\mathrm{f}}}{\delta_{\mathrm{c-f,fine}}}} + \frac{c_{\mathrm{E,coarse}}}{\frac{1}{w_{\mathrm{s,f,coarse}}} + \frac{A_{\mathrm{f}}+A_{\mathrm{c}}+A_{\mathrm{d}}}{\delta_{\mathrm{o-od,coarse}}} + \frac{A_{\mathrm{f}}+A_{\mathrm{c}}}{\delta_{\mathrm{od-c,coarse}}} + \frac{A_{\mathrm{f}}}{\delta_{\mathrm{c-f,coarse}}}} \tag{24}$$

where:

R_c	: Critical sea level rise for the flats	$[mm/year]$
$\delta_{(o-od),(od-c),(c-f)}$	: horizontal exchange coefficient o = outside, od=ebb-tidal delta, c=channel, f=flats	$[m^3/s]$
$A_{c,f,od}$	: Area of the (c) channel, (f) flats and (od) ebb-tidal delta	$[m^2]$
$w_{s,f}$	: fall velocity the flats	$[m/s]$
$coarse, fine$	: indicates the fine (mud) and the coarse (sand) sediment fraction	

	Description	**unit**	**flats-channel**	**channel-ebb-tidal delta**	**ebb-tidaldelta-outside world**
P	Prism per tidal element	m^3	$P_f = A_f * H - V_f$	$P_c = A_c * H + P_f$	$P_{od} = A_{od} * H + P_c$
H	Average element boundary depth	m	$\frac{1}{2}$ H	Average depth inlet	Average depth edge ebb-tidal delta
b	Length of element boundary	km	Perimeter tidal flats	Width inlet	edge of ebb-tidal delta
S	Cross-sectional area of element boundary, so area through which water exchanges between the elements	m^2	$H \cdot b$	$H \cdot b$	$H \cdot b$
u_{avg}	Time- and spatially averaged exchange velocity at element boundary	m/s	$\frac{Pf}{S \cdot T}$	$\frac{Pc}{S \cdot T}$	$\frac{Pod}{S \cdot T}$
α	Multiplication factor for velocity	-	-	-	-
u	Characteristic velocity as used in definition for D	m/s	$u_{\text{avg}} \cdot \alpha$	$u_{\text{avg}} \cdot \alpha$	$u_{\text{avg}} \cdot \alpha$
w_s	Settling velocity of sediment	m/s	Defined by sediment size	Defined by sediment size	Defined by sediment size
ϵ	dimensionless parameter	-	-	-	-
D	Intertidal diffusion/dispersion coefficient	m^2	$\epsilon \cdot u^2 \cdot H/w_s$	$\epsilon \cdot u^2 \cdot H/w_s$	$\epsilon \cdot u^2 \cdot H/w_s$
L	Distance that sediment travels between adjacent elements.	km	Average weighted distance from the centerline of the channel towards the tidal flats (visual estimation)	Average weighted distance of each point in the channel towards the center of mass of the ebb-tidal delta (visual estimation)	Representative exchange length between the ebb-tidal delta and the coast and off-shore (visual estimation)
δ	Horizontal exchange coefficient	m^3/s	$\frac{D \cdot S}{L}$	$\frac{D \cdot S}{L}$	$\frac{D \cdot S}{L}$

Table B.2: Parameter definitions for determining the horizontal exchange coefficient, with H = tidal range [m] and T = tidal period [s]

Using the definitions in Table B.2 the horizontal exchange parameter can be calculated. This caluclation and values for the horizontal exchange parameter between each element is visible in Table B.3.

Using the calculated horizontal exchange parameter and the global equilibrium concentrations, the critical sea level rise for the flats can be determined using Equation (24). This yields a value of 4.3 mm/year. This value is lower than the critical sea-level rise for flats in the Wadden Sea, which are located in basins of similar size. However, this R_c value is still suggested to be acceptable, for explanation see Section 5.2.2.

	unit	flats-channel	channel-ebb-tidal delta	ebb-tidaldelta-outside world
P	m^3	$P_f = 117 \times 10^6 * 3.36 - 91 \times 10^6 = 302 \times 10^6$	$P_c = 239 \times 10^6 * 3.36 + 302 \times 10^6 = 1110 \times 10^6$	$P_{od} = 280 \times 10^6 * 3.36 + 1119 \times 10^6 = 2050 \times 10^6$
H	m	1.68	16	10
b	km	190	5	40
S	m^2	319200	80000	400000
u_{avg}	m/s	0.042	0.62	0.23
α	-	2	1	2
u	m/s	0.085	0.62	0.46
w_s	m/s	$w_{s,sand} = 0.006$ $w_{s,mud} = 0.001$	$w_{s,sand} = 0.015$ $w_{s,mud} = 0.001$	$w_{s,sand} = 0.015$ $w_{s,mud} = 0.000001$
ϵ	-	0.8	0.1	0.1
D	m^2	$D_{sand} = 1.61$ $D_{mud} = 9.67$	$D_{sand} = 40.9$ $D_{mud} = 613$	$D_{sand} = 14$ $D_{mud} = 210056$
L	km	2.5	20	12
δ	m^3/s	$\delta_{sand} = 205 \quad \delta_{mud} = 1234$	$\delta_{sand} = 163 \quad \delta_{mud} = 2451$	$\delta_{sand} = 476$ $\delta_{mud} = 7502041$

Table B.3: Horizontal exchange coefficient calculation with the definitions used in Table B.2

B.4 Horizontal exchange parameter values for the sensitivity run

Because the horizontal exchange parameter is defined based on average aggregated distances a sensitivity analysis is done. The distances that are changed are the average element boundary depth H, the length of the element boundary b and the distance that sediment travels between adjacent cells L. A larger H, b and L leads to a smaller δ. Smaller horizontal exchange parameter δ results in less sediment exchange between the tidal element. This means more time is needed to reach their equilibrium volume, while for larger δ less time is needed to reach is equilibrium.

The averaged distances of H, L, and b in Table B.3 are adjusted to reflect a range 15% higher and lower than their base values. Within this range the minimum, maximum and mean are used to compute the respective minimum and maximum, and mean values for the horizontal exchange parameter. The values for H,b and L with their calculated horizontal exchange parameters are shown in Table B.4. The mean values are identical to those in Table 4.4, which represents the most likely estimates for the average distances in the Eastern Scheldt.

	Description	**unit**	**flats-channel**	**channel-ebb-tidal delta**	**ebb-tidaldelta-outside world**
H	Average element boundary depth	m	$\frac{1}{2}$ H	Average depth inlet	Average depth edge ebb-tidal delta
b	Length of element boundary	m	Perimeter tidal flats	Width inlet	edge of ebb-tidal delta
L	Distance that sediment travels between adjacent elements.	m	Average weighted distance from the centerline of the channel towards the tidal flats (visual estimation)	Average weighted distance of each point in the channel towards the center of mass of the ebb-tidal delta (visual estimation)	Representative exchange length between the ebb-tidal delta and the coast and off-shore (visual estimation)
H	**Maximum**	m	1.68	18.4	11.5
b	**Maximum**	km	218.5	5.75	46
L	**Maximum**	km	2.875	23	13.8
δ	**Minimum**	m^3/s	$\delta_{f-c,s} = 155$ $\delta_{f-c,m} = 933$	$\delta_{c-od,s} = 123$ $\delta_{c-od,m} = 1853$	$\delta_{od-o,s} = 352$ $\delta_{od-o,m} = 5294548$
H	**Mean**	m	1.68	16	10
b	**Mean**	km	190	5	40
L	**Mean**	km	2.5	20	12
δ	**Mean**	m^3/s	$\delta_{f-c,s} = 205$ $\delta_{f-c,m} = 1234$	$\delta_{c-od,s} = 163$ $\delta_{c-od,m} = 2451$	t $\delta_{od-o,s} = 466$ $\delta_{od-o,m} = 7502041$
H	**Minimum**	m	1.68	13.6	8.5
b	**Minimum**	km	161.5	4.25	34
L	**Minimum**	km	2.125	17	10.2
δ	**Maximum**	m^3/s	$\delta_{f-c,s} = 284$ $\delta_{f-c,m} = 1708$	$\delta_{c-od,s} = 226$ $\delta_{c-od,m} = 3393$	$\delta_{od-o,s} = 646$ $\delta_{od-o,m} = 9691406$

Table B.4: Values of the average distances which are used to calculate a minimum, maximum and mean value for the horizontal exchange parameter. The subscripts indicate the elements, i.e. f = flat, c = channel, od = ebb-tidal delta and o = outside world and the fractions, s =sand sediment fraction and m =mud sediment fraction

B.5 Parameter values for the sensitvity run on the shape parameter of the bruun-profile

The ebb-tidal volume was calculated using an undisturbed bed profile. Typically, such a profile is constructed by extending depth contours from an undisturbed section of the coast adjacent to the ebb-tidal delta. In this thesis, however, the undisturbed bed profile was constructed using the Bruun profile, see Section 3.2.1. This approach introduces some uncertainty due to the choice of the shape parameter A, which determines the steepness of the undisturbed bed profile, read also Section 3.2.1 and Section 3.3.3. The parameter was selected so that the -20-meter depth contour aligns with the measured depth. Parameters in the range of A=0.35 to A=0.40 provided a reasonable fit, see Section 4.1.2. Using these shape parameters, the ebb-tidal delta volumes were calculated for the year 1964. This is the equilibrium volume of the ebb-tidal delta by assuming the Eastern Scheldt was in equilibrium at that time, see Appendix B.2. Using this ebb-tidal delta volume and the recorded tidal prism, the empirical equilibrium parameter for the ebb-tidal delta is computed using the relation in Equation (20). The initial volumes were recalculated using the bed level of 2019 according to the different shape parameters. The values used in the sensitivity analysis calculated for the different shape parameters A, are shown in Table B.5.

Parameter	A	Ebb-tidal volume in 1964	Empirical equilibrium parameter ebb-tidal delta (α_{od})	Initial volume ebb-tidal delta
Unit	[$m^{2/3}$]	[$\cdot 10^6$ m^3]	[$\cdot 10^{-3}$ $m^{-0.69}$]	[$\cdot 10^6$ m^3]
minimum values	0.35	226	1.54	226
reference run	0.38	480	3.27	486
maximum values	0.4	639	4.35	649

Table B.5: Parameter values used in the sensitivity run of the bruun profile